UC San Diego
Scripps Institution of Oceanography Technical Report

Title

The Natural Geochemistry of Tetrafluoromethane and Sulfur Hexafluoride : Studies of Ancient Mojave Desert Groundwaters, North Pacific Seawaters and the Summit Emissions of Kilauea Volcano

Permalink

https://escholarship.org/uc/item/1hp1f3bd

Author

Deeds, Daniel A

Publication Date

2008-05-20

UNIVERSITY OF CALIFORNIA, SAN DIEGO

The Natural Geochemistry of Tetrafluoromethane and Sulfur Hexafluoride: Studies of

Ancient Mojave Desert Groundwaters, North Pacific Seawaters and the Summit

Emissions of Kilauea Volcano

A dissertation submitted in partial satisfaction of the

requirements for the degree Doctor of Philosophy

in

Earth Sciences

by

Daniel Arthur Deeds

Committee in Charge:

　　　Professor Ray F. Weiss, Chairman
　　　Professor David R. Hilton
　　　Professor Ralph F. Keeling
　　　Professor Kimberly A. Prather
　　　Professor Jeffrey P. Severinghaus

2008

The dissertation of Daniel A. Deeds is approved, and it is

acceptable in quality and form for publication on microfilm:

_____

_____

_____

_____
                                            Chairman

University of California, San Diego

2008

TABLE OF CONTENTS

LIST OF FIGURES

LIST OF TABLES

ACKNOWLEDGEMENTS

I consider myself very fortunate to have had Ray Weiss as an advisor during my doctoral study. Ray has always offered unstinting support and encouraged me to independently pursue my research goals. He has kept my focus on the big picture, keeping me from bogging down in the little details of the science. Perhaps most importantly, he's always stood up for my interests, from getting the correct SIO acceptance letter sent to me when I received another student's letter by mistake to supporting my decision to be a more involved father.

I am grateful to David Hilton, Ralph Keeling, Kim Prather and Jeff Severinghaus for serving on my doctoral committee. Despite very busy schedules, they were always accessible and willing to apply their considerable expertise to any part of my research that I brought to them.

I also owe a big debt of gratitude to the other members of the Weiss lab. Chris Harth has been an unending source of advice about anything I've ever wanted to discuss, from experimental design to ethical eating practices and everything between. Her guidance was especially valuable during the design of the dissolved gas extraction line that was used in most of the research in this thesis. Peter Salameh was always available to help with data analysis and Matlab advice. When the data didn't make complete sense, a chat with Ben Miller or Jens Mühle would often help straighten things out. Martin Vollmer and Erin Shields have both been excellent

officemates and not complained once about my frequent outbursts, questions, diatribes or digressions.

My experience at SIO has been greatly enhanced by the kindness of my fellow students. Martin Vollmer and Justin Kulongoski have been good friends and wonderful collaborators. The Mojave Desert and Big Bear CF_4 measurements would not exist without their invitation to join the sampling expeditions. Even though the results were inconclusive, I still count myself lucky to also have collaborated with Martin on a study of halogenated gas concentrations in Mammoth Mountain soil gases. An agreement with Katie Phillips garnered me travel funds to sample Kilauea's summit fumaroles in exchange for my help on her research cruise of Hawaii. Although not for my research, I had another chance to experience the planning and execution of a scientific cruise when Evan Solomon invited me along for a week-long cruise to the Gulf of Mexico.

My work in the Mojave Desert would also not have been possible without the financial and logistical support of David Hilton and John Izbicki (US Geological Survey). Both Dave and John were also very willing to share their expertise when it came to dissolved gases in groundwater and the hydrogeology of the Mojave. Jeff Severinghaus generously opened his laboratory so that I could use his vacuum line to extract dissolved gases from the Mojave Desert groundwaters collected in 2002.

The groundwater sampling trips to the Big Bear Lake Watershed coincided with the due date of my daughter. I am very grateful to Greg Smith (US Geological Survey), who graciously volunteered to collect groundwater samples for me, so that I

During my stay at SIO I've met many wonderful people who've become friends, including Evan Solomon, who was always willing to head to a show to check out a new band, Patrick Rafter (another great officemate!), Brian Hopkinson, Mario

and Melissa (and Kai!) Soldevilla, Lisa Munger, Sarah Glaser and Melissa Headly. Difficult times were made easier with the help of friends like these.

The love, support and encouragement of my parents and brother have been priceless. I treasure my wife Geneviève Boisvert and our daughter Léanore, I love them greatly, and know that they give me the strength and purpose to persevere. I feel truly blessed to have my family in my life.

Vita

Education:

2001 – 2008   Ph.D. in Earth Sciences, Scripps Institution of Oceanography,
University of California, San Diego

1997 – 2001   Bachelor of Sciences in Chemistry,
University of California, Berkeley

Professional Work Experience:

2001 – 2008   Graduate Student Researcher
Research Advisor: Professor Ray Weiss
Scripps Institution of Oceanography, UC San Diego

1999 – 2001   Undergraduate Research Assistant
Research Advisor: Professor Ron Cohen
Department of Chemistry, UC Berkeley

Languages: English (mother tongue), French (intermediate comprehension), German and Spanish (basic comprehension)

Peer-reviewed Manuscripts:

Deeds D. A., J. Mühle and R. F. Weiss (2008) Tetrafluoromethane in the deep North Pacific Ocean, Geophys. Res. Lett., in review.

Deeds D. A., Vollmer M. K., Kulongoski J. T., Miller B. R., Mühle J., Harth C. M., Izbicki J. A., Hilton D. R. and Weiss R. F. (2008) Evidence for crustal degassing of

CF$_4$ and SF$_6$ in Mojave Desert groundwaters, Geochim. Cosmochim. Acta 72, 999 – 1013.

Meeting Abstracts:

Deeds D. A., Vollmer M. K., Kulongoski J. T., Miller B. R., Hilton D. R., Izbicki J. A., Harth C. M., and Weiss R. F. (2004) Terrestrial Sources of Perfluorinated Gases: Excess CF$_4$ and SF$_6$ in Mojave Desert Groundwaters. EOS Trans. AGU, 85(47), Fall Meet. Suppl., Abstract H21F-1093.

Day D. A., Deeds D. A., Woolridge P. J., Dillon M. B., McKay M., Shade G. W., Goldstein A. H. and Cohen R. C. (2001) The Seasonal Cycle of NO$_2$, Total Peroxy Nitrates, Total Alkyl Nitrates, and HNO$_3$ at the U. C. Blodgett Forest Research Station. EOS Trans. AGU, 82(47), Fall Meet. Suppl., Abstract A41B-0033, 2001.

ABSTRACT OF THE DISSERTATION

The Natural Geochemistry of Tetrafluoromethane and Sulfur Hexafluoride: Studies of

Ancient Mojave Desert Groundwaters, North Pacific Seawaters and the Summit

Emissions of Kilauea Volcano

by

Daniel Arthur Deeds

Doctor of Philosophy in Earth Science

University of California, San Diego, 2008

Professor Ray F. Weiss, Chairman

Tetrafluoromethane (CF_4) and sulfur hexafluoride (SF_6) are potent, long-lived greenhouse gases whose natural atmospheric sources and sinks are poorly understood. CF_4 and SF_6 concentrations were measured in groundwater, deep and surface seawater, and volcanic gas samples to provide a better constraint on their lithospheric sources to the atmosphere.

Groundwaters collected from the Mojave Desert and nearby Big Bear Lake Watershed contain CF_4 and SF_6 concentrations well in excess of air-saturated water concentrations for the conditions of recharge, providing in situ evidence for a crustal

degassing of CF_4 and SF_6. Excess CF_4 and SF_6 concentrations can be attributed to release during weathering of the surrounding granitic alluvium and to a deeper crustal flux of CF_4 and SF_6 entering the study aquifers through the crystalline basement. The crustal flux of CF_4, but not SF_6, is enhanced in the vicinity of local active fault systems due to release of crustal fluids during episodic crustal fracturing driven by tectonic activity. When the crustal degassing rate of CF_4 and SF_6 into studied groundwaters is extrapolated to a global scale, it is consistent with the lithospheric flux required to sustain their preindustrial atmospheric abundances using best-estimate atmospheric lifetimes.

CF_4 and SF_6 in volcanic emissions from Kilauea summit originate from air entrained into rising volcanic gases and from gases exsolved from Kilauea's hydrothermal system. An upper limit to a hypothetical volcanic flux of CF_4 and SF_6 is negligible when compared to the continental flux, indicating that the upper mantle is not a significant source of either gas to the atmosphere.

Surface seawaters collected off of Scripps Pier during calm weather are in equilibrium with expected air-saturated seawater CF_4 concentrations. Deep Pacific seawater samples are oversaturated by roughly 4%, consistent with a predicted 5% oversaturation for these waters. The oceanic crust is therefore not a significant source of lithospheric CF_4. This suggests that CF_4 is conservative in seawater, and, combined with its rapid accumulation in the atmosphere, indicates that dissolved anthropogenic CF_4 concentrations are an effective time-dependent tracer of ocean circulation and mixing processes.

Chapter 1

Introduction

Gases of relatively low atmospheric abundance (i.e. "trace gases") can have a significant impact on the chemical and physical state of the atmosphere. One example that has received significant recent attention are the greenhouse gases, such as carbon dioxide and methane, which are infrared (IR) active trace gases that absorb a portion of the outgoing long-wave radiation emitted from the Earth. Some of the absorbed energy is reemitted back towards the Earth, resulting in an enhanced warming of the Earth's surface. In this manner, emissions of greenhouse gases related to human industry and activity can have a considerable influence on global climate.

The class of fully fluorinated greenhouse gases, comprised of perfluorocarbons (PFCs) and SF_6, are of particular scientific interest, not only because of their strong absorption of IR radiation (Ko et al., 1993; Sihra et al., 2001), but also because they are effectively inert in the majority of the atmosphere (Ravishankara et al., 1993; Morris et al., 1995). The loss processes for these compounds are either chemically or dynamically limited, leading to atmospheric lifetimes on the order of millennia (Morris et al., 1995; Ravishankara et al., 1993). Fully fluorinated species thus not only have an impact on the radiative budget of the atmosphere, but due to their long lifetimes, their presence in the atmosphere will persist for thousands of years after

human-induced perturbations in the abundances of other greenhouse gases disappear. Although on a time-scale of hundreds of years the fully fluorinated gases may play only a small role in anthropogenic climate change compared to other more abundant greenhouse gases (e.g. CO_2) (Isaksen et al., 1992), their emissions lead to a lasting climate legacy.

The two most abundant fully fluorinated species present in the atmosphere, tetrafluoromethane (CF_4) and sulfur hexafluoride (SF_6), have atmospheric mole fractions that have increased rapidly since the first half of the 20th century (Maiss and Brenninkmeijer, 1998; Worton et al., 2007). Currently the atmospheric dry-air mixing ratios of CF_4 and SF_6 have reached roughly 75 ppt and 6 ppt, respectively (1 ppt = 10^{-12} mole mole^{-1}). The natural background of these gases prior to the start of anthropogenic emissions is estimated to be approximately 34 ppt CF_4 and <6.4 ppq SF_6 (1 ppq = 10^{-15} mole mole^{-1}) (Harnisch et al., 1996; Vollmer and Weiss, 2002; Worton et al., 2007). The relatively rapid increases in the CF_4 and SF_6 content of the atmosphere are attributed solely to anthropogenic emissions of these gases.

The current understanding of the natural geochemistry of CF_4 and SF_6 is limited, as it is difficult to directly observe sources and sinks of these gases in the atmosphere, partly because of the remote nature of atmospheric sinks of CF_4 and SF_6 but also because of the very small magnitude expected for sinks and sources of the gases to the atmosphere (Ravishankara et al., 1993). However, it is critical that scientists and policymakers have a more complete understanding of the natural geochemistry of these gases, as the rate at which they are naturally released and

destroyed will influence the rate at which anthropogenic perturbations of their atmospheric abundances will diminish in the future.

For my doctoral research, I have taken up the challenge of quantifying the natural sources of CF_4 and SF_6, to better understand their preindustrial geochemistry and thus the response in atmospheric CF_4 and SF_6 abundances to current and future anthropogenic emissions. I have focused mainly on ancient waters in the crust and in the oceans, as they are isolated from the atmosphere for sufficiently long periods of time (i.e. thousands of years) that they can accumulate quantifiable amounts of natural CF_4 or SF_6. In addition, I have investigated whether perfluorinated gases and other halogenated gases are present in magmatic emissions, a question that has spurred considerable debate in recent years (Stoiber et al., 1971; Isidorov et al., 1990; Jordan et al., 2000). Before detailing my doctoral research, I present a brief description of the available literature concerning the geochemistry of CF_4 and SF_6, and I describe the general method by which I analyzed gas and water samples for CF_4 and SF_6. Results from groundwater studies in the Mojave Desert (Chapter 4) and Big Bear Valley (Chapter 5), a study of gas emissions from Kilauea volcano (Chapter 6) and results from a study of surface and deep North Pacific seawaters (Chapter 7) are then presented.

1.1 References

Harnisch, J., Borchers, R., Fabian, P., Gaggeler, H.W., and Schotterer U. (1996) Effect of natural tetrafluoromethane, *Nature* **384**, 32.

Harnisch, J. and Eisenhauer A. (1998) Natural CF_4 and SF_6 on Earth, *Geophys. Res. Lett*. **25**, 2401 – 2404.

Isaksen, I.S.A., Bruhl, C., Molina, M., Schiff, H., Shine, K., and Stordal F. (1992) An assessment of the role of CF_4 and C_2F_6 as greenhouse gases, *Policy Note 1992-06.* Oslo, Norway, CICERO.

Isidorov V. A., Zenkevich I. G. and Ioffe B. V. (1990) Volatile organic compounds in solfataric gases, *J. Atmos. Chem.* **10**, 329 – 340.

Jordan A., Harnisch J., Borchers R., Le Guern F. and Shinohara H. (2000) Volcanogenic Halocarbons, *Envrion. Sci. Technol.* **36**, 1122 – 1124.

Ko M. K. W., Sze N. D., Wang W. C., Shia G., Goldman A., Murcray F. J., Murcray D. G. and Rinslan C. P. (1993) Atmospheric sulfur hexafluoride – sources, sinks and greenhouse warming, *J. Geophys. Res.-Atmos.* **98**, 10,499 – 10,507.

Maiss, M. and Brenninkmeijer C. A. M. (1998) Atmospheric SF_6: Trends, sources, and prospects, *Environ. Sci. Tech.* **32**, 3077 – 3086.

Morris, R.A., Miller, T.M., Viggiano, A.A., Paulson, J.F., Solomon, S., and Reid G. (1995) Effects of Electron and Ion Reactions on Atmospheric Lifetimes of Fully Fluorinated Compounds, *J. Geophys. Res.-Atmos.* **100**, 1287 – 1294.

Ravishankara, A.R., Solomon, S., Turnipseed, A.A., and Warren R. F. (1993) Atmospheric Lifetimes of Long-Lived Halogenated Species, *Science* **259**, 194 – 199.

Sihra, K., Hurley, M.D., Shine, K.P., and Wallington T. J. (2001), Updated radiative forcing estimates of 65 halocarbons and nonmethane hydrocarbons, *J. Geophys. Res.-Atmos.* **106**, 20,493 – 20,505.

Stoiber R. E., Leggett D. C., Jenkins T. F., Murrmann R. P. and Rose W. I. Jr. (1971) Organic compounds in volcanic gas from Santiaguito Volcano, Guatemala, *Geol. Soc. Am. Bull.* **82**, 2299 – 2302.

Vollmer, M. K. and Weiss R. F. (2002), Simultaneous determination of sulfur hexafluoride and three chlorofluorocarbons in water and air, *Marine Chem.* **78**, 137 – 148.

Worton D. R., Sturges W. T., Gohar L. K., Shine K. P., Martinerie P., Oram D. E., Humphrey S. P., Begley P., Gunn L., Barnola J.-M., Schwander J. and Mulvaney R. (2007) Atmospheric Trends and Radiative Forcings of CF_4 and C_2F_6 Inferred from Firn Air, *Environ. Sci. Technol.* **41**, 2184 – 2189.

Chapter 2

The Geochemistry of CF_4 and SF_6

2.1 Sources of CF_4 to the atmosphere

The current primary source of CF_4 to the atmosphere is production from the electrolysis of cryolite during aluminium production (Taberaux, 1994):

$$4\,Na_3AlF_6 + 3\,C \longrightarrow 4\,Al + 12\,NaF + 3\,CF_4 \qquad \textbf{(2.1)}$$
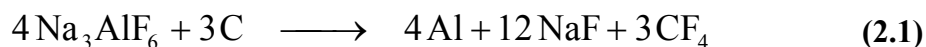
Emissions of CF_4 vary depending on the cell technology used, with older Al reduction cells tending to have higher emissions factors (kg CF_4 per ton Al produced) due to more frequent and longer-lasting cryolite-decomposition events (Taberaux, 1994). Annual global emissions of CF_4 from the production of aluminum indicate an increase from about 1,000 tons CF_4 yr^{-1} in the 1940s to a peak of roughly 16,000 tons CF_4 yr^{-1} in the late 1980s, with emissions afterwards declining to around 9,200 tons CF_4 yr^{-1} for 2000 (Harnisch et al., 1999; Olivier, 2002). Modernization of aluminum

reduction plants has led to a general decrease in CF_4 emissions, despite increases in Al production (Harnisch et al., 1999). The only other significant anthropogenic source of CF_4 to the atmosphere that has been identified is emission from the semiconductor industry, with a source strength increasing from effectively 0 tons CF_4 yr^{-1} in 1980 to about 1,400 tons CF_4 yr^{-1} in 2000 (Victor and MacDonald, 1999).

Recently, several scientific groups have independently discovered the presence of CF_4 in the preindustrial atmosphere (Fabian et al., 1987; Harnisch et al. 1995; Harnisch et al., 1996; Worton et al. 2007), with the oldest-reaching reconstructed CF_4 history indicating a preindustrial CF_4 mole fraction of 34 ± 1 ppt (Worton et al., 2007). Measurements in our laboratory of ancient air extracted from ice cores, with an age of around 1300 years, have shown a similar atmospheric CF_4 mole fraction of 34.8 ± 0.2 ppt, suggesting that, prior to the start of emissions of CF_4 from aluminum production, the Holocene atmosphere has been in steady-state with respect to CF_4 (J. Mühle, personal communication). Harnisch and Eisenhauer (1998) and Harnisch et al. (2000) detected significant amounts of CF_4 in fluid inclusions trapped in fluorites and granites, with CF_4 mass contents ranging from <1 ppt to 61,000 ppt and from 2 ppt to 265 ppt, respectively. These authors proposed that weathering, metamorphism and other alterations of the continental crust would result in a lithospheric flux of $0.1 - 1$ t CF_4 yr^{-1}, of similar magnitude to the natural flux the authors calculated was necessary to maintain the preindustrial atmospheric CF_4 abundance ($0.4 - 4$ t CF_4 yr^{-1}) based on an atmospheric CF_4 lifetime of 170,000 years (Ravishankara et al., 1993). However, this estimate does not include all proposed losses for CF_4 (Morris et al., 1995; see

following section), which, when combined in parallel, result in a lower limit atmospheric CF_4 lifetime of 110,000 years. If this lifetime is used in place of the 170,000-year estimate of Ravishankara et al. (1993), the estimated lithospheric flux of $0.1 - 1$ t CF_4 yr^{-1} cannot sustain the observed preindustrial atmospheric abundance of CF_4.

2.2 Atmospheric CF$_4$ loss processes

The principle loss process for CF_4 in the atmosphere is thought to be destruction by reaction with atomic hydrogen in high temperature combustors at the Earth's surface (i.e. incinerators, internal combustion engines, etc.), with an estimated atmospheric lifetime of >50,000 years (Ravishankara et al., 1993). CF_4 is lost naturally to reaction with atomic hydrogen and positive oxygen ions (O^+) and to photolysis by H Lyman α radiation in the upper atmosphere (Ravishankara et al., 1993; Morris et al., 1995). However, natural loss processes for CF_4 are estimated to be significantly slower than anthropogenic loss at the Earth's surface, since the low atmospheric pressures of the upper atmosphere (on the order of 10^{-6} bar) require air to cycle through this region roughly a million times to process the entire atmosphere (Morris et al., 1995). Estimated atmospheric lifetimes for natural CF_4 loss processes are 170,000 years for loss to H, 330,000 years for loss to O^+ and 6,200,000 years for photolysis by H Lyman α radiation (Ravishankara et al., 1993; Morris et al., 1995).

When combined in parallel, the natural atmospheric loss processes for CF_4 give a best-estimate "preindustrial" atmospheric CF_4 lifetime of 110,000 years.

2.3 Sources of SF_6 to the atmosphere

SF_6 is mainly used as an insulating gas in high voltage electrical applications, and as a degassing agent of molten metals (Ko et al., 1993; Maiss and Brenninkmeijer, 1998), but it is also used in other applications such as filling of tires, sound insulating windows, and shoe soles, and in semiconductor production. Electrical applications currently make up around 60% of total SF_6 sales, with 40% split between the non-electrical applications. Of the amount of SF_6 used in electrical applications, such as circuit breakers and switchgear, 30% is released to the atmosphere due to leaking from gaskets and seals, and release during servicing of the equipment, with the latter usually occurring after a delay of several years (Maiss and Brenninkmeijer, 1998). Blanketing of molten metals, chiefly aluminium and magnesium, is the next largest use of SF_6, comprising 5-10% of the total SF_6 production (Ko et al., 1993; Maiss and Brenninkmeijer, 1998). SF_6 emissions from degassing of aluminium are small due to destruction of SF_6 in the aluminium melt, while practically all the SF_6 used for blanketing molten magnesium is emitted to the atmosphere (roughly half of the total SF_6 used to blanket molten metals). Emissions of SF_6 to the atmosphere have increased roughly linearly from 760 t yr^{-1} in 1972 to 6,300 t yr^{-1} in 1996 (Maiss and Brenninkmeijer, 1998).

In addition to CF_4, Harnisch and Eisenhauer (1998) and Harnisch et al. (2000) also detected smaller amounts of SF_6 in the fluid inclusions of fluorites and granites. Busenberg and Plummer (2000) confirmed the presence of SF_6 in granitic rocks and in fluorite, and in a variety of other minerals and rocks as well, including calcite, dolomite, and halite. Busenberg and Plummer (2000) also observed elevated SF_6 concentrations in groundwaters in contact with granitic and carbonate aquifers. Measured SF_6 mass concentrations in fluorites range from <0.2 ppt to 30,000 ppt and from <0.2 ppt to 45 ppt in granites. The majority of granites studied had SF_6 mass concentrations below detection limits (Harnisch and Eisenhauer, 1998; Busenberg and Plummer, 2000; Harnisch et al., 2000). SF_6 concentrations in other minerals are on the order of 100 to 10,000 times smaller than in fluorite and granites (Busenberg and Plummer, 2000).

Harnisch and Eisenhauer (1998) estimate a flux of SF_6 to the atmosphere of 0.006 to 0.06 tons yr^{-1}, resulting in a natural background of 0.001 to 0.01 ppt (by mole). This is consistent with current estimates of a natural SF_6 background of less than 0.0064 ppt in Antarctic firn air (Vollmer and Weiss, 2000).

2.4 Atmospheric SF_6 loss processes

SF_6 attaches electrons and reacts with O^+ at the theoretical limit (Morris et al., 1995), and so it is destroyed at altitudes higher than the stratopause, similar to CF_4. Photolysis by H Lyman α radiation in the upper atmosphere may also be a significant

loss process: in one study, it accounted for an estimated 24% of the total loss of SF_6 from the atmosphere (Ravishankara et al., 1993). Thermal destruction in high temperature combustors was also suggested as a significant loss process for SF_6 (Ravishankara et al., 1993).

While considering only electron attachment leading to SF_5^- and F, and thermal destruction as loss processes of SF_6, Ravishankara et al. (1993) estimated an atmospheric lifetime for SF_6 of 3,200 years. Morris et al. (1995) added attachment of electrons leading to SF_6^-, and loss to O^+ in the upper atmosphere to the scenario proposed by Ravishankara et al. (1993), resulting in a lower limit to the SF_6 lifetime of 800 years. In either case, the atmospheric cycling of SF_6 seems dependent mainly on electron scavenging in the upper atmosphere. The atmospheric lifetime for SF_6 should thus be in the range 800 – 3200 years.

2.5 References

Busenberg, E. and Plummer L. N. (2000) Dating young groundwater with sulfur hexafluoride: Natural and anthropogenic sources of sulfur hexafluoride, *Water Resources Research* **36**, 3011 – 3030.

Fabian, P., Borchers, R., Kruger, B.C., and Lal S. (1987) CF_4 and C_2F_6 in the Atmosphere, *J. Geophys. Res.-Atmos.* **92**, 9831 – 9835.

Harnisch, J., Borchers, R., and Fabian P. (1995) Estimation of tropospheric trends (1980 - 1995) for CF_4 and C_2F_6 from stratospheric data, *Proc. Int. Soc. for Opt. Eng. / Europ. Opt. Soc., Europ.-Series.* **2506**, 384 – 393.

Harnisch, J., Borchers, R., Fabian, P., Gaggeler, H.W., and Schotterer U. (1996) Effect of natural tetrafluoromethane, *Nature* **384**, 32.

Harnisch J. and Eisenhauer A. (1998) Natural CF_4 and SF_6 on Earth. *Geophys. Res. Lett.* **25**, 2401 – 2404.

Harnisch, J., Borchers, R., Fabian, P., and Maiss M. (1999) CF_4 and the age of mesospheric and polar vortex air, *Geophys. Res. Lett.* **26**, 295 – 298.

Harnisch, J., Frische, M., Borchers, R., Eisenhauer, A., and Jordan A. (2000) Natural fluorinated organics in fluorite and rocks, *Geophys. Res. Lett.* **27**, 1883 – 1886.

Ko M. K. W., Sze N. D., Wang W. C., Shia G., Goldman A., Murcray F. J., Murcray D. G. and Rinslan C. P. (1993) Atmospheric sulfur hexafluoride – sources, sinks and greenhouse warming, *J. Geophys. Res.-Atmos.* **98**, 10,499 – 10,507.

Maiss, M. and Brenninkmeijer C. A. M. (1998) Atmospheric SF_6: Trends, sources, and prospects, *Environ. Sci. Tech.* **32**, 3077 – 3086.

Morris, R.A., Miller, T.M., Viggiano, A.A., Paulson, J.F., Solomon, S., and Reid G. (1995) Effects of Electron and Ion Reactions on Atmospheric Lifetimes of Fully Fluorinated Compounds, *J. Geophys. Res.-Atmos.* **100**, 1287 – 1294.

Olivier J. (2002), EDGAR Database; http://www.mnp.nl/edgar/

Ravishankara, A.R., Solomon, S., Turnipseed, A.A., and Warren R. F. (1993) Atmospheric Lifetimes of Long-Lived Halogenated Species, *Science* **259**, 194 – 199.

Tabereaux, A. T. (1994) Anode Effects, PFCs, Global Warming, and the Aluminum Industry, *JOM*. Nov. 1994, 30 – 34.

Victor, D. G. and MacDonald G. J. (1999) A model for estimating future emissions of sulfur hexafluoride and perfluorocarbons, *Climatic Change* **42**, 633 – 662.

Vollmer, M. K. and Weiss R. F. (2002) Simultaneous determination of sulfur hexafluoride and three chlorofluorocarbons in water and air, *Marine Chem.* **78**, 137 – 148.

Worton D. R., Sturges W. T., Gohar L. K., Shine K. P., Martinerie P., Oram D. E., Humphrey S. P., Begley P., Gunn L., Barnola J.-M., Schwander J. and Mulvaney R. (2007) Atmospheric Trends and Radiative Forcings of CF_4 and C_2F_6 Inferred from Firn Air, *Environ. Sci. Technol.* **41**, 2184 – 2189.

Chapter 3

Extraction and Measurement of Dissolved Perfluorinated Gases

One significant challenge when studying perfluorinated gases, especially CF_4, is their high volatility. CF_4 has a significant vapor pressure (roughly 0.8 Torr) at even the relatively low temperature of its triple point (89.6 K) (Lobo and Staveley, 1979), and so complete extraction and collection of CF_4 from a sample using common cryogenics is not possible. To completely extract CF_4 from water and gas samples, I adapted an ice-core noble gas extraction protocol devised by Severinghaus et al. (2003). In this protocol, gases are transferred from a sample flask into a vacuum line (Fig. 3.1) for collection into an evacuated 40 mL cold finger immersed in liquid helium (~4 K). The following is a description of a typical dissolved gas extraction from a groundwater sample. Modifications of this general protocol for other types of analyses are discussed in chapters describing individual research projects.
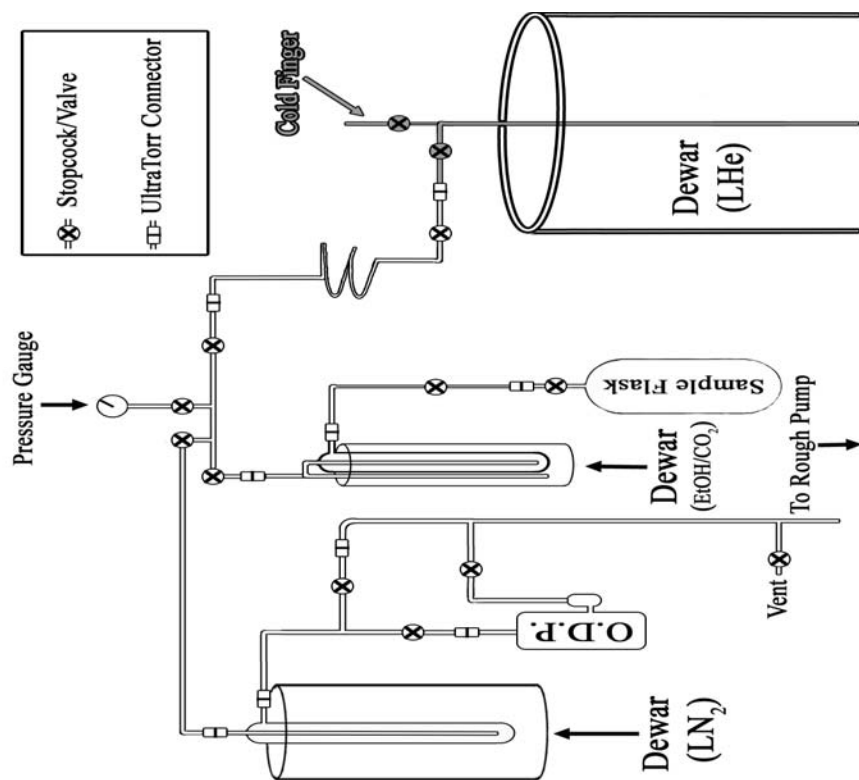
Figure 3.1: Photograph and schematic of the dissolved gas extraction line. The dewars contain liquid nitrogen (LN$_2$), liquid helium (LHe), or an ethanol/dry-ice slurry (EtOH/CO$_2$). (O.D.P. = Oil Diffusion Pump)

At the start of an extraction, the evacuated cold finger is immersed in liquid helium, and both the flask and cold finger are connected to the evacuated (p <1 mTorr) extraction line. An initial static leak test of the line is performed to ensure that the sample will not be significantly contaminated by room air. Typical static leaks are 0.1 – 0.2 mTorr min^{-1}, contributing <0.2 fmol CF_4 per extraction.

After the integrity of the extraction line is confirmed through static leak testing, the flask is exposed to the line, and the internal pressure of the line is allowed to build for several seconds before the cold finger is opened. The pressure differential between the flask headspace and cold finger drives sample gases into the cold finger, where they absorbs onto its internal surfaces, maintaining the pressure differential and flow into the finger. Most water vapor is removed from the line upstream of the finger by a double-chamber vacuum trap cooled by an ethanol-dry ice slurry (T~195 K). Upstream of this trap, water vapor acts as a flushing gas, aiding the movement of gas out of the flask's headspace. The extraction continues for 10 minutes, at which point the flask is isolated from the line, the pressure in the line is allowed to drop to <1 mTorr, and the cold finger is closed and removed from the line and the liquid helium. Extraction times of 10 minutes are sufficient to remove >99% of the headspace of a sample.

Once removed from the liquid helium, the cold finger is warmed to the touch and is connected in line with the "Medusa" cryotrapping quadrupole gas chromatograph/mass spectrometer (Miller et al., 2008). The cold finger has been fitted with a dip-tube through which analyte-free nitrogen is flushed to completely

transfer extracted gases into the Medusa's cryotrapping module. A general description of the treatment of a sample by the Medusa-GC/MS is given in the Methods section of Chapter 4. The full details of the Medusa-GC/MS can be found in Miller et al. (2008).

Each measurement is blank-corrected and calibrated by comparison to a known volume (~1 L) of a whole air standard with assigned dry-air mole fractions based on the SIO-2005 gravimetric calibration scale (Prinn et al., 2000; C. Harth, personal communication). Standard volumes were determined using the Medusa-GC/MS's integrating digital mass flow controller, which was calibrated using a precision quartz pressure transducer fitted to a volume-calibrated 6 L stainless-steel flask pressurized with dry air and immersed in a temperature-stabilizing water bath (see Appendix A). Using this technique, I can accurately determine the number of moles standard introduced into the GC/MS to within ±0.5%. The CF_4 calibration in mole fraction of gas is then converted to an absolute molar calibration.

Gases dissolved in the liquid phase of a sample during extraction are not collected, since the time-scale of diffusion in water for most gases is long compared to the extraction period (e.g. the characteristic length-scale of diffusion for CF_4 at 20°C is roughly 1 mm in 10 min in water (Yaws, 1995)). However, the solubilities of CF_4 and SF_6 in water are extremely low, with ~98% of the CF_4 and SF_6 in a sample located in the headspace of the flask at laboratory temperatures. Multiple headspace extractions of several samples have confirmed that ~2% of the dissolved CF_4 and SF_6 remains in the sample after the first extraction. Thus, analysis of perfluorinated gases

in groundwater samples requires only extraction of the headspace, with a small correction for the residual gas dissolved in the water phase.

The total number of moles initially present in a water sample (n_T) can be estimated from:

$$n_T = n_G + n_D \qquad \textbf{(3.1)}$$

where n_G is the number of moles gas extracted from a water sample, and n_D is the number of moles gas remaining in the aqueous phase of a sample after extraction. Assuming that the aqueous and vapor phases were in equilibrium prior to extraction, then n_G and n_D can be related through the Ostwald solubility coefficient:

$$L = \frac{n_D / V_S}{n_G / V_{HS}} \quad \rightarrow \quad n_D = L \times n_G \times \frac{V_S}{V_{HS}} \qquad \textbf{(3.2)}$$

where V_S is the volume of water in the flask and V_{HS} is the volume of the flask's headspace.

Recognizing that the molar concentration of gas X in a collected sample ([X], in moles X per liter water) is equal to n_T/V_S, and subsituting Equation 2 into Equation 1 gives:

$$[X] = n_G \times \left(\frac{V_{HS} + V_S \times L}{V_{HS} \times V_S} \right) \qquad \textbf{(3.3)}$$

The volume of the headspace V_{HS} can be estimated from $V_F - V_S$, where V_F is the volume of the flask. The flask volume is calibrated using the mass of the flask when completely filled with distilled water at a known temperature (m_F) and the density of freshwater at that temperature (ρ_F). Sample volumes can be estimated from the mass of the flask after sample collection (m_S) and the density of water at the temperature of the flask during the headspace extraction (ρ_S). Water densities are estimated using the International One-Atmosphere Equation of State of Seawater (Millero and Poisson, 1981). Both m_F and m_S are corrected for the mass of the flask material (i.e. the mass of the flask when evacuated).

Volume terms in Equation 3.3 can be replaced with the more easily measured mass terms, resulting in Equation 3.4:

$$[X] = n_g \times \left(\frac{m_F/\rho_F - m_S/\rho_S + L \times m_S/\rho_S}{\left(m_F/\rho_F - m_S/\rho_S \right) \times m_S/\rho_S} \right) \qquad (3.4)$$

which can be rearranged to give:

$$[X] = n_g \times \rho_S \times \left(\frac{m_F/m_S \times \rho_S + \{L-1\} \times \rho_F}{m_F \times \rho_S - m_S \times \rho_F} \right) \qquad (3.5)$$

Since the molar concentration of a gas is temperature dependent, a more convenient concentration term is the molality of a gas (i.e. moles of gas X per kilogram water), which can be estimated by dividing Equation 3.5 by ρ_S.

SF$_6$ has been previously used as a time-dependent tracer of water mass movement, and its solubility in fresh water and seawater as functions of temperature have been well described (Bullister et al., 2002). No single source of freshwater solubility data for CF$_4$ covers a sufficiently dynamic range of temperatures for the studies in this thesis, and so I compiled available freshwater solubility data for CF$_4$ and fit it with a Clark-Glew-Weiss equation (see Appendix B). The resulting function is valid over a temperature range of $275 - 330$ K, and gives calculated CF$_4$ solubilities that in general agree to within 1% with the literature values.

Total uncertainties associated with this analytical technique are $\pm$ 3% for CF$_4$ and $\pm$4% for SF$_6$. Duplicate measurements tend to agree to within $\pm$ 5% for CF$_4$, although more recent measurements (e.g. 2005 analyses of Mojave Desert groundwaters) are in significantly better agreement (i.e. reproducibilities for duplicate samples of $\pm\ 0.5 - 1\%$.)

3.1 References

Bullister J. L., Wisegarver D. P., and Menzia F. A. (2002) The solubility of sulfur hexafluoride in water and seawater, *Deep Sea Res., Part I* **49**, 175 – 187.

Lobo L. Q. and Staveley L. A. K. (1979) The vapour pressure of tetrafluoromethane, *Cryogenics* **19**, 335 – 338.

Miller B. R., Weiss R. F., Salameh P. K., Tanhua T., Greally B. R., Mühle J. and Simmonds P. G. (2008) Medusa: a sample preconcentration and GC/MS detector system for in situ measurements of atmospheric trace halocarbons, hydrocarbons and sulfur compounds, *Anal. Chem.* **80**, 1536 – 1545.

Millero F. J. and Poisson A. (1981) International one-atmosphere equation of state of seawater. *Deep Sea Res. A* **28**, 625-629.

Prinn R.G., R. F. Weiss, P. J. Fraser, P. G. Simmonds, D. M. Cunnold, F. N. Alyea, S. O'Doherty, P. Salameh, B. R. Miller, J. Huang, R. H. J. Wang, D. E. Hartley, C. Harth, P. L. Steele, G. Sturrock, P. M. Midgley and A. McCulloch (2000), A history of chemically and radiatively important gases in air deduced from ALE/GAGE/AGAGE. *J. Geophys. Res.–Atmos.* **105(D14)**, 17,751–17,792.

Severinghaus J.P., Grachev A., Luz B., and Caillon N. (2003), A method for precise measurement of argon 40/36 and krypton/argon ratios in trapped air in polar ice with applications to past firn thickness and abrupt climate change in Greenland and at Siple Dome, Antarctica, *Geochim. Cosmochim. Acta*. **67**, 325 – 343.

Yaws C. L. (1995) Diffusion Coefficient in Water. In : *Handbook of transport property data: viscosity, thermal conductivity, and diffusion coefficients of liquids and gases*. Library of physico-chemical property data. Gulf Pub.Co., Houston, Texas.

Chapter 4

Crustal Degassing of CF_4 and SF_6: Evidence from Mojave Desert Groundwaters

4.1 Abstract

Dissolved tetrafluoromethane (CF_4) and sulfur hexafluoride (SF_6) concentrations were measured in groundwater samples from the Eastern Morongo Basin (EMB) and Mojave River Basin (MRB) located in the southern Mojave Desert, California. Both CF_4 and SF_6 are supersaturated with respect to equilibrium with the preindustrial atmosphere at the recharge temperatures and elevations of the Mojave Desert. These observations provide the first in situ evidence for a flux of CF_4 from the lithosphere. A gradual basin-wide enhancement in dissolved CF_4 and SF_6 concentrations with groundwater age is consistent with release of these gases during weathering of the surrounding granitic alluvium. Dissolved CF_4 and SF_6 concentrations in these groundwaters also contain a deeper crustal component associated with a lithospheric flux entering the EMB and MRB through the

underlying basement. The crustal flux of CF_4, but not of SF_6, is enhanced in the vicinity of local active fault systems due to release of crustal fluids during episodic fracture events driven by local tectonic activity. When fluxes of CF_4 and SF_6 into Mojave Desert groundwaters are extrapolated to the global scale they are consistent, within large uncertainties, with the fluxes required to sustain the preindustrial atmospheric abundances of CF_4 and SF_6.

4.2 Introduction

Tetrafluoromethane (CF_4) and sulfur hexafluoride (SF_6) are among the longest-lived atmospheric trace gases, with estimated lifetimes of >50 kyr and 0.8-3.2 kyr, respectively (Ravishankara et al, 1993; Morris et al. 1995). Prior to 1996, consensus held that atmospheric CF_4 and SF_6 were derived solely from anthropogenic emissions. However, measurements of preindustrial air trapped in ice (Harnisch et al., 1996a) and of stratospheric air (Harnisch et al., 1996b) led to the discovery of a natural atmospheric abundance of CF_4, with a dry-air mole fraction (or "mixing ratio") of 39 ± 6 ppt (parts-per-trillion, or parts in 10^{12}). In a more recent study of air trapped in firn, Worton et al. (2007) estimated the preindustrial atmospheric CF_4 mole fraction as 34 ± 1 ppt, based on samples of older firn air than those measured by Harnisch and coworkers. Measurements of air trapped in Antarctic firn have shown a preindustrial atmospheric SF_6 abundance of less than 6.4 ppq (parts-per-quadrillion, or parts in 10^{15}) (Vollmer and Weiss, 2002).

The detection of several parts-per-million by weight of CF_4 and SF_6 in the extracted gas of a fluorite sample led Harnisch et al. (1996a) to propose a lithospheric origin for the natural atmospheric abundance of these gases. In subsequent studies (Harnisch and Eisenhauer, 1998; Harnisch et al., 2000), up to 60 parts-per-billion by weight of CF_4 and 30 parts-per-billion by weight of SF_6 were detected in a wider range of fluorite samples, as well as in accessory fluorites in granites, granodiorites and gneisses. In a later study, Busenberg and Plummer (2000) detected SF_6 in a wider range of minerals, and found elevated concentrations of dissolved SF_6 in groundwaters collected from carbonate and granitic aquifers, providing further evidence for a lithospheric source of SF_6.

Considering surficial weathering and subsurface alteration of the continental crust, Harnisch and Eisenhauer (1998) calculated a lithospheric source of CF_4 to the atmosphere of $100 - 1000$ kg CF_4 per year. This estimate agrees with these authors' model-derived source strength of $400 - 4000$ kg CF_4 per year necessary to maintain a preindustrial atmospheric CF_4 abundance of 40 ppt with an atmospheric lifetime in the range of 170 to 1700 kyr (Ravishankara et al., 1993). However, if all natural loss processes proposed by Ravishankara et al. (1993) are active in the atmosphere, then the lithospheric source of CF_4 to the atmosphere must be roughly three to four times larger than the Harnisch and Eisenhauer (1998) lithospheric source strength estimate, depending on whether the preindustrial atmospheric CF_4 mole fraction is taken as 34 ppt (Worton et al., 2007) or 40 ppt (Harnisch and Eisenhauer, 1998). Additionally, the lifetime estimate of Ravishankara et al. (1993) does not include the loss of CF_4 to

reaction with mesospheric O^+ (Morris et al., 1995). When this loss mechanism is combined in parallel with the loss processes proposed by Ravishankara et al. (1993), a lower limit of 110 kyr is calculated for the preindustrial atmospheric lifetime of CF_4, increasing the likelihood that a larger weathering flux or additional lithospheric sources are needed to balance the preindustrial atmospheric budget. Harnisch and Eisenhauer (1998) also explored several possible release mechanisms for lithospheric CF_4 in the laboratory, but no actual releases of lithospheric CF_4 have been observed in nature.

In this study, we report the first measurements of dissolved CF_4 in groundwaters, and use CF_4 and SF_6 concentrations, together with other geochemical constraints, to identify release mechanisms of lithospheric CF_4 and SF_6 to the atmosphere. We estimate the strengths of the weathering and deep crustal sources of CF_4 and SF_6 and assess their potential impact on the global geochemistry of these gases.

4.3 Study Areas

Groundwater samples were collected in the southern region of the Mojave Desert, California, from the Eastern Morongo Basin (EMB) and Mojave River Basin (MRB). The Mojave Desert is a semi-arid region with low rainfall (<150 mm yr^{-1}), low humidity, and high summer temperatures (Londquist and Martin, 1991). The

MRB and EMB are located ~130 km and ~200 km east-northeast of Los Angeles, respectively (Fig. 4.1).

The EMB and MRB are underlain by an impermeable crystalline basement complex of Precambrian igneous and metamorphic rock, filled with unconsolidated to moderately consolidated granitic alluvium of Tertiary to Tertiary-Quaternary age derived from the surrounding mountain ranges (Riley and Worts, 1953; California Department of Water Resources, 1967). Deposit thicknesses are greater than 1000 m in some areas of the EMB and MRB (Riley and Worts, 1953; Subsurface Surveys, 1990).

The EMB deposits consist of an upper unit of Tertiary to Quaternary deposits overlying a lower unit of more poorly-sorted, less-permeable, Tertiary deposits with larger amounts of igneous and metamorphic fragments (Londquist and Martin, 1991). Though the two units are interconnected hydrologically, waters from the lower unit have significantly different chemistries from waters residing in the upper unit (Londquist and Martin, 1991). The EMB wells studied here draw water from the upper geologic unit, with the exception of well 3N/7E-32D2 and well 3N/7E-28D2, which penetrate into the lower geologic unit.

The EMB is recharged by infiltration of runoff and streamflow from seasonal precipitation along the eastern edge of the San Bernardino Mountains (~1.3 km above sea level). Mean modern surface temperatures at the recharge site are ~8 °C in winter (Engstrom, 1981). Wells sampled for this study lie within the Surprise Spring sub-Basin (SSB), located at the center of the EMB (Fig. 4.1d). Groundwater flows from
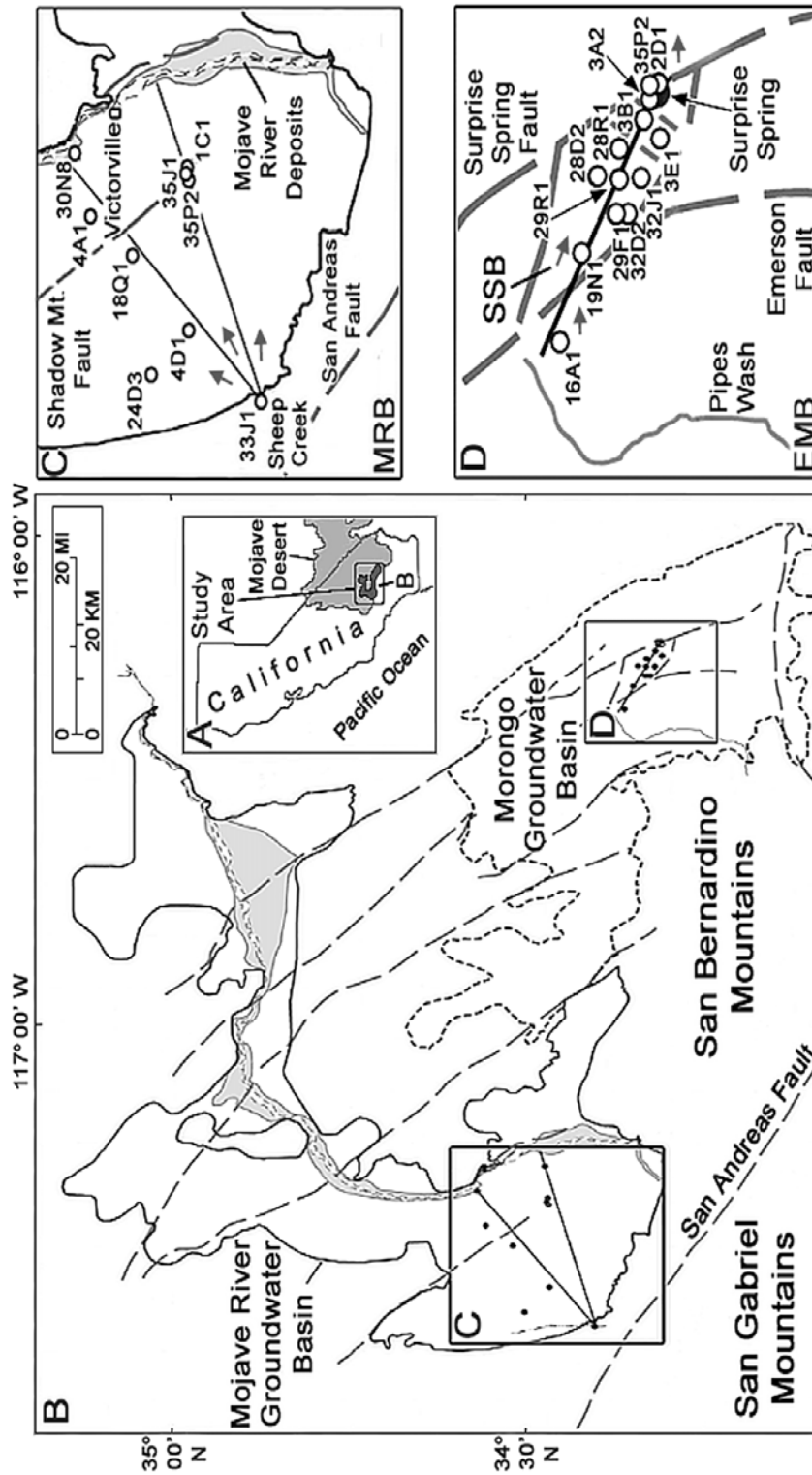
Figure 4.1 A) Locations of the Mojave Desert and the study area within California; B) The Mojave River Basin and Morongo Basin, with boxes indicating areas sampled in this study; C) Borehole locations (circles) within the Mojave River Basin (MRB), and D) Eastern Morongo Basin (EMB) study areas. The Surprise Spring sub-Basin (SSB) is located in the center of the EMB. Well labels are the last four digits of the corresponding USGS identification in Table 1 (e.g. −16A1 from 3N/6E-16A1). Long dashed lines in B – D are local fault systems, while solid black lines indicate the study flowpaths. Gray arrows indicate the general direction of groundwater flow (see Stamos et al. (2001) for a more detailed description of groundwater flow). Shaded regions in the Mojave River Basin show the location of the Mojave River Deposits.

the northwest to the east-southeast in the SSB, entering the sub-basin from recharge along the lower reaches of Pipes Wash to the west. In the east, the Surprise Spring Fault acts as a barrier to groundwater flow, which resulted in natural surface discharge at Surprise Spring prior to well field development in 1955 (Londquist and Martin, 1991).

In the Mojave River Basin, we focused our research on the much older waters of the underlying deep regional aquifer, rather than the shallow Mojave River Deposits, which contain modern water from infiltration during storm-flow events along the Mojave River (Izbicki and Michel, 2004). Groundwater enters the regional aquifer in the western part of the MRB as mountain-front recharge from infiltration of winter stormflows and snowmelt runoff in the upper reaches of ephemeral streams on the flanks of the San Bernardino and San Gabriel Mountains (~1.5 km above sea level). Recharging groundwater flows radially outward from Sheep Creek to the north-northeast (Fig. 4.1c). Recharge from direct infiltration of precipitation does not occur away from the mountain front in the regional aquifer (Izbicki et al., 2000). Measured groundwater temperatures for recently recharging groundwater into the regional aquifer are ~12 ºC (Kulongoski et al, 2003). Two flowpaths (Fig. 4.1c) are studied here, extending through the regional aquifer from the recharge site to discharge sites near the Mojave River.

4.4 Methods

4.4.1 Sample Collection

During five expeditions between October 2000 and January 2005, we collected samples for SF_6 and/or CF_4 analyses from 14 wells in the EMB and 12 wells in the MRB. The sampled wells were mainly production wells (24 cm or 36 cm I.D.) equipped with electric turbine pumps. Wells 3N/6E-16A1 and 3N/7E-19N1 in the EMB are observation wells (10 cm I.D.) that were sampled with a mobile submersible pump. Inactive wells were pumped for >30 min prior to sampling, to purge more than three times the well volume in an attempt to avoid sampling stagnant water previously in contact with modern air. Observation wells were pumped for roughly three hours, as the flow rate of the mobile pump (roughly 10 L min^{-1}) is relatively low compared to the flow rate of the turbine pumps (around 1000 L min^{-1}) installed in production wells. Prior to each sampling, the spigot of the well was struck repeatedly to dislodge any air bubbles that may have been trapped on its inner walls.

Groundwater samples were flame sealed into 0.35L glass ampoules for SF_6, CFC-12 (CCl_2F_2), CFC-11 (CCl_3F), and CFC-113 ($CClF_2C$ Cl_2F) analyses (Vollmer and Weiss, 2002). During the 2002 field study to the EMB several samples were also collected in annealed copper tubes for dissolved He and Ne extraction and analysis (Kulongoski, 2003; 2005).

Groundwater samples were also collected into evacuated (<1 mTorr) 2.5 L glass flasks for CF_4, SF_6 and chlorofluorocarbon (CFC) analyses by the Medusa-GC/MS system (described below). The glass flasks are fitted with a glass-plug o-ring stopcock with two sidearms that permit purging of the stopcock with groundwater prior to sample collection. One sidearm of the flask was connected to the production well with ~1 m of 3/8" O.D. Tygon tubing that was soaked in water for 24 hours prior to sampling to reduce bubble adhesion during sample collection. Another ~1 m length of 3/8" O.D. Tygon tubing was connected to the second sidearm of the flask to prevent the incursion of modern air into the stopcock during sampling. Each flask was filled with approximately 2 L of sample, leaving roughly 0.5 L of headspace containing exsolved gas and water vapor. Once returned to the laboratory, the flasks were allowed to equilibrate with the controlled room temperature of ~24 °C.

4.4.2 Sample Analyses

4.4.2.1 Noble Gas and SF_6 Analyses

Helium and neon concentrations presented here are a subset of data published previously by Kulongoski et al. (2003; 2005), supplemented by the 2002 EMB data. Measurement precisions for He and Ne were determined from the reproducibility of duplicate analyses (usually ±2%). Errors in ^{3}He abundances, derived from the

measured $^3He/^4He$ ratio, principally reflected counting statistics for the ^3He ion beam ($\pm4\%$).

Dissolved SF_6 and CFC concentrations in ampoule samples were measured using a purge-and-trap electron capture gas chromatography (GC/ECD) technique described by Vollmer and Weiss (2002). The overall precision of the analyses is ~2% as determined from 15 pairs of duplicate samples. Results are reported on the SIO-1998 calibration scale with an estimated accuracy of 2% (Vollmer and Weiss, 2002).

Supersaturation of gases in groundwaters drawn from well 6N/4W-30N8 resulted in bubble formation and loss of exsolved gas during flame-sealing of ampoules for GC/ECD analysis. Measured SF_6 concentrations for well 6N/4W-30N8 by GC/ECD are thus compromised, and are excluded from the data set presented in Table 4.1.

4.4.2.2 CF₄ Sample Extraction and Analysis

CF_4 analysis begins by freezing the headspace gases in the sample flask into an evacuated (<0.1 mTorr) cold finger cooled with liquid helium (T ≈ 4 K). This procedure was adapted from an ice core noble gas analytical protocol used by Severinghaus et al. (2003). A 10-minute extraction was found to be sufficient to remove >99% of the headspace of a sample.

Gases dissolved in the water in the flask are not removed by this technique, since the time-scale of diffusion in water is long compared to the extraction period

(e.g. the characteristic length-scale of diffusion for CF_4 at 20°C is roughly 1 mm in 10 min in water (Yaws, 1995)). However, because the solubility of CF_4 in water is extremely low, ~98% of the CF_4 in the sample is located in the headspace of the flask at ambient temperatures. Multiple headspace extractions of several samples have confirmed that ~2% of the dissolved CF_4 remains in the sample after the first extraction. Thus, analysis of CF_4 in groundwater samples requires only extraction of the headspace, with a small correction for the residual CF_4 dissolved in the water phase. We use compiled CF_4 solubility data from Ashton et al. (1968), Wilhelm et al. (1977) and Scharlin and Battino (1995) to calculate the residual dissolved CF_4 for each flask.

After sample extraction, the cold finger is removed from the liquid helium, heated until warm to the touch, and connected in line with the "Medusa" cryotrapping quadrupole gas chromatograph/mass spectrometer (GC/MS) system. The 80 cm long 3/8" O.D. cold finger is fitted with a 1/16" O.D. internal dip-tube, through which ultra-high purity nitrogen is flushed to transfer the sample into the Medusa-GC/MS. During early groundwater analyses by GC/MS (i.e. 2002 analyses and analyses for wells 3N/6E-16A1 and 3N/7E-28D2) the extraction tube was not actively heated, although sufficient time was usually allotted for the tube to thaw to room temperature (30 minutes – 1 hour). However, the extraction tube may not have thawed sufficiently for the GC/MS analysis of groundwater drawn from well 3N/7E-28D2 (thaw time of ~10 minutes), resulting in possible incomplete transfer of extraction gases, and results

for this well by GC/MS should be consider lower limits to the measured concentrations.

The Medusa-GC/MS was designed for the Advanced Global Atmospheric Gases Experiment (AGAGE) network (http://agage.eas.gatech.edu) by a collaboration of scientists from Scripps Institution of Oceanography and the University of Bristol. The Medusa-GC/MS system measures ~40 atmospheric trace gases, including CF_4, SF_6, CFC-12, CFC-11, and CFC-113. Samples introduced to the Medusa system are cryogenically preconcentrated on a HayeSep D trap (T1) at -165 °C. The CF_4, along with some bulk air components (e.g. N_2, O_2 and CO_2), is then desorbed and refocused on a second HayeSep D microtrap (T2), followed by separation of the CF_4 from the residual bulk air on a MS-4A/HiSiv-3000 precolumn and CP-PoraBond Q capillary column. The non-CF_4 analytes are subsequently desorbed from T1 and refocused on T2, and are injected directly into the GC/MS, where they are separated on the capillary column prior to MS detection. These separation steps greatly reduce the amounts of more abundant atmospheric gases that would otherwise interfere with chromatographic separation and mass spectrometric detection, including N_2, O_2, H_2O, CO_2, CH_4, and the noble gases.

The detection limit for measurement of CF_4 by the Medusa-GC/MS is currently 15 fmol (i.e. ~7 fmol CF_4 kg^{-1} H_2O for this study), based on 3 times the baseline noise, with instrumental precisions of $\pm$ 0.2% for routine measurements of the current atmospheric CF_4 background abundance. The total estimated analytical uncertainty associated with the measurement of CF_4 by this method is $\pm$ 3%, including

a conservatively estimated uncertainty of ± 1% associated with the correction for incomplete extraction. Duplicate measurements of dissolved CF_4 concentrations in this study typically agree within 5%.

After blank correction, CF_4 mole fractions in a sample are determined by comparison to known volumes (1 L) of a whole air standard with an assigned CF_4 dry-air mole fraction of 75.0 ± 0.4 ppt, based on the SIO-2005 gravimetric calibration scale (Prinn et al., 2000; C. Harth, personal communication). Standard volumes were determined using the Medusa-GC/MS's integrating digital mass flow controller (Redwood Microsystems), which was calibrated using a precision quartz pressure transducer (Paroscientific Instruments) fitted to a volume-calibrated 6 L stainless-steel flask pressurized with dry air and immersed in a temperature-stabilizing water bath. The volume of the 6 L flask is calibrated using the gravimetric method of Bullister (1984).

4.5 Results

Table 4.1 lists CF_4 and SF_6 concentration results for the EMB and the regional aquifer of the MRB. We report measured CF_4 and SF_6 concentrations (X), as well as "excess" concentrations (X_{ex}) that are corrected for modern air and water contamination (X_{mod}), air-bubble entrainment (X_a) and air-water equilibration (X_{eq}) during recharge, as discussed below. Reported CF_4 and SF_6 concentrations are generally the mean of duplicate samples. ^{3}He, ^{4}He, and Ne_a concentrations (see

Section 4.2.2.1), distances from wells to the apparent recharge locations and interpreted groundwater ages derived from radiocarbon (^{14}C) data ("groundwater radiocarbon ages") are also tabulated. Interpreted groundwater ages are from Kulongoski et al. (2003; 2005) and Izbicki and Michel (2004), and are calculated from dissolved inorganic ^{14}C activity using the computer program NETPATH (Plummer et al., 1991). These authors tuned the program by adjusting the reaction set and modeled mass transfers between rock and water, minimizing the differences between observed and calculated inorganic δ^{13}C compositions, to account for chemical reactions that alter inorganic ^{14}C content (Izbicki and Michel, 2004).

4.5.1 Chlorofluorocarbon-derived Contamination Estimates

Dissolved chlorofluorocarbons can be used to quantify X_{mod}, the component of measured CF_4 or SF_6 that is due to modern contamination, since CFCs have not been detected in preindustrial air (Butler et al., 1999). Measured CFC-12, CFC-11, and CFC-113 concentrations for the EMB and MRB from GC/ECD and Medusa-GC/MS analyses are tabulated in Electronic Annex EA-1. Most ampoule samples collected for analysis by GC/ECD had no detectable CFC concentrations, though some had CFC-12, CFC-11 and/or CFC-113 concentrations consistent with the addition of between 0.03-0.12 millimoles modern air per kg H_2O (i.e. roughly $0.6 - 3$ mL STP air kg^{-1} H_2O). CFC-113 was undetectable for the majority of ampoule samples. Samples

Table 4.1
CF$_4$ and SF$_6$ groundwater concentrations and crustal fluxes (J_X) for the Eastern Morongo Basin and Mojave River Basin

Borehole identification	D (km)[a]	^{14}C age (yr)	Ne$_a$ (nmol kg^{-1} H$_2$O)	^{4}He$_{ex}$ (nmol kg^{-1} H$_2$O)	^{3}He$_{ex}$ (fmol kg^{-1} H$_2$O)	Year sampled	CF$_4$ (fmol kg^{-1} H$_2$O)	SF$_6$ (fmol kg^{-1} H$_2$O)	CF$_{4ex}$ (fmol kg^{-1} H$_2$O)	SF$_{6ex}$ (fmol kg^{-1} H$_2$O)	J_{CF_4} (fmol cm^{-2} yr^{-1})	J_{SF_6} (fmol cm^{-2} yr^{-1})
Eastern Morongo Basin												
3N/6E-16A1[c]	5.0	<50	4.7	1.03	1.4	2003	16.7	13.5	0	13.3	—	—
3N/7E-19N1[c]	10.7	1430	3.1	1.7	2.0	2003	33*	11.6*	27	9.4	0.13	—
3N/7E-29F1	11.8	3800	27	4.0	6.2	2002	—	0.38*	—	0.36	—	—
3N/7E-28D2[d]	12.0	5800	54	7.2	10.8	2002	—	12.1	—		2.3	—
						2003	>1250	12.3*	>1130	12.3		
3N/7E-32D2	12.2		7.0	46	11.6	2000	—	2.19	—	2.18		0.0026
3N/7E-29R1	12.7	3900	4.4	2.9	2.5	2000	—	0.50*	—	0.49	0.082	0.00085
						2002	—	0.59	—	0.47		
						2003	85*	0.61*	61	0.57		
3N/7E-32J1	14.5		8.5	4.6	0.9	2000	—	1.52	—	1.31	—	—
3N/7E-28R1	15.2	7700	8.6	6.3	4.0	2000	—	4.38	—	4.18		0.0030
						2002	—	4.07*	—	3.93		
						2003	—	4.29	—	4.09		
2N/7E-3E1	17.0		6.6	4.8	1.5	2002	1960	4.08	1920	3.81	1.4	—
						2003	—	5.7	—	4.9		
2N/7E-3B1	17.2	6500	6.9	2.9	1.9	2000	1760	4.70*	1720	4.50	0.61	0.0024
						2003	—	5.2*	—	4.5		
2N/7E-3A2	17.8	5000	12	1.9	0.9	2000	1190*	3.16	1160	3.16	0.54	0.0021
						2002	—	3.29*	—	3.28		
						2003	—	2.7	—	2.7		
2N/7E-2D1	17.9	6550	6.4	3.4	1.7	2002	770*	2.81*	740	2.65	0.34	0.0015
						2003	980	3.5*	940	3.0		
3N/7E-35P2	18.2	5090	6.8	2.4	1.2	2000	650*	3.02	620	2.32	0.61	0.0026
						2002	580*	2.77*	550	2.51		
						2003	580	3.02	550	2.03		
Mojave River Basin												
4N/7W-33J1	0.5	0	4.8	1.7	1.3	2003	170	0.68	97	0.22	0.17	0.0011
4N/6W-4D1	11.9	5580	8.5	3.4	1.6	2003	214	0.92*	176	0.82	0.081	0.00036
5N/7W-24D3	14.1	19,990	8.8	2.3	1.1	2003	140*	1.13*	101	0.81	0.022	0.00015
5N/5W-18Q1	20.9	11,880	8.1	4.5	1.6	2003	—	0.91	—	0.58	—	—
						2005	—	1.39*	—	0.54		
5N/5W-4A1	26.5	28,500	8.0	1270	210	2003	13,500	0.156	13,400	0.141	3.55	0.00005
						2005	14,500*	0.49*	14,400	0.01		
6N/4W-30N8	31.8	38,500	9.0	4500	690	2003	39,000*	6.73*	39,000	2.5	4.05	0.00017
						2005	31,500*	1.46*	31,500	1.40		
5N/5W-35P2	23.5	16,800	12	11.5	0.26	2003	120	1.13	80	1.08	0.018	0.00049
5N/5W-35J1	24.1	14,890	19	10.6	3.1	2003	118	1.07*	62	1.01	0.013	0.00051
4N/5W-1C1	24.6	12,300	5.4	15	1.6	2003	91*	0.77*	64	0.73	0.026	0.00045

Borehole identification follows the naming protocol of the US Geological Survey (Township/Range–Well ID#) 2002 GC/MS precisions were ±4% for CF$_4$ and ±14% for SF$_6$.

An ''ex'' subscript denotes measured values (X) corrected for addition from contamination, and from air–water equilibration and bubble entrainment during recharge.

Ne$_a$ values are the contribution to neon concentrations from entrapped air bubbles that are partially dissolved during recharge.

Groundwater radiocarbon ages from Izbicki and Michel (2004) and Kulongoski et al. (2003, 2005). Noble gas data from Kulongoski et al. (2003, 2005) 1 nmol He kg^{-1} = 2.3 × 10^{-8} cc He STP g^{-1}

[a] Distance along the studied flowpath(s) from the apparent recharge site (km).

[b] Year in which groundwater samples for CF$_4$ and/or SF$_6$ analyses were collected.

[c] Observation wells were sampled with a portable pump.

[d] Incomplete transfer of extracted gases for GC/MS analysis. CF$_4$ value is a lower limit for this well.

analyzed by GC/MS tend to show higher concentrations for CFC-12 and CFC-11, as well as small amounts (<0.06 pmol kg^{-1} H$_2$O) of CFC-113, indicating slightly higher modern air contributions (0.04 – 0.3 millimoles modern air per kg H$_2$O). Some wells in the EMB contained CFC concentrations that suggest the presence of 0.005 – 0.02 kg modern water per kg sample.

The presence of modern air in our samples probably results from introduction of lab air during analysis, but may also originate as bubble entrainment into samples from leaks in well plumbing. Since no significant local recharge is observed in the Mojave Desert away from mountain-fronts (Izbicki and Michel, 2004), modern water is likely to be residual air-equilibrated water not flushed from the borehole prior to sampling. Contamination present in this study was not necessarily present in previous groundwater samples collected for He and ^{14}C analyses (Izbicki and Michel, 2004; Kulongoski et al., 2003; 2005). CF$_4$ corrections due to contamination are typically in the range of 0 – 10 fmol CF$_4$ kg^{-1} H$_2$O, less than 5% in most cases. SF$_6$ measurements require a more significant correction, typically 0 – 0.5 fmol SF$_6$ kg^{-1} H$_2$O, or 0 – 30% of measured values. However, as shown graphically in Electronic Annex EA-2, the agreement between SF$_6$ measurements by GC/ECD and GC/MS improves significantly after correction for contamination. SF$_6$ concentrations used in the following discussion are error-weighted averages of the GC/ECD and GC/MS measurements where both are available.

Groundwaters collected from observation wells in the EMB (wells 3N/6E-16A1 and 3N/7E-19N1) contain CFC-11 and CFC-113 concentrations in excess of

those expected from air contamination, based on CFC-12 measurements. CFC-11 and CFC-113 concentrations decreased in the order that samples were collected from each well, and also decreased in the order in which boreholes were sampled, with groundwaters from well 3N/7E-19N1 containing less CFC-11 and CFC-113 than from well 3N/6E-16A1. These trends in CFC-11 and CFC-113 concentrations are qualitatively consistent with degassing of CFCs from plastics, with possible sources including nylon pump parts, Teflon tubing attached to the mobile pump, or PVC pipe present in the boreholes (Busenberg and Plummer, 1992; Reynolds et al., 1990). Groundwater samples from wells 3N/6E-16A1 and 3N/7E-19N1 also contain significantly higher SF_6 concentrations than expected for their groundwater ages and proximity to the recharge site for the EMB. In contrast, CF_4 and He concentrations for these wells are attributable almost entirely to addition during recharge, as shown by relatively low excess concentrations and helium isotope ratios of $R/R_a = 1$, where R is the measured $^3He/^4He$ ratio and R_a is the atmospheric $^3He/^4He$ ratio (Kulongoski et al., 2005).

Measured SF_6 concentrations for wells 3N/6E-16A1 and 3N/7E-19N1 in general follow the patterns observed for CFC-11 and CFC-113, with decreasing concentrations in order of sample collection and increased borehole purging. Elevated SF_6 concentrations for these wells are not the result of a modern groundwater contaminant plume, since the transit time between the two wells is on the order of a thousand years (see Table 4.1). Also, groundwaters drawn from wells 3N/6E-16A1 and 3N/7E-19N1 do not contain detectable amounts of tritium (Izbicki

and Michel, 2004), a radioactive isotope of hydrogen with a sufficiently short half-life (12.43 years) that is expected to be present at detectable concentrations only in recently recharged water. It also does not seem likely that elevated SF_6 concentrations for wells 3N/6E-16A1 and 3N/7E-19N1 are the result of natural input to the EMB, since groundwaters drawn from wells in the vicinity of 3N/7E-19N1 (e.g. wells 3N/7E-29F1 and 3N/7E-29R1) contain significantly less SF_6. The source of the elevated SF_6 concentrations for these wells therefore originates from a source external to the groundwater aquifer. The borehole and pump components that release CFC-11 and CFC-113 into groundwaters drawn from these wells are not thought to degas SF_6 (Busenberg and Plummer, 2000), although the significant length of time between flushing of observation wells (on the order of years) may allow a degassing source, which is insignificant on timescales of minutes to hours, to release significant amounts of SF_6 into stagnant borehole waters. Another possibility is that ambient air in the region occasionally had elevated SF_6 mole fractions as a result of emissions from Marine Corps military applications, nearby urban centers (Santella et al., 2003) or high voltage switchboxes or transformers (Maiss and Brenninkmeijer, 1998), so that observation wells which are infrequently flushed would contain stagnant water in equilibrium with time-integrated atmospheric SF_6 mole fractions that are significantly higher than the atmospheric background values.

Either of these sources would have a less significant impact on groundwaters drawn from production wells, which are continuously pumped for water supply. With the exception of well 3N/7E-28D2, we observe good agreement between GC/ECD

and GC/MS contaminant-corrected SF_6 concentrations for groundwater samples drawn from production wells (see Electronic Annex EA-2), confirming the lack of significant borehole SF_6 contamination in collected samples. Groundwater samples collected from EMB well 3N/7E-28D2 contained similar SF_6 concentrations as groundwater drawn from wells 3N/6E-16A1 and 3N/7E-19N1. However, well 3N/7E-28D2 draws water that does not contain detectable amounts of CFCs and that originates in part from the lower geologic unit of the EMB. SF_6 concentrations for this well may therefore be elevated as a result of natural subsurface phenomena, rather than modern contamination.

4.5.2 Air-saturated water and entrained air estimates

The initial dissolved gas concentrations of recharging groundwaters are composed of two components, i) dissolved gases resulting from air-water equilibration at the temperature and elevation of recharge ("air-saturated water", X_{eq}), and ii) dissolved gases resulting from dissolution of trapped air bubbles near the water table during recharge ("entrained air", X_a) (Kipfer et al., 2002). Air-saturated water contributions to measured CF_4 and SF_6 concentrations are calculated using preindustrial atmospheric CF_4 and SF_6 dry-air mole fractions and an estimated temperature and elevation of recharge (Torgersen, 1980). Low preindustrial atmospheric mole fractions and low solubilities lead to relatively small X_{eq} values for CF_4 and SF_6, on the order of 10 fmol CF_4 kg^{-1} H_2O and 0.003 fmol SF_6 kg^{-1} H_2O.

Entrapped-air concentrations of CF_4 and SF_6 are estimated assuming complete dissolution of air bubbles trapped during recharge. The concentration of a dissolved gas resulting from entrapped air (*"X_a"*) can then be estimated from $X_a = Ne_a R_X$ (Kulongoski et al., 2003; 2005), where Ne_a is the neon concentration from entrapped-air (Table 1), and R_x is the ratio of the atmospheric mole fraction of the gas to the atmospheric mole fraction of neon. For Mojave Desert groundwaters, entrapped-air concentrations (*X_a*) of CF_4 and SF_6 are small, and are of similar magnitude to air-saturated water concentrations for these gases (i.e. roughly 10 fmol CF_4 kg^{-1} H_2O and 0.001 fmol SF_6 kg^{-1} H_2O). Previous groundwater studies indicate that entrapped air is generally fractionated with respect to atmospheric air, most likely as a result of only partial dissolution of air bubbles trapped during recharge (Kipfer et al., 2002; Klump et al., 2007). Soluble gases will therefore have a more significant entrapped-air component than insoluble gases. Regardless, unfractionated entrapped-air CF_4 and SF_6 estimates in this study are not significantly different (to within 1% for CF_4 and 0.01% for SF_6, on average) from entrapped-air concentrations that are estimated assuming a degree of entrapped-air fractionation typically observed in groundwaters (Aeschbach-Hertig et al., 2000; Klump et al., 2007).

4.5.3 Excess CF_4 and SF_6 concentrations

The "excess" concentration of a dissolved gas, X_{ex}, is defined as $X - (X_{mod} + X_a + X_{eq})$. A positive X_{ex} indicates the presence of an additional, non-atmospheric source.

CF_{4ex} and SF_{6ex} values are greater than zero for all Mojave Desert groundwater samples, with the exception of wells in close proximity to the recharge sites for the EMB and MRB. Supersaturation of CF_4 and SF_6 with respect to the preindustrial atmosphere suggests that discharge at springs and dry lakes and into the Mojave River has constituted a source of these gases to the preindustrial atmosphere.

4.6 Discussion

4.6.1 Identifying Sources of Lithospheric CF_4 and SF_6 to Mojave Desert Groundwaters

The spatial patterns of excess CF_4 and SF_6 in Mojave Desert groundwaters, as well as their correlations with other dissolved species and groundwater residence times, may be used to identify and characterize subsurface sources of these gases. Loss processes for SF_6 are probably insignificant in Mojave Desert groundwaters, as SF_6 is thought to be insensitive to biodegradation or sorption onto aquifer material (Busenberg and Plummer, 2000; Wilson and Mackay, 1996). CF_4 is chemically inert, and has a similar size, mass and solubility to SF_6, and it is reasonable to assume that CF_4 is insensitive to these loss processes as well. Excess CF_4 and SF_6 concentrations, when plotted versus estimated groundwater radiocarbon age (Fig. 4.2), show different trends for the EMB and the MRB.
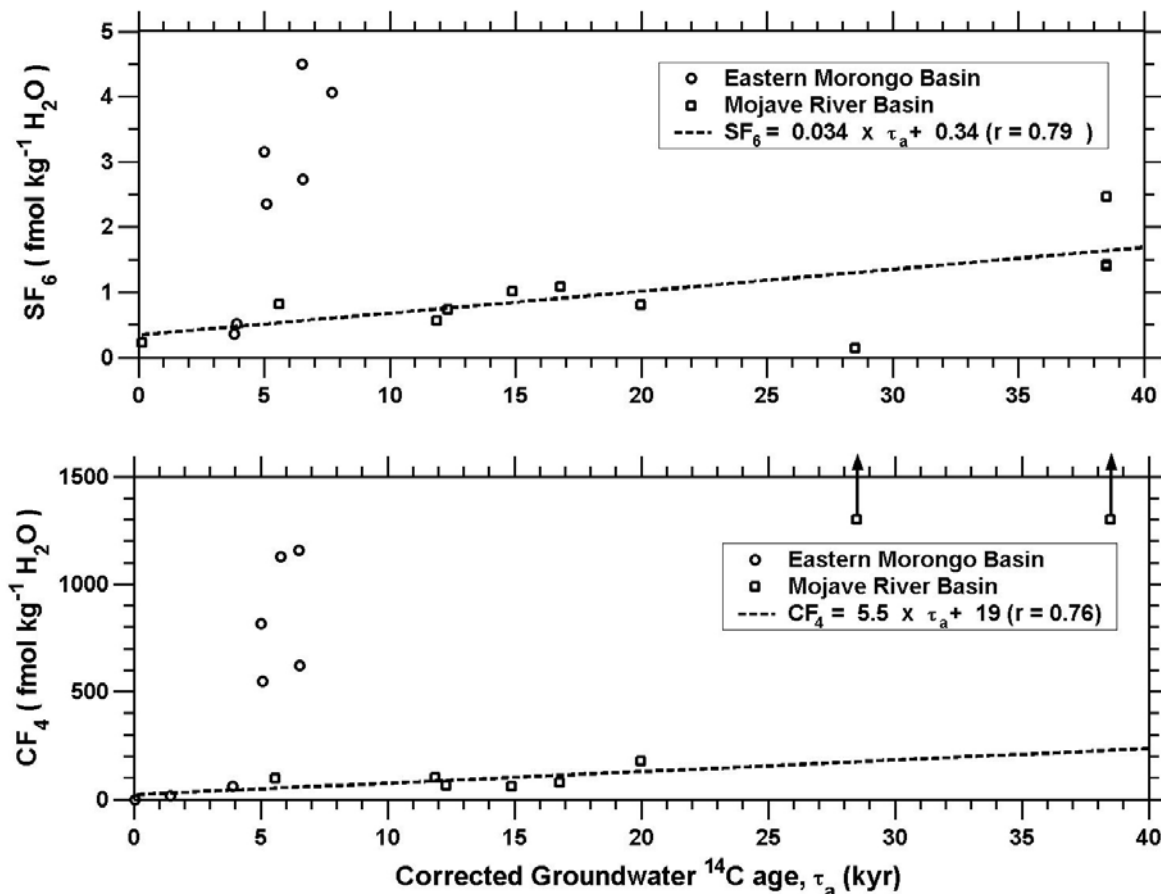
Figure 4.2 "Excess" CF_4 and SF_6 (i.e. concentrations with atmospheric contributions removed) plotted against groundwater ^{14}C ages from Izbicki and Michel (2004) and Kulongoski et al. (2003; 2005). Both gases show a gradual, regional increase with water mass age in the Mojave River Basin. CF_4 results at 28.5 and 38.5 kyr are off-scale at roughly 14 and 31 – 39 pmol kg^{-1} H_2O, respectively. Significant deviations from the observed regional trends are associated with local fault systems (see Fig. 4.3).

In the MRB, CF_4 and SF_6 gradually accumulate with increasing groundwater age, providing evidence for a regional source of CF_4 and SF_6 to the aquifer. Given the similar hydrogeology of the MRB and EMB, we expect a corresponding enrichment of CF_4 and SF_6 in EMB groundwaters with time, but this is not expressed as clearly in EMB groundwater samples. This may be explained by the disruption of groundwater flow by two inactive faults along the EMB flowpath (Fig. 4.3).
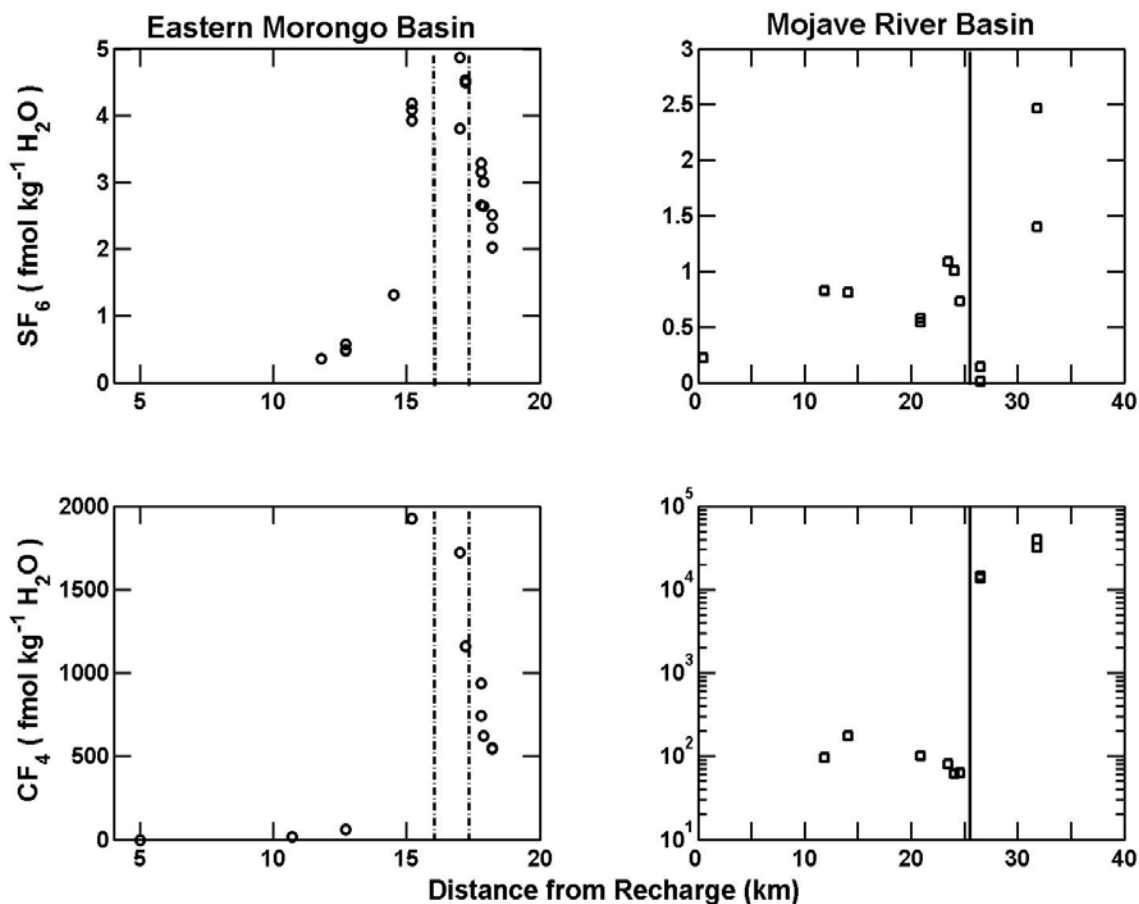
Figure 4.3 "Excess" CF_4 and SF_6 (i.e. concentrations with atmospheric contributions removed) plotted against approximate distance from the recharge sites for the Eastern Morongo Basin (EMB) and Mojave River Basin (MRB). Vertical lines denote the approximate distance where two inferred faults (dashed lines) and the Shadow Mountain fault (solid line) transect the study flowpaths in the EMB and MRB, respectively. Large changes in CF_4 in the proximity of faults in both basins and in SF_6 for the EMB are shown.

A fault transecting the MRB also appears to influence CF_4 concentrations, with waters sampled down-flow of the Shadow Mountain fault in the MRB containing elevated CF_4 concentrations, in excess of those expected solely from the observed regional input. Interestingly, SF_6 concentrations down-flow of the Shadow Mountain

fault do not appear to be enhanced in a similar manner to CF_4 concentrations in this region.

Harnisch and Eisenhauer (1998) proposed that lithospheric CF_4 and SF_6 are released to the atmosphere by weathering of fluorite minerals present in the continental crust. Since large fluorite veins are not found in the study region (Wright et al., 1953), the probable source of lithospheric CF_4 and SF_6 to Mojave Desert groundwaters is accessory fluorites contained in granitic rock. Another common fluorine-rich mineral in Mojave Desert alluvium is apatite (J. Izbicki, personal communication), but its CF_4 and SF_6 contents are currently unknown. The molar CF_4/SF_6 source ratio for the regional increases in CF_4 and SF_6 is 150 ± 60, as derived from the increase in CF_4 and SF_6 concentrations with increasing groundwater age (Fig. 4.2). This is consistent with the range of $10 - 150$ for molar CF_4/SF_6 ratios measured in fluids extracted from granitic rocks (Harnisch and Eisenhauer, 1998; Harnisch et al., 2000).

4.6.1.1 Diffusive loss of CF_4 and SF_6 from Mojave Desert alluvium

Potential release mechanisms for CF_4 and SF_6 trapped in granitic rock include diffusive loss, release during mineral breakdown/alteration, and a crustal flux through the underlying basement (Ballentine and Burnard, 2002; Kulongoski et al., 2003; 2005). The diffusivities of CF_4 and SF_6 in granite under the conditions of the upper continental crust (T<150°C) are unknown. Kinetic theory predicts that the ratio of the diffusivities of two gases will be proportional to the ratios of the inverse-square-roots

of their molecular masses and inverse-squared atomic/molecular radii (Bird et al., 1960). The diffusivities of CF_4 and SF_6 can be estimated by analogy to gases whose crustal diffusivities have previously been studied. For example, the upper limit for the diffusivity of Ar under upper crustal conditions is less than 10^{-25} cm^2 sec^{-1} (McDougall and Harrison, 1988). Using their respective masses of 40, 88 and 146 g mol^{-1} and atomic/molecular radii of 1.9 Å, 2.33 Å and 2.55 Å for Ar, CF_4 and SF_6, respectively (Birnbaum and Cohen, 1976; Ozima and Podosek, 1983; Wilson and Mackay, 1996), the diffusivities of CF_4 and SF_6 in the upper crust are estimated to be $<4 \times 10^{-26}$ cm^2 sec^{-1} and $<3 \times 10^{-26}$ cm^2 sec^{-1}, respectively. The fraction of a gas lost from a spherical grain due to diffusive loss can then be estimated from:

$$F_L = \frac{6}{\pi^2}\left[\frac{\left(\pi^2 Dt\right)}{a^2}\right]^{\frac{1}{2}} - \frac{3}{\pi^2}\left[\frac{\left(\pi^2 Dt\right)}{a^2}\right] \tag{4.1}$$

where D is the diffusivity of the gas, t is time, and a is the effective grain size (Musset 1969). For coarse sand (a ≈ 0.75 mm), the age of Mojave Desert deposits (t < 7Myr), and the estimated diffusivities for CF_4 and SF_6, F_L is <0.008 percent for CF_4 and <0.006 percent for SF_6. We calculate average CF_4 and SF_6 mass contents for granitic rock of 40 ppt and 7 ppt from the combined data sets of Harnisch and Eisenhauer (1998) and Harnisch et al. (2000). The fraction of CF_4 and SF_6 lost from 7 Myr old Mojave Desert deposits should then be less than 36 fmol CF_4 kg^{-1} granite and less than 2.9 fmol SF_6 kg^{-1} granite. Assuming a porosity of 0.2 − 0.3 for Mojave Desert

deposits and a density of 2.8 kg/L for the granitic deposits (Kulongoski et al., 2003; 2005), these fluxes would result in an ubiquitous increase in Mojave Desert groundwaters of <0.07 fmol CF_4 kg^{-1} H_2O kyr^{-1} and <0.006 fmol SF_6 kg^{-1} H_2O kyr^{-1}. Diffusive release of CF_4 and SF_6 from the aquifer material is therefore expected to be significantly smaller than the observed input of these gases to the MRB, and another source of these gases is needed to account for their observed regional enhancement in Mojave Desert groundwaters.

4.6.1.2 Release of CF_4 and SF_6 from weathering of Mojave Desert alluvium

Izbicki and Michel (2004) estimate a weathering rate for granitic alluvium in the MRB of 0.005 - 0.01 g rock kg^{-1} H_2O kyr^{-1}. Assuming an average CF_4 content of 40 ppt by mass for granites (Harnisch and Eisenhauer, 1998; Harnisch et al., 2000), the release rate of CF_4 expected to be associated with weathering of Mojave Desert deposits would be 2.3 – 4.5 fmol CF_4 kg^{-1} H_2O kyr^{-1}, which is of similar magnitude to the regional increase rate observed in the MRB, 5.5 (± 1) fmol CF_4 kg^{-1} H_2O kyr^{-1}. From the combined data sets of Harnisch and Eisenhauer (1998) and Harnisch et al. (2000) we calculate an average CF_4/SF_6 molar ratio of 56 for granite samples where both gases were above detection limits. The expected weathering input of SF_6 would then be 0.04 – 0.08 fmol SF_6 kg^{-1} H_2O kyr^{-1}, which is on average larger, but still consistent with the observed regional increase in SF_6 in the MRB, 0.034 (± 0.01) fmol SF_6 kg^{-1} H_2O kyr^{-1}. The estimated weathering flux may indeed be larger than the actual weathering flux, given that 10 out of 17 granite samples analyzed by Harnisch

and coauthors had SF_6 contents below their detection limit. Regardless, the general agreement between observed regional CF_4 and SF_6 enrichment rates and CF_4 and SF_6 release estimates based on chemical modeling of water-rock interactions suggest that weathering of granitic rock is a significant mechanism for release of lithospheric CF_4 and SF_6 into Mojave Desert groundwaters.

Another possible source for lithospheric CF_4 and SF_6 is carbonate sediments, since the majority (>75%) of fluorine-bearing minerals in carbonate sediments are fluorite (Koritnig, 1951), and since previous measurements in groundwaters drawn from carbonate aquifers have shown elevated dissolved SF_6 concentrations (Busenberg and Plummer, 2000). However, the carbonate content of Mojave Desert deposits in the study area is low (Izbicki and Michel, 2004), and saturation indices calculated for carbonate in studied groundwaters are positive, indicating that precipitation, not dissolution, of carbonates in Mojave Desert groundwaters is favored (Izbicki and Michel, 2004). It therefore seems unlikely that weathering of carbonates is a significant source of CF_4 and SF_6 to groundwaters in this study.

4.6.1.3 Basal fluxes of CF_4 and SF_6 into study aquifers

It is also possible that the observed CF_4 and SF_6 concentrations in the Mojave Desert are in part attributable to a diffusive and/or advective crustal flux of these gases entering the aquifer through the underlying basement. In analogy to the release

of helium from the continental crust, the relationship between groundwater age and excess CF_4 or SF_6 should be (from Stute et al., 1992):

$$\tau = \frac{X_{ex}}{\dfrac{J_0}{\phi z_0 \rho} + W} \tag{4.2}$$

where τ is the groundwater age (in years), J_0 is the crustal flux entering the aquifer from depth (in fmol X cm^{-2} yr^{-1}), ϕ is the effective aquifer porosity, z_0 is the depth (in meters) at which the crustal flux enters the aquifer, ρ is the density of water, and W is the "in situ" (i.e. weathering) release rate of X (in fmol X kg^{-1} H$_2$O yr^{-1}). Values of z_0 are calculated as the distance between the midpoint of borehole perforations and the contact with the basement (Kulongoski et al., 2003; 2005). For CF_4, we use the weathering release rate estimated from the chemical modeling work of Izbicki and Michel (2004), W_{CF_4} = 2.3 – 4.5 fmol CF_4 kg^{-1} H$_2$O kyr^{-1}. Using groundwater radiocarbon ages, crustal CF_4 fluxes for each study region can then be estimated from Equation 4.2. The results are presented in Table 4.1 and are displayed in Fig. 4.4.

The smallest crustal fluxes of CF_4 (J_{CF_4}) observed in this study are associated with MRB groundwaters up-flow of the Shadow Mountain fault and with young groundwaters in the EMB (0.01 – 0.2 fmol CF_4 cm^{-2} yr^{-1}), with an average crustal CF_4 flux of 0.07 fmol CF_4 cm^{-2} yr^{-1}. This is consistent with the interpretation of the helium basal flux in the MRB (Kulongoski et al., 2003) and elsewhere (Stute et al.,

1992; Torgersen and Clarke, 1985), which suggests that relatively young groundwaters are dominated by in situ production/release.
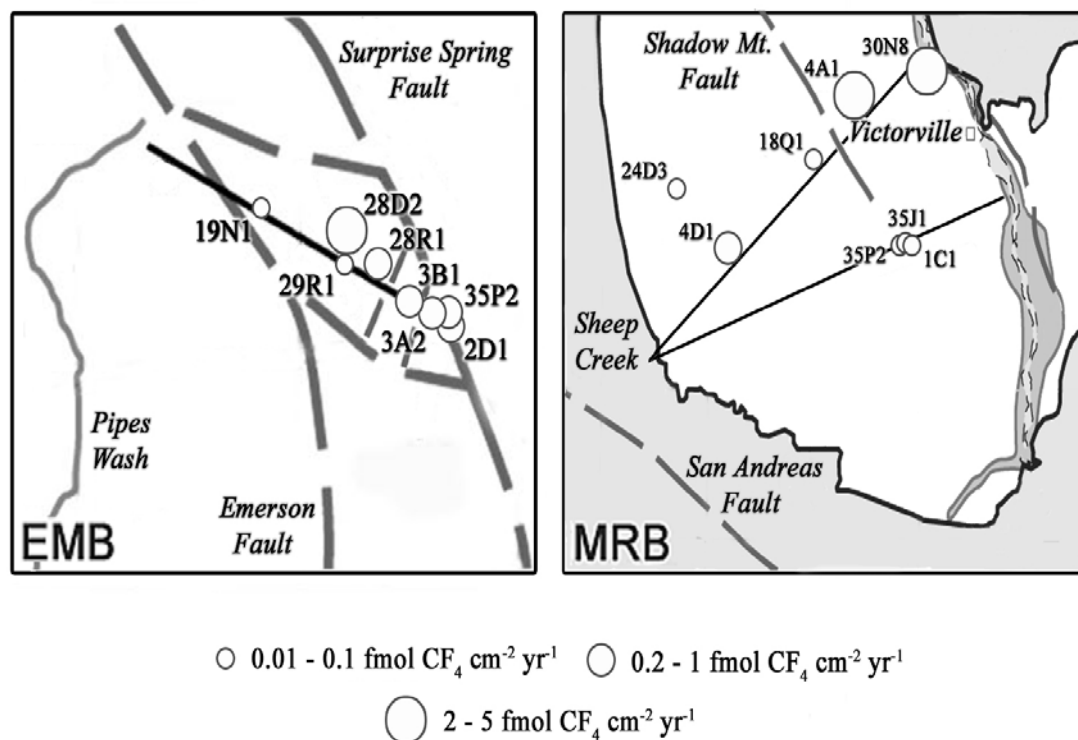
Figure 4.4 The estimated flux of CF_4 entering the Eastern Morongo Basin (EMB) and Mojave River Basin (MRB) through the underlying crystalline basement. The concentrations of CF_4 in young EMB groundwaters and MRB groundwaters located up-flow of the Shadow Mountain are dominated by in situ releases associated with granitic weathering, with relatively small estimated crustal CF_4 input. A more significant crustal CF_4 flux is observed in the southeast region of the EMB study area, where the shoaling basement results in groundwater being drawn from closer proximity to the basal CF_4 flux. An enhanced CF_4 crustal flux down-flow of the Shadow Mountain fault is associated with fluids advecting vertically through the fault.

The average crustal CF_4 flux observed in older EMB groundwaters is roughly an order of magnitude higher, 0.7 fmol CF_4 cm^{-2} yr^{-1}, with crustal CF_4 fluxes in individual wells ranging between 0.3 and 1 fmol CF_4 cm^{-2} yr^{-1}. Basal helium fluxes observed in older waters in the Surprise Spring sub-Basin (SSB) of the EMB are also

roughly an order of magnitude higher than MRB crustal fluxes (Kulongoski et al., 2005). Groundwaters in the EMB may contain a greater proportion of CF_4 from a basal flux because the basement shoals in the southeast of the SSB (see Fig. 2 in Kulongoski et al., 2005), driving deep groundwater toward the surface. Restriction of horizontal fluid-flow across inactive faults internal to the SSB results in pooling of groundwater up-flow of the faults, which also contributes to the mixing of older, deep groundwaters from the lower geologic unit with groundwaters from the upper geologic unit.

Groundwaters drawn from wells down-flow of the Shadow Mountain fault show a crustal flux almost two orders of magnitude higher than other MRB groundwaters (roughly 4 fmol CF_4 cm^{-2} yr^{-1}). Kulongoski et al. (2003) also observed a two order of magnitude enhancement in the crustal helium flux down-flow of the Shadow Mountain fault. Implications of this enhanced crustal CF_4 flux associated with the Shadow Mountain fault are discussed in the following section. The consistency between crustal helium and CF_4 fluxes indicates that a basal flux of CF_4, when combined with in situ release of CF_4 from weathering of granites, is sufficient to satisfy the magnitude and variability of observed dissolved CF_4 concentrations in Mojave Desert groundwaters.

Equation 4.2 cannot be used directly to estimate crustal SF_6 fluxes into the MRB and EMB, since the SF_6 weathering flux estimated from the SF_6 content of granites (Harnisch and Eisenhauer, 1998; Harnisch et al., 2000) and the chemical modeling work of Izbicki and Michel (2004) overestimates the weathering input into

Mojave Desert groundwaters due to its bias toward high SF_6 content in granites (i.e.

granites with SF_6 above detection limits). Since Mojave Desert alluvium is derived

from nearby mountains with similar lithology to the underlying basement, we can

assume that the CF_4/SF_6 molar weathering ratio is equal to the molar crustal flux ratio

(i.e. $W_{CF_4}/W_{SF_6} = J_{CF_4}/J_{SF_6}$). Rearranging this equation and substituting into

Equation 4.2 to replace W_{SF_6} results in an equation that can be solved for J_{SF_6} using

groundwater radiocarbon ages (τ), calculated excess SF_6 concentrations (SF_{6ex}), CF_4

weathering release rates (W_{CF_4}) calculated from the modeling work of Izbicki and

Michel (2004), and crustal CF_4 fluxes (J_{CF_4}) calculated from Equation 4.2:

$$J_{SF_6} = \frac{\dfrac{SF_{6ex}}{\tau}}{\left(\dfrac{1}{\phi z_0 \rho} + \dfrac{W_{CF_4}}{J_{CF_4}}\right)} \qquad \textbf{(4.3)}$$

The aquifer porosity (φ), density of water (ρ) and depth-to-basement (z_0)

values are the same as those used in Equation 4.2. Once crustal fluxes of J_{SF_6} are

calculated from Equation 4.3, the weathering release rate of SF_6 can be calculated

from $W_{SF_6} = \left(W_{CF_4} \times J_{SF_6}\right)/J_{CF_4}$. Values of W_{SF_6} for the EMB and MRB groundwaters

range from $0.01 - 0.02$ fmol SF_6 kg^{-1} H$_2$O kyr^{-1}, on average slightly less than half the

total observed regional increase in SF_6 with groundwater age.
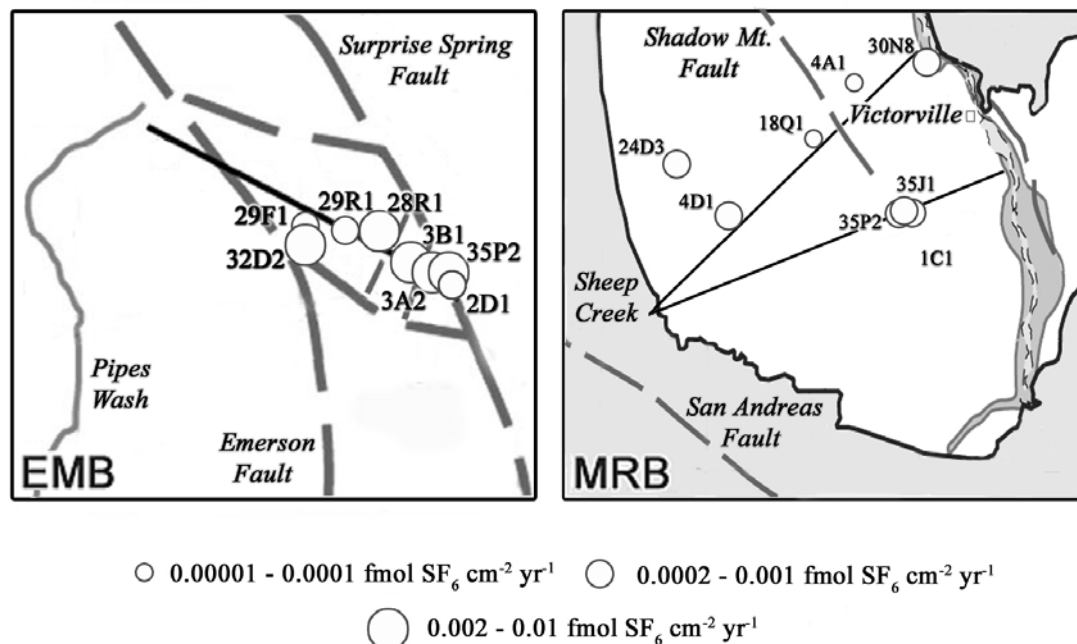
Figure 4.5 The estimated flux of SF_6 entering the Eastern Morongo Basin (EMB) and Mojave River Basin (MRB) through the underlying crystalline basement. The concentrations of SF_6 in young EMB groundwaters and MRB groundwaters located up-flow of the Shadow Mountain are dominated by in situ releases associated with granitic weathering, with relatively small estimated crustal SF_6 input. A more significant crustal SF_6 flux is observed in the southeast region of the EMB study area, where the shoaling basement results in groundwater being drawn from closer to the basal SF_6 flux. In contrast to CF_4 (Figure 4.4), the crustal SF_6 flux is not enhanced down-flow of the Shadow Mountain fault.

For most Mojave Desert groundwaters, average crustal SF_6 flux estimates derived from groundwater radiocarbon ages show similar regional variability as the corresponding crustal fluxes of CF_4 and He (Figure 4.5). The crustal SF_6 flux for groundwaters in the MRB and young groundwaters in the EMB is small ($0.0002 - 0.001$ fmol SF_6 cm^{-2} yr^{-1}), with an average crustal SF_6 flux of 0.0006 fmol SF_6 cm^{-2} yr^{-1}. Older groundwaters in the EMB show an average crustal SF_6 flux of 0.002 fmol SF_6 cm^{-2} yr^{-1}, with a range of $0.001 - 0.003$ fmol SF_6 cm^{-2} yr^{-1}. In contrast to crustal

CF_4 and He fluxes, the crustal SF_6 flux does not increase across the Shadow Mountain fault.

4.6.2 Tectonic influences on dissolved CF_4 and SF_6 in Mojave Desert groundwaters

In order to explain large increases in ^{3}He and ^{4}He concentrations down-flow of active faults in the southern Mojave, Kulongoski et al. (2003; 2005) suggest that faulting associated with extensional tectonics allows for the upward transport of mantle volatiles through the continental crust. In this scenario, faults in the Mojave Desert either directly tap mantle volatiles by penetrating completely through the thinned crust, or indirectly collect mantle fluids through a connection to a mid-crustal décollement (Kulongoski et al., 2005). Episodic hydrofracturing events associated with tectonic activity along these faults increase local permeability, facilitating the upward movement of fluids and volatiles (Nur and Walder, 1990; Torgersen and O'Donnell, 1991). These fracturing events also release ^{4}He-rich fluids from the nearby crust, which are then entrained into the rising mantle fluids (Torgersen and O'Donnell, 1991; Kulongoski et al., 2005). CF_4 concentrations support the assertion that hydrofracture associated with tectonic activity controls transport of fluids and volatiles into Mojave Desert groundwaters, as CF_4 concentrations rise dramatically down-flow of an active fault in the study region (the Shadow Mountain fault) but show no corresponding change down-flow of 2 inactive faults in the EMB.

There are two possible sources for the elevated CF_4 concentrations that we observe down-flow of active faults in the Mojave Desert: mantle fluids transported through the fault, or crustal fluids that are released by episodic fracturing events and entrained into the rising mantle fluid. To help identify this source, we analyzed several samples for CF_4 that were collected from two hot springs in Yellowstone National Park, which had $^3He/^4He$ isotope ratios ~16 times atmospheric (Craig et al., 1978). CF_4 was consistently below detection limit. These springs (Black Dragon's Cauldron and Sizzling Basin) best represent a pure mantle source of helium in Yellowstone National Park (R. Poreda, personal communication). That CF_4 was not detected in these samples, or in previously collected volcanic gases (Frische et al., 2006; Jordan et al., 2000), provides evidence against a mantle source of CF_4. Therefore, crustal fluids released during tectonic fracture events are the most likely source of lithospheric CF_4 to groundwaters collected down-flow of the Shadow Mountain fault.

Given that CF_4 and SF_6 in other regions of the Mojave Desert appeared to be derived from a mutual granitic source, we would expect a correspondingly enhanced crustal SF_6 flux through the Shadow Mountain fault. However, SF_6 concentrations down-flow of the Shadow Mountain fault require a crustal SF_6 flux of similar magnitude to groundwaters in other areas of the MRB (see Fig. 4.5 or section 4.6.1.3). Diffusive fractionation associated with degassing during hydrofracture events should be small, given the similar expected diffusivities of CF_4 and SF_6 in granite (see Section 4.6.1.1). We propose two possible explanations for the lack of SF_6 in fault

fluids rising through the Shadow Mountain fault. As we mentioned previously, SF_6 is not always present above detection limits in granite samples where CF_4 is detectable, and the source rock for CF_4 in upwelling fault fluids may be relatively poor in SF_6 with respect to the granitic alluvium and directly underlying basement. Alternatively, SF_6 in fault fluids may be removed through thermal decomposition, as SF_6 has been observed to decompose in the presence of alkali metals at temperatures as low as 200˚C and in the presence of quartz at temperatures $\geq$700˚C (Padma and Vasudeva Murthy, 1975), while CF_4 is effectively inert up to temperatures of around 2000˚C (Gaßman, 1974). With a typical geothermal gradient in southern California being between 25 – 35 ˚C per km depth (Wright, 1991), a temperature of 200 - 700˚C would correspond to depths of 5 – 27 km (i.e. depths ranging the thickness of the underlying crust (Kohler and Davis, 1997)). Depending on the extent to which faults in the Mojave Desert penetrate the crust, it may be possible that SF_6 is thermally destroyed in upwelling fluids before they encounter MRB groundwaters.

4.6.3 Atmospheric Implications

For a steady-state atmosphere, the lifetime of a gas, τ, will equal the ratio between M, the amount of trace gas present in the atmosphere, and P, the rate at which it enters into or is produced in the atmosphere. The ratio of lifetimes for two

gases, rearranged to solve for the input ratio, P_x/P_y, gives:

$$\frac{P_X}{P_Y} = \frac{M_X \tau_Y}{M_Y \tau_X}$$

(4.4)

For preindustrial atmospheric mole fractions of <6.4 ppq SF_6 and 34 ± 1 ppt CF_4, and lifetimes in the range of $0.8 - 3.2$ kyr for SF_6 and $110 - 1700$ kyr for CF_4, Equation 4.4 gives a range of potential SF_6/CF_4 molar input ratios of $0 - 0.4$. Our observed input ratio of SF_6 to CF_4 in Mojave Desert groundwaters $(1/(150 \pm 60) = 0.007 \pm 0.003 \ \text{mol} \ SF_6 \ \text{mol}^{-1} \ CF_4)$ is therefore consistent with the input ratio required to maintain the preindustrial atmospheric ratio of these gases. The ratio of SF_6 to CF_4 increase in Mojave Desert groundwater thus provides evidence of a connection between lithospheric CF_4 and SF_6 present in granitic rocks and the preindustrial atmospheric abundances of these gases.

Due to the local nature of this study, it is not clear whether CF_4 and SF_6 enrichments observed in Mojave Desert groundwaters are representative of their global lithospheric fluxes. Nevertheless, we estimate global lithospheric CF_4 and SF_6 fluxes based on these results to illustrate the potential influence crustal degassing mechanisms may have on the preindustrial atmospheric abundances of CF_4 and SF_6.

4.6.3.1 Release by Weathering

There is no a priori reason to assume that the weathering rate of granitic deposits in the Mojave Desert reflects the global average weathering of granitic rock. A weathering estimate from the Mojave Desert would likely underestimate weathering rates for granites at the Earth's surface, since surficial weathering of rock typically occurs at a faster rate than groundwater-rock interaction (Berner and Berner, 1996). It is probably more reasonable to adopt the global CF_4 and SF_6 weathering flux estimates of Harnisch and Eisenhauer (1998), $100 - 1000$ kg yr^{-1} and $6 - 60$ kg yr^{-1}, respectively, which are based on total loss of crustal material and rely on data from a wider spatial sampling of the crust. However, Harnisch and Eisenhauer (1998) assumed that the removal rate of granitic material from the continental crust is the same as that for the entire crust, which may overestimate the resulting CF_4 and SF_6 fluxes because granitic rocks are especially resistant to weathering processes (Meybeck, 1987; Amiotte-Suchet et al., 2003).

4.6.3.2 Crustal flux of CF$_4$ and SF$_6$

Noble gas geochemical studies indicate that crustal degassing is controlled by regional tectonic events, such as orogeny and crustal extension (Ballentine and Burnard, 2002). To maintain a steady-state atmospheric helium abundance, the crustal degassing of ^{4}He must be roughly equivalent to its radiogenic production from crustal U- and Th-series nuclides (Torgersen, 1989; Torgersen and Clarke, 1985). The

relation between average crustal CF_4, SF_6 and ^4He fluxes in the Mojave Desert, a region of active crustal extension, might therefore be used to estimate a degassing flux of CF_4 and SF_6 from the crust.

^4He degassing estimates for the whole crust (e.g., O'Nions and Oxburgh, 1983) include U- and Th-containing rocks that may not contain significant CF_4 or SF_6 (Busenberg and Plummer, 2000; Harnisch and Eisenhauer, 1998; Harnisch et al., 2000). Assuming that the degassing rate of ^4He from granitic rocks is equivalent to its radiogenic production rate, an estimated mass of known CF_4-containing granitic rocks (i.e. granites, granodiorites and gneisses) in the continental crust of 7.34×10^{24} g (Ronov and Yaroshevsky, 1969), and average U and Th contents in granitic rock of 4.0 ppm and 15 ppm, respectively (Li, 2000), we calculate a global ^4He production rate (Ballentine and Burnard, 2002) of 3.0×10^8 mol per year from these rock types. Average $CF_4/^4He$ molar crustal flux ratios for the Mojave Desert range from 3×10^{-5} to 1.5×10^{-4}, while average $SF_6/^4He$ molar crustal flux ratios range from 1.5×10^{-7} to 4.5×10^{-7}. From these ratios we calculate ranges of tectonically driven global crustal CF_4 and SF_6 degassing rates of $800 - 4\,000$ kg yr^{-1} and $7 - 20$ kg yr^{-1}, respectively. These are of comparable magnitude to the weathering release rates of $100 - 1000$ kg CF_4 yr^{-1} and $6 - 60$ kg SF_6 yr^{-1} estimated by Harnisch and Eisenhauer (1998).

Combining the crustal flux estimates with the estimated weathering flux of Harnisch and Eisenhauer (1998) results in a total lithospheric CF_4 and SF_6 flux to the atmosphere of $(0.9 - 5) \times 10^3$ kg CF_4 yr^{-1} and $13 - 80$ kg SF_6 yr^{-1}. For a CF_4 source of $(0.9 - 5) \times 10^3$ kg CF_4 yr^{-1} to sustain a steady-state preindustrial atmospheric CF_4

abundance of 34 ± 1 ppt CF_4, the preindustrial atmospheric CF_4 lifetime would need to be between $100 - 620$ kyr. Though our flux extrapolation has large uncertainties due to limited geographic sampling and broad assumptions regarding global $CF_4/^4He$ flux ratios, the range of CF_4 lifetimes we obtain is nevertheless in good agreement with the range of $110 - 1700$ kyr for the preindustrial atmospheric CF_4 lifetime, based on its expected atmospheric loss processes (Morris et al., 1995; Ravishankara et al., 1993).

Since the atmospheric lifetime of SF_6 is relatively well known, the total lithospheric SF_6 release rate may instead be used to estimate the preindustrial atmospheric SF_6 abundance. A crustal degassing flux of $13 - 80$ kg SF_6 yr^{-1} would sustain an atmospheric abundance of $0.40 - 9.8$ ppq, assuming an estimated atmospheric SF_6 lifetime in the range of $800 - 3200$ years. This range is consistent with the upper limit of 6.4 ppq SF_6 for the preindustrial atmosphere measured by Vollmer and Weiss (2000).

Though global lithospheric CF_4 and SF_6 flux estimates presented in this study are based on a small region of the continental crust, they agree well with global source strength estimates based on atmospheric lifetime (Morris et al., 1995; Ravishankara et al., 1993) and preindustrial atmospheric abundance (Harnisch et al., 1996a; Vollmer and Weiss, 2000) constraints. These estimates could be strengthened by further work on continental groundwaters, particularly in other areas of crustal extension, as well as in carbonate aquifers and groundwaters where SF_6 concentrations have been found to be significantly enhanced over air-water equilibrium concentrations (Busenberg and

Plummer, 2000). Although Harnisch and coauthors did not find detectable amounts of CF_4 and SF_6 in basaltic rocks (Harnisch and Eisenhauer, 1998; Harnisch et al., 2000), it would also be helpful to test for lithospheric CF_4 and SF_6 fluxes from oceanic crust and sediments, or from hydrothermal sources such as mid-ocean ridges. A study of CF_4/He and SF_6/He molar ratios in the fluid inclusions of granitic rocks could test the assumption of constant molar ratios inherent in our crustal flux estimates. Clearly, more work is needed to improve our understanding of the natural geochemistries of CF_4 and SF_6.

4.7 Conclusion

Nearly all the groundwaters collected in this study contain dissolved CF_4 and SF_6 in excess of the concentrations expected from atmospheric solubility at their recharge conditions, providing evidence for a lithospheric source of perfluorinated gases. Groundwaters from the Mojave River Basin show a regional enhancement in dissolved CF_4 and SF_6 concentrations with increasing water mass age, which is consistent with the release of these gases during weathering of the surrounding granitic alluvium. The variability and magnitude of measured excess CF_4 and SF_6 concentrations also require a contribution from a crustal flux of CF_4 and SF_6 that enters the Mojave River Basin and nearby Eastern Morongo Basin through the underlying crystalline basement. Groundwaters sampled down-flow of the Shadow Mountain fault in the Mojave River Basin also contain an enhanced crustal flux

expeditions to the Mojave Desert, I was responsible for the GC/MS measurements of dissolved CF_4, SF_6 and chlorofluorocarbon concentrations in collected groundwaters, I was responsible for interpretation of the resulting halogenated gas data, and I was responsible for the preparation and revision of this manuscript.

4.9 References

Aeschbach-Hertig W., Peeters F., Beyerle U. and Kipfer R. (2000) Palaeotemperature reconstruction from noble gases in ground water taking in to account equilibration with entrapped air, *Nature* **405**, 1040-1044.

Amiotte-Suchet P., Probst J.-L. and Ludwig W. (2003) Worldwide distribution of continental rock lithology : Implications for the atmospheric/soil CO_2 uptake by continental rock weathering and alkalinity river transport to the oceans, *Global Biogeochem. Cycles,* 1038*,* doi:10.1029/2002GB001891.

Ashton J. T., Dawe R. A., Miller K. W., Smith E. B. and Sticking B. J. (1968) Solubility of certain gaseous fluorine compounds in water. *J. Chem. Soc. A* **8**, 1793-1796.

Ballentine C.J. and Burnard P. (2002) Production of noble gases in the continental crust. In *Noble gases in geochemistry and cosmochemistry*, vol. 47 (eds. D. Porcelli, C. J. Ballentine and R. Wieler), Mineral. Soc. Am., Washington D. C. pp. 481-538.

Berner E. K. and Berner R. A. (1996), *Global Environment: Water, Air and Geochemical Cycles*, Prentice Hall, New Jersey. pp. 3, 164.

Bird R. B., Stewart W. E. and Lightfoot E. N. (1960) *Transport Phenomena*, John Wiley & Sons, NY, pp. 510-513.

Birnbaum G. and Cohen R. (1976) Determination of molecular multipole moments and potential function parameters of nonpolar molecules from far infrared-spectra. *Mol. Phys.* **32**, 161-167.

Bullister J. (1984) Atmospheric Chlorofluorocarbons as Tracers of Ocean Circulation and Mixing: Measurement and Calibration Techniques and Studies in the

Greenland and Norwegian Seas, PhD Thesis, University of California, San Diego, pp. 61-64.

Busenberg E. and Plummer L. N. (1992) Use of chlorofluorocarbons (CCl$_3$F and CCl$_2$F$_2$) as hydrologic tracers and age-dating tools: The alluvium and terrace system of central Oklahoma, *Water Resour. Res.* **28**, 2257-2283.

Busenberg E. and Plummer L. N. (2000) Dating young groundwater with sulfur hexafluoride: natural and anthropogenic sources of sulfur hexafluoride. *Water Resour. Res.* **36**, 3011-3030.

Butler J. H., Battle M., Bender M., Montzka S. A., Clarke A. D., Saltzman E. S., Sucher C., Severinghaus J., and Elkins J. W. (1999), A twentieth century record of atmospheric halocarbons in polar firn air, *Nature* **399**, 749-765.

California Department of Water Resources (1967) Mojave River groundwater basin investigation. *Bull. Calif. Dept. Water Res.* **84**.

Craig H., Lupton J. E., Welhan J. A. and Poreda R. (1978) Helium isotope ratios in Yellowstone and Lassen Park volcanic gases. *Geophys. Res. Lett.* **5**, 897-900.

Engstrom W. N. (1981) Quantitative geomorphology of some desert mountain drainage basins. *Z. Geomorphol. N. F.* **25**, 383-390.

Frische M., Garofalo K., Hansteen T. H., Borchers R. And Harnisch J. (2006) The origin of stable halogenated compounds in volcanic gases, *Environ. Sci. Pollution Res.* **13**, 406-413.

Gaßman M. (1974) Freon 14 im "Krypton reinst" und in der Atmosphäre, *Naturwissenschaften* **61**, 127.

Harnisch J., Borchers R., Fabian P., Gäggeler H. W. and Schotterer U. (1996a) Effect of natural tetrafluoromethane. *Nature* **384**, 32.

Harnisch J., Borchers R., Fabian P. and Maiss M. (1996b) Tropospheric trends for CF$_4$ and C$_2$F$_6$ since 1982 from SF$_6$ dated stratospheric air. *Geophys. Res. Lett.* **23**, 1099-1102.

Harnisch J. and Eisenhauer A. (1998) Natural CF$_4$ and SF$_6$ on Earth. *Geophys. Res. Lett.* **25**, 2401-2404.

Harnisch J., Frische M., Borchers R., Eisenhauer A. and Jordan A. (2000) Natural fluorinated organics in fluorite and rocks. *Geophys. Res. Lett.* **27**, 1883-1886.

Izbicki J. A., Radyk J. and Michel R. L. (2000) Water movement through a thick unsaturated zone underlying an intermittent stream in the western Mojave Desert, southern California, USA. *J. Hydrol.* **238**, 194-217.

Izbicki J. A. and Michel R. L. (2004) Movement and age of ground water in the western part of the Mojave Desert, southern California, USA. USGS Water-Resources Investigations Report 03-4314.

Jordan A., Harnisch J., Borchers R., Le Guern F. and Shinohara H. (2000) Volcanogenic halocarbons, *Environ. Sci. Technol.* **34**, 1122-1124.

Kipfer R., Aeschbach-Hertig W., Peeters F. and Stute M. (2002) Noble Gases in Lakes and Groundwaters. In *Noble gases in geochemistry and cosmochemistry*, vol. 47 (eds. D. Porcelli, C. J. Ballentine and R. Wieler), Mineral. Soc. Am., Washington D. C. pp. 615-700.

Klump S., Tomonaga Y., Kienzler P., Kinzelbach W., Baumann T., Imboden D. I. and Kipfer R. (2007) Field experiments yield new insights into gas exchange and excess air formation in natural porous media, *Geochim. Cosmochim. Acta* **71**, 1385-1397.

Kohler, M. D. and Davis P. M. (1997) Crustal thickness variations in Southern California from Los Angeles Region Seismic Experiment passive phase teleseismic travel times, *Bull. Seis. Soc. Am.* **87**, 1330-1344.

Koritnig S. (1951) Ein Beitrag zur Geochemie des Fluor. *Geochim. Cosmochim. Acta* **1**, 89-116.

Kulongoski J. T., Hilton D. R. and Izbicki J.A. (2003) Helium isotope studies in the Mojave Desert, California: implications for groundwater chronology and regional seismicity. *Chem. Geol.* **202**, 95-113.

Kulongoski J. T., Hilton D. R. and Izbicki J. A. (2005) Source and movement of helium in the Morongo groundwater basin: the influence of regional tectonics on crustal and mantle helium fluxes. *Geochim. Cosmochim. Acta* **69**, 3857-3872.

Li, Y.-H. (2000) Igneous rocks and the composition of the Earth. In *A compendium of geochemistry*. Princeton Univ. Press, Princeton. pp. 189-249.

Londquist C. J. and Martin P. (1991) Geohydrology and groundwater-flow simulation of the Surprise Spring Basin aquifer system, San Bernardino county, CA. USGS Water-Resources Investigations Report 89-4099.

Maiss, M. and C. A. M. Brenninkmeijer (1998), Atmospheric SF_6: Trends, sources, and prospects, *Environ. Sci. Tech.* **32**, 3077-3086.

McDougall I. and Harrison T. M. (1988) Geochronology and thermochronology by the $^{40}Ar/^{36}Ar$ method, Oxford University Press, Oxford.

Meybeck M. (1987) Global chemical weathering of surficial rocks estimated from river dissolved loads, *Am. J. Sci.* **287**, 401-428.

Morris R. A., Miller T. M., Viggiano A. A., Paulson J. F., Solomon S. and Reid G. (1995) Effects of electron and ion reactions on atmospheric lifetimes of fully fluorinated compounds. *J. Geophys. Res* **100 (D1)**, 1287-1294.

Musset A. E. (1969) Diffusion measurements and the Potassium-Argon method of dating. *Geophys. J. Roy. Astron. Soc.* **18**, 71-92.

Nur A. and Walder J. (1990) Time-dependent hydraulics of the Earth's crust. In *The role of fluids in crustal processes*, National Academy of Sciences, pp. 113-127.

O'Nions R. K. and Oxburgh E. R. (1983) Heat and helium in the Earth, *Nature* **306**, 429-431.

Ozima M. and Podosek F. A. (1983) Noble Gas Geochemistry. Cambridge University Press, Cambridge.

Padma D. K. and Vasudeva Murthy A. R. (1975) Thermal decomposition of sulphur hexafluoride, *J. Fluor. Chem.* **5**, 181-184.

Plummer L. N., Prestemon E. C. and Parkhurst D. L. (1991) An interactive code (NETPATH) for modelling net geochemical reactions along a flow path, U.S. Geological Survey Water-Resources Investigations Report 94-4078.

Prinn R.G., Weiss R. F., Fraser P. J., Simmonds P. G., Cunnold D. M., Alyea F. N., O'Doherty S., Salameh P., Miller B. R., Huang J., Wang R. H. J., Hartley D. E., Harth C., Steele L. P., Sturrock G., Midgley P. M. and McCulloch A. (2000) A history of chemically and radiatively important gases in air deduced from ALE/GAGE/AGAGE. *J. Geophys. Res.* **105 (D14)**, 17751-17792.

Ravishankara A. R., Solomon S., Turnipseed A. A. and Warren R. F. (1993) Atmospheric lifetimes of long-lived halogenated species. *Science* **259**, 194-199.

Reynolds G. W., Hoff J. T. and Gillham R. W. (1990) Sampling Bias Caused by Materials Used to Monitor Halocarbons in Groundwater. *Environ. Sci. Technol.* **24**, 135-142.

Riley F. S. and Worts Jr. G. F. (1953) Geology and groundwater appraisal of the Twentynine Palms Marine Corps Training Center, CA. USGS Open File Report 98-617.

Ronov A. B. and Yaroshevsky A. A. (1969) Chemical composition of the Earth's crust. In *The Earth's crust and upper mantle*. (ed. P. J. Hart) Am. Geophys. Union, Washington D. C. pp. 37-57.

Santella N., Ho D. T., Schlosser P. and Stute M. (2003), Distribution of Atmospheric SF_6 near a Large Urban Area as Recorded in the Vadose Zone, *Environ. Sci. Technol.* **37**, 1069-1074.

Scharlin P and Battino R (1995) Solubility of CCl_2F_2, $CClF_3$, CF_4 and CH_4 in water and seawater at 288.15 – 303.15K and 101.325 kPa. *J. Chem. Eng. Data* **40**, 167-169.

Severinghaus J. P., Grachev A., Luz B. and Caillon N. (2003) A method for precise measurement of argon 40/36 and krypton/argon ratios in trapped air in polar ice with applications to past firn thickness and abrupt climate change in Greenland and at Siple Dome, Antarctica. *Geochim. Cosmochim. Acta* **67**, 325-343.

Stamos C. L., Martin P., Nishikawa T. and Cox B. F. (2001) Simulation of ground-water flow in the Mojave River Basin, CA. USGS Water-Resources Investigations Report 01-4002.

Stute M., Sonntag C., Deak J. and Schlosser P. (1992) Helium in deep circulating groundwater in the Great Hungarian Plain: Flow dynamics and crustal helium fluxes, *Geochim. Cosmochim. Acta* **56**, 2051-2067.

Subsurface Surveys (1990) Inventory of groundwater stored in the Mojave River Basins. Subsurface Surveys and Associates, Inc., Solana Beach, California.

Torgersen T. (1980) Controls on pore-fluid concentration of He-4 and Rn-222 and the calculation of He-4-Rn-222 ages. *J. Geochem. Explor.* **13**, 57-75.

Torgersen T. and Clarke W. B. (1985) Helium accumulation in groundwater I: An evaluation of sources and the continental flux of [4]He in the Great Artesian Basin, Australia, *Geochim. Cosmochim. Acta* **49**, 1211-1218.

Torgersen T. (1989) Terrestrial helium degassing fluxes and the atmospheric helium budget: Implications with respect to the degassing processes of continental crust, *Chem. Geol.* **79**, 1-14.

Torgersen T. and O'Donnell J. (1991) The degassing flux from the solid earth: release by fracturing. *Geophys. Res. Lett.* **18**, 951-954.

Vollmer M. K. and Weiss R. F. (2002) Simultaneous determination of sulfur hexafluoride and three chlorofluorocarbons in water and air. *Mar. Chem.* **78**, 137-148.

Wilhelm E., Battino R. and Wilcock R. J. (1977) Low-pressure solubility of gases in liquid water. *Chem. Rev.* **77**, 219-262.

Wilson R. D. and Mackay D. M. (1996) SF_6 as a Conservative Tracer in Saturated Media with High Intragranular Porosity or High Organic Carbon Content, *Ground Water* **34**, 241-249.

Worton D. R., Sturges W. T., Gohar L. K., Shine K. P., Martinerie P., Oram D. E., Humphrey S. P., Begley P., Gunn L., Barnola J.-M., Schwander J. and Mulvaney R. (2007) Atmospheric Trends and Radiative Forcings of CF_4 and C_2F_6 Inferred from Firn Air, *Environ. Sci. Technol.* **41**, 2184 -2189.

Wright L. A., Stewart R. M., Gay Jr. T. E. and Hazenbush G.C. (1953) Mines and Mineral Deposits of San Bernardino County, California, *Calif. J. Mines Geol.* **49**, 165.

Wright T. L. (1991) Structural geology and tectonic evolution of the Los Angeles basin, California. In: *Active Margin Basins,* vol. 52 (Ed. K. T. Biddle), Am. Assoc. Petroleum Geologists Memoir, Tulsa, Oklahoma, 35-134.

Yaws, C. L. (1995) Diffusion Coefficient in Water. In : *Handbook of transport property data: viscosity, thermal conductivity, and diffusion coefficients of liquids and gases*. Library of physico-chemical property data. Gulf Pub.Co., Houston, Texas.

4.10 Electronic Annexes

Electronic Annexes EA-1 and EA-2 can be found in the online version of this article,

at http://dx.doi.org/10.1016/j.gca.2007.11.027.

4.11 Appendix

This appendix was written subsequent to publication, for further clarification of the continental crustal flux of CF_4 and SF_6 to the atmosphere. In this chapter I propose that there is a crustal flux of CF_4 and SF_6 entering the groundwater basins through the underlying basement, and demonstrate that the regional variability in the estimated crustal CF_4 and SF_6 fluxes would be consistent with the corresponding variability in crustal helium fluxes (see Section 4.6.1.3). A potential weakness in the argument presented herein is the initial assumption that a crustal flux of CF_4 and SF_6 does indeed exist. A more rigorous approach would be to statistically link excess CF_4 and SF_6 with crustal helium entering Mojave Desert groundwaters from depth.

To begin, I consider whether water-rock interactions are responsible, within uncertainty, for the total accumulation of lithospheric CF_4 and SF_6 in Mojave Desert groundwaters. To do this I take the extreme case of setting the weathering fluxes of CF_4 and SF_6 to their maximum value presented in Sections 4.6.1.2 and 4.6.1.3, 4.5 fmol CF_4 kg^{-1} H_2O kyr^{-1} and 0.02 fmol SF_6 kg^{-1} H_2O kyr^{-1}, and estimate the residual CF_4 or SF_6 concentration not accounted for by weathering (X_R). X_R can be estimated from $X_R = X_{ex} - W_X \times \tau$, where X_{ex} is the excess concentration, W_X is the weathering flux, and τ is the water mass (radiocarbon) age. A value of X_R that is smaller than its uncertainty would indicate that only a weathering flux is necessary to accumulate the measured concentration of the gas. There are no significant residual CF_4 and SF_6 concentrations for wells 5N/7W-24D3, 5N/5W-18Q1, 5N/5W-35P1, 5N/5W-35J1 and

4N/5W-1C1 in the regional aquifer of the Mojave River Basin. The remaining groundwaters presented in Chapter 4 contain significant residual concentrations of CF_4 and SF_6, indicating that an additional source of lithospheric CF_4 and SF_6 is necessary to account for their observed concentrations in collected groundwaters. As stated in Section 4.6.1.3, this is consistent with noble gas studies that indicate that accumulation of lithospheric gases in young groundwaters is dominated by in-situ production or release (Stute et al., 1992; Kulongoski et al., 2003; 2005).

The residual excesses of CF_4 and SF_6 for Mojave Desert groundwaters are plotted versus the deep crustal component of measured ^{4}He concentrations in Figure 4.6. There is a strong correlation (r = 0.99) between CF_4 residuals and deeply-sourced ^{4}He, providing supporting statistical evidence for a crustal flux of lithospheric CF_4 entering Mojave Desert groundwaters through the underlying basement. This also provides further evidence that crustal degassing is driven by advection of gases associated with fluid flow through the crust (Kulongoski et al., 2005).

There is no correlation between SF_6 residuals and deep ^{4}He. However, it may be premature to dismiss a crustal SF_6 flux, given that the residuals in CF_4 and SF_6 correlate well (r = 0.88), and that the only weathering flux estimate available for SF_6 is derived with the assumption of a crustal flux of SF_6, possibly making it inappropriate for this consideration. Combined measurements of SF_6 concentrations in groundwaters and in the surrounding aquifer material would provide a better understanding of the weathering flux of SF_6, and improve our understanding of its crustal degassing.

Alternatively, a groundwater study in a non-granitic aquifer, preferably in a region of tectonic activity, could test for the presence of crustal SF_6 fluxes as well.
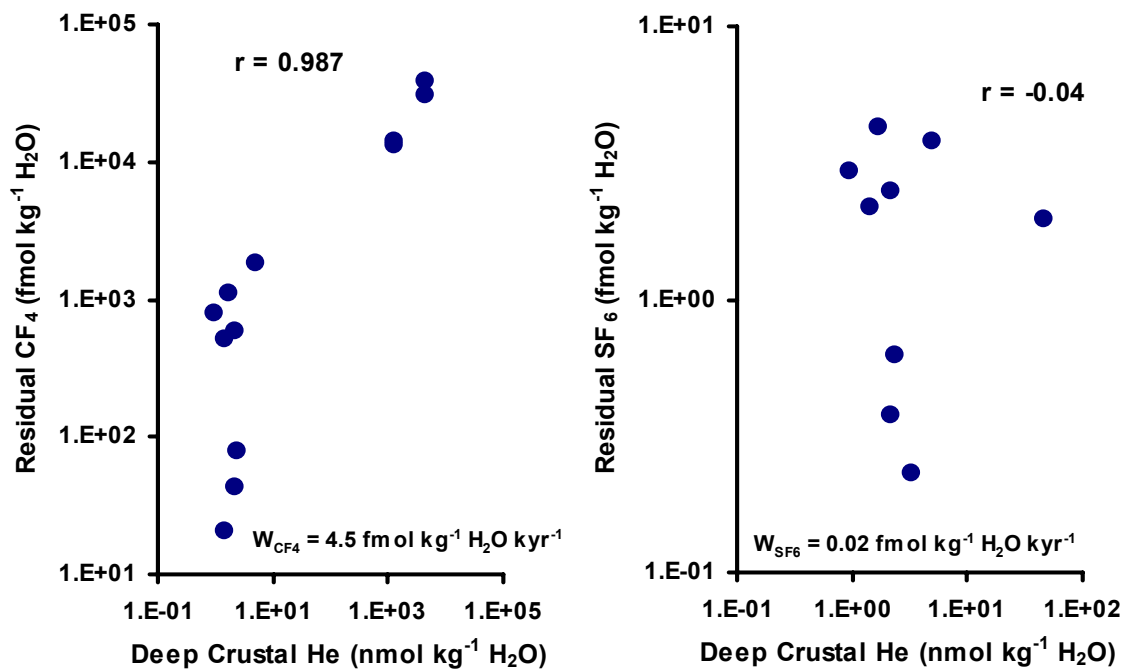
Figure 4.6 Residual excesses of CF_4 and SF_6 in Mojave Desert groundwaters, after removal of contributions from release during weathering of aquifer material, plotted against the deep crustal component of measured ^4He concentrations. A strong correlation between the residual excesses of CF_4 and deep ^4He indicates that the external source of CF_4 to Mojave Desert groundwaters is a crustal degassing flux migrating through the underlying basement. No corresponding correlation between SF_6 and deep-sourced ^4He is observed, possibly a result of a bias in the estimated weathering flux of SF_6.

Chapter 5

Dissolved CF_4 and SF_6 concentrations in the Big Bear Lake Watershed

5.1 Introduction

In the fall of 2005, I returned to the southern Mojave to collect groundwaters from the Big Bear Lake Watershed (BBLW) for dissolved CF_4 and SF_6 analyses. The BBLW is located on the northern face of the San Bernardino Mountains to the south/southwest of the Mojave River Basin (MRB) and Eastern Morongo Basin (EMB) discussed in Chapter 4 (Fig. 5.1). Average daily temperatures range from around 18 °C in the summer to around 3 °C in the winter. The average annual precipitation in the Big Bear Valley ranges from 580 to 740 mm yr^{-1} (California Department of Water Resources, 2003).

The aquifer is comprised of Cenozoic alluvium overlying a pre-Tertiary crystalline basement that also forms the surrounding mountains (Flint et al., 2008). The basement rocks are composed of large granitic bodies, metamorphosed sedimentary rock, and gneiss (Miller, 2004). The alluvium consists of Tertiary deposits directly overlying the basement rocks, and older and younger Quaternary

deposits that overly both the Tertiary deposits and basement rocks throughout much

of the basin (GeoScience Support Services, Inc., 2003). The deposits are relatively

thin, with thicknesses of less than 300 meters in most places (Flint et al., 2008).
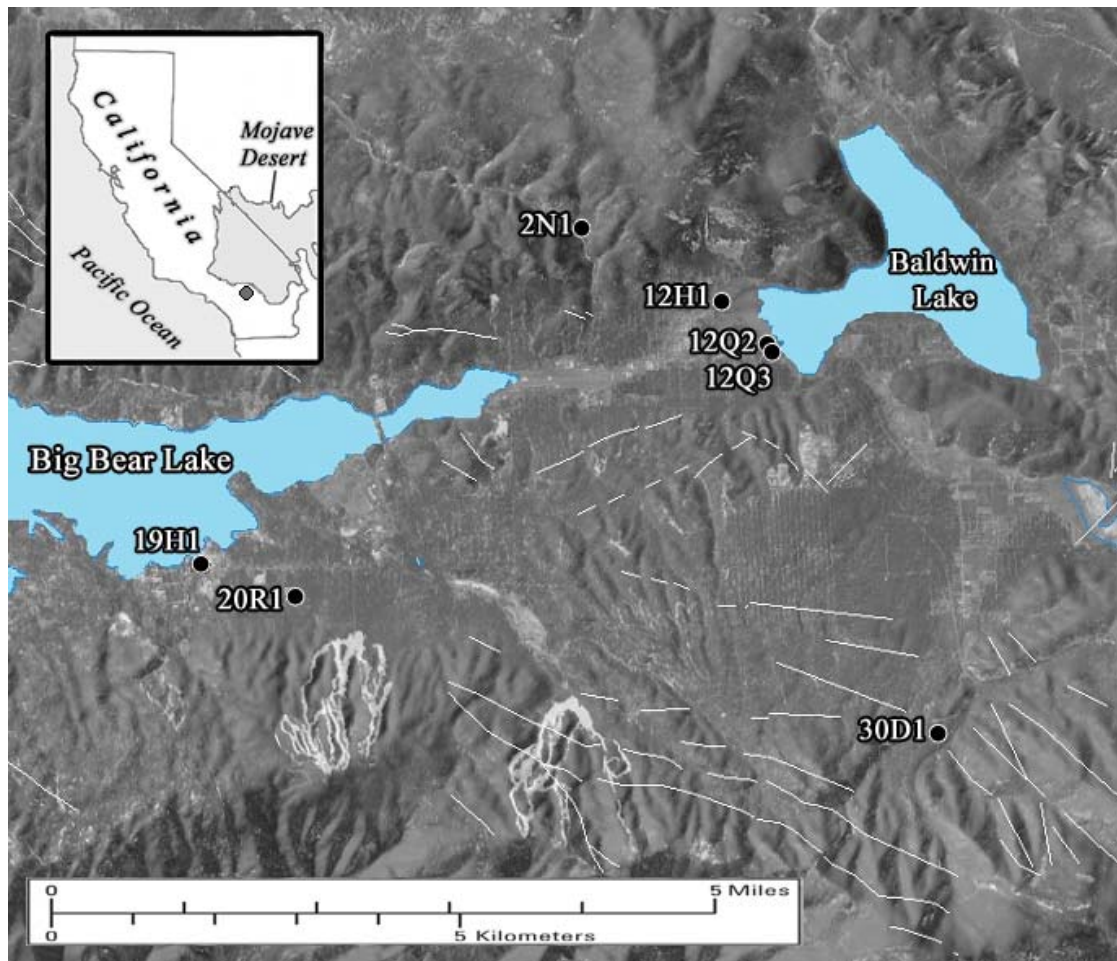
Figure 5.1 Topographic map of the Big Bear Lake Watershed study area, with well locations shown. Well names are the last four digits of the respective USGS well identifications presented in Table 5.1 (e.g. 12H1 for well 2N/1E-12H1). White lines indicate the location of known fault zones. The insert shows the location of the study area (gray dot) with respect to California and the Mojave Desert.

The older Quaternary deposits are considered the major water-bearing deposits

of the aquifer (Flint et al., 2008), and are composed of interbedded layers of coarse

sand, gravel and clay. Given the similar lithology of the BBLW and MRB/EMB

alluvium, the BBLW is a suitable location to test the weathering and basal flux mechanisms proposed in Chapter 4 for crustal degassing of lithospheric CF_4 and SF_6.

5.2 Methods

Groundwater samples for CF_4 and SF_6 analyses were collected in Fall 2005 from eight wells in the Big Bear Lake Watershed. Wells were sampled in an identical manner to those studied in the Mojave River Basin and Eastern Morongo Basin (see Chapter 4 for details). Dissolved gases were extracted and analyzed by Medusa-GC/MS, as detailed in Chapter 3 and 4 (or see Miller et al., 2008). Precision of dissolved CF_4 and SF_6 measurement were estimated at ±3%. The reproducibility of duplicate CF_4 and SF_6 measurements in this study was typically in the range of 2 – 4 %, consistent with the estimated precisions. The Medusa-GC/MS also measures a wide variety of halogenated gases, including CFC-12 (CCl_2F_2), CFC-11 (CCl3F), CFC-113 (CCl_2FCClF_2), CFC-13 ($CClF_3$), Halon 1301 ($CBrF_3$) and Halon 1211 ($CClBrF_2$). The precision of measurement of CFC-12, CFC-11 and CFC-113 were also estimated at ±3%. The precision of measurement for CFC-13, Halon-1301 and Halon-1211 were poorer due to low signal-to-noise ratios, with precision estimates of ±5% for Halon-1211 and ±10% for CFC-13 and Halon-1301.

5.3 Results

Dissolved CF_4 and SF_6 concentrations for groundwaters in the Big Bear Lake Watershed are presented in Table 5.1, as well as helium isotope, fluoride and tritium concentrations, the hydrogen and oxygen isotopic composition of collected groundwaters, and radiocarbon water mass ages (http://waterdata.usgs.gov/nwis; Flint et al., 2008).

Table 5.1 Radiocarbon water mass ages, helium isotope, tritium (in tritium units, 1 TU = 3.19 pCi kg^{-1} H_2O), CF_4 and SF_6 concentrations, and the hydrogen and oxygen isotope composition of water in groundwaters drawn from wells in the Big Bear Lake Watershed.

Well Identification	^{14}C age	$^4He_{ex}$	^3H	δD	$\delta^{18}O$	^3He	CF_4	SF_6	F^-
	years	nmol kg^{-1} H_2O	TU	‰			fmol kg^{-1} H_2O		mg L^{-1}
2N/2E-2N1	–	0	–	–	–	0.03	400	14.5	–
2N/2E-30D1	–	0	–	–	–	0	19.1	1.26	–
2N/2E-20R1	1849	0	0.60	-80.6	-11.57	0	28.1	0.82	0.1
2N/1E-12Q2	3749	106	0.16	-94.4	-12.93	8.4	102000	3.01	7.5
2N/1E-19H1	4328	2.7	0.06	-81.5	-11.61	0	326	1.09	0.2
2N/1E-12Q3	6074	325	0.09	-95.3	-12.97	34	109000	3.4	10.5
							107000	3.4	
2N/1E-12H1	16791	655	0	-99.7	-13.66	63	197000	0.57	17.1
							190000	0.73	

The highest concentrations of CF_4 in the BBLW are associated with thermal waters drawn by well 2N/1E-12H1 to the west of Baldwin Lake (Fig 5.1). Dissolved CF_4 concentrations are also exceptionally high in wells 2N/1E-12Q2 and 2N/1E-12Q3, which draw waters containing stable isotope ratios and high fluoride concentrations

that more closely resemble thermal waters drawn from 2N/1E-12H1 than the remainder of the BBLW groundwaters. Flint et al. (2008) propose that the aquifer underneath wells 2N/1E-12Q2 and 2N/1E-12Q3 is hydrologically connected to the thermal waters under well 2N/1E-12H1 by a permeable horizon, such as a fault zone. Crustal fracturing events associated with tectonic activity facilitate the vertical migration of mantle fluids through fault zones in the southern Mojave Desert (Kulongoski et al., 2003; 2005). Fracturing of the basement surrounding a fault zone also releases crustal ^{4}He and CF_4 into vertically migrating fluids (see Chapter 4). The presence of elevated concentrations of ^{4}He and CF_4 in the region west of Baldwin Lake suggests that crustal fracturing events may facilitate the migration of thermal fluids from depth, similar to fluid flow through active fault zones in the southern Mojave.

5.3.1 Modern water contamination and excess CF_4 and SF_6 concentrations

The water-bearing Quaternary deposits filling the Big Bear Lake Watershed have been separated into three aquifers, labeled the "upper", "middle" and "lower" aquifers (GeoScience Support Services, Inc., 2003). The upper and middle aquifers are the primary water producers in the BBLW, with the upper aquifer containing recently recharged water, while the middle aquifer contains water recharged between 2,000 and 6,000 years ago (Flint et al., 2008). Young groundwater drawn from the

upper aquifer will contribute modern CF_4 and SF_6 to collected well waters, which needs to be accounted for if measured CF_4 and SF_6 concentrations are to be used to study the subsurface release of these gases.

The chlorofluorocarbon (CFC) and bromohalocarbon ("halon") gases can provide a constraint on the modern water content of collected groundwaters, as they will only be present in groundwaters drawn from the upper aquifer, since there are no known natural sources of these gases (Butler et al., 1999; Reeves et al., 2005). Measured concentrations of CFC-12, CFC-11, CFC-113, CFC-13, Halon-1301 and Halon-1211 are presented in Table 5.2.

Table 5.2 Dissolved halogenated gas concentrations in Big Bear Lake Watershed groundwaters. Excess CF_4 and SF_6 concentrations (X_{ex}) corrected for recharge and modern inputs to collected groundwaters are also presented. m_H is the modern water content of collected groundwaters (in %, by mass), estimated from halocarbon concentrations. n.d. = not detected.

Well Identification	CFC 12	CFC 11	CFC 113	CFC 13	Halon 1301	Halon 1211	m_H	CF_{4ex}	SF_{6ex}
	pmol kg^{-1} H$_2$O						%	fmol kg^{-1} H$_2$O	
2N/2E-2N1	1.22	2.46	0.155	n.d.	0.001	0.0025	63	380	13.3
2N/2E-30D1	1.66	2.76	0.268	0.0017	0.006	0.0187	70	0	0
2N/2E-20R1	0.905	1.79	0.095	0.0007	0.003	0.0082	25	14.9	0.37
2N/1E-12Q2	0.113	1.62	0.045	0.0002	n.d.	0.0004	4	102000	2.9
2N/1E-19H1	0.070	0.906	n.d.	n.d.	n.d.	0.0005	3	316	1.04
2N/1E-12Q3	0.073	0.217	0.003	0.0001	n.d.	0.0014	3	109000	3.4
	0.068	0.207	0.006	0.0006	n.d.	0.0013	3	107000	3.3
2N/1E-12H1	0.067	0.206	0.012	n.d.	0.001	0.0011	3	197000	0.52
	0.072	0.070	0.003	0.0001	n.d.	0.0021	2	190000	0.70

The modern water content of collected groundwater samples (m_H) can be estimated by the ratio of the dissolved CFC and halon concentrations in Table 5.2 to their freshwater solubilities (compiled in Appendix B). BBLW groundwaters have a modern water content that ranges from several percent for the oldest groundwaters to

70% for the youngest groundwaters. Most wells contained CFC-11 concentrations in excess of those expected based on the modern water contents listed in Table 5.2. However, this may not be surprising given that groundwater samples often contain at least one CFC in excess of air-saturated water concentrations (Höhner et al., 2003). Use of CFC-13, Halon-1301 and Halon-1211 measurements in addition to CFC-12, CFC-11 and CFC-113 ensured that at least 3 uncontaminated gases were available to constrain the modern water content of collected samples for each well.

"Excess" dissolved CF_4 and SF_6 concentrations (X_{ex}), corrected for modern water contributions, and for equilibration with the preindustrial atmosphere and entrainment of air during recharge, are presented in Table 5.2. A recharge temperature of 9°C and entrained air concentrations of $0 - 0.02$ mL kg^{-1} H_2O were estimated from a partial-reequilibration recharge model (Aeschbach-Hertig et al., 2000) constrained by dissolved Ne, Ar, Kr and Xe concentrations (J. Kulongoski, personal communication). In most cases, the low atmospheric mole fractions and low solubilities of CF_4 and SF_6 result in relatively small differences between measured and excess concentrations for these gases.

5.4 Discussion

5.4.1 The source of perfluorinated gases to Big Bear Lake Watershed groundwaters

To test whether the crustal degassing mechanisms observed in the Mojave Desert can satisfy the observed concentrations of CF_4 and SF_6 in Big Bear groundwaters, we can compare water mass ages derived from CF_4 and SF_6 concentration excesses and Mojave Desert weathering and crustal flux estimates to an independent measure of water mass age (e.g radiocarbon ages). CF_4- and SF_6- based water mass ages (τ) can be estimated from (modified from Stute et al., 1992):

$$\tau = \frac{[X]}{\dfrac{J}{\phi z \rho} + W} \qquad (5.1)$$

where [X] is the measured excess concentration of gas X (in fmol X kg^{-1} H_2O) , J is the crustal flux of gas X (in fmol X cm^{-2} yr^{-1}) , φ is the aquifer porosity, z is the depth from the midpoint of a well's perforation(s) to the underlying basement (in cm), ρ is the density of freshwater (in kg cm^{-3}), and W is the weathering flux of gas X (in fmol X kg^{-1} H_2O yr^{-1}). The weathering flux into Mojave Desert groundwaters was estimated at $2.3 - 4.5$ fmol CF_4 kg^{-1} H_2O kyr^{-1} and $0.01 - 0.02$ fmol SF_6 kg^{-1} H_2O kyr^{-1}, based on the silicate weathering rate estimates of Izbicki and Michel (2004). The

crustal fluxes of CF_4 and SF_6 varied by several orders of magnitude over relatively short distances (kilometers), and crustal fluxes of CF_4 were significantly enhanced down-flow of an active fault in the region. Crustal fluxes of CF_4 varied from 0.07 fmol CF_4 cm^{-2} yr^{-1} to 4 fmol CF_4 cm^{-2} yr^{-1}, while crustal SF_6 fluxes varied from 0.0006 fmol SF_6 cm^{-2} yr^{-1} to 0.002 fmol SF_6 cm^{-2} yr^{-1}.

CF_4 and SF_6 water mass ages estimated from Equation 5.1 are presented graphically as functions of radiocarbon age in Figures 5.2 and 5.3. The dashed lines in Figures 5.2 and 5.3 are 1:1 lines that indicate complete agreement between perfluorinated-gas-based and radiocarbon-based water mass ages. If the Mojave Desert crustal degassing rates are sufficient to produce the observed CF_4 and SF_6 concentrations in the Big Bear Lake Watershed, then CF_4 and SF_6 water mass age estimates should scatter around the 1:1 line when plotted against ^{14}C water mass age.

CF_4 ages in Figure 5.2 suggest that a regional crustal CF_4 flux of similar magnitude to that observed in the Mojave Desert, 0.07 – 0.7 fmol CF_4 cm^{-2} yr^{-1}, combined with an average weathering flux of 3.4 fmol CF_4 kg^{-1} H_2O kyr^{-1}, is sufficient to explain observed concentrations of wells tapping shallow, young groundwaters in the BBLW (i.e. wells 2N/2E-20H1 and 2N/2E-19H1). A much larger crustal flux, 30 fmol CF_4 cm^{-2} yr^{-1}, is needed to reproduce the observed CF_4 concentrations in groundwaters drawn from well 2N/1E-12H1.
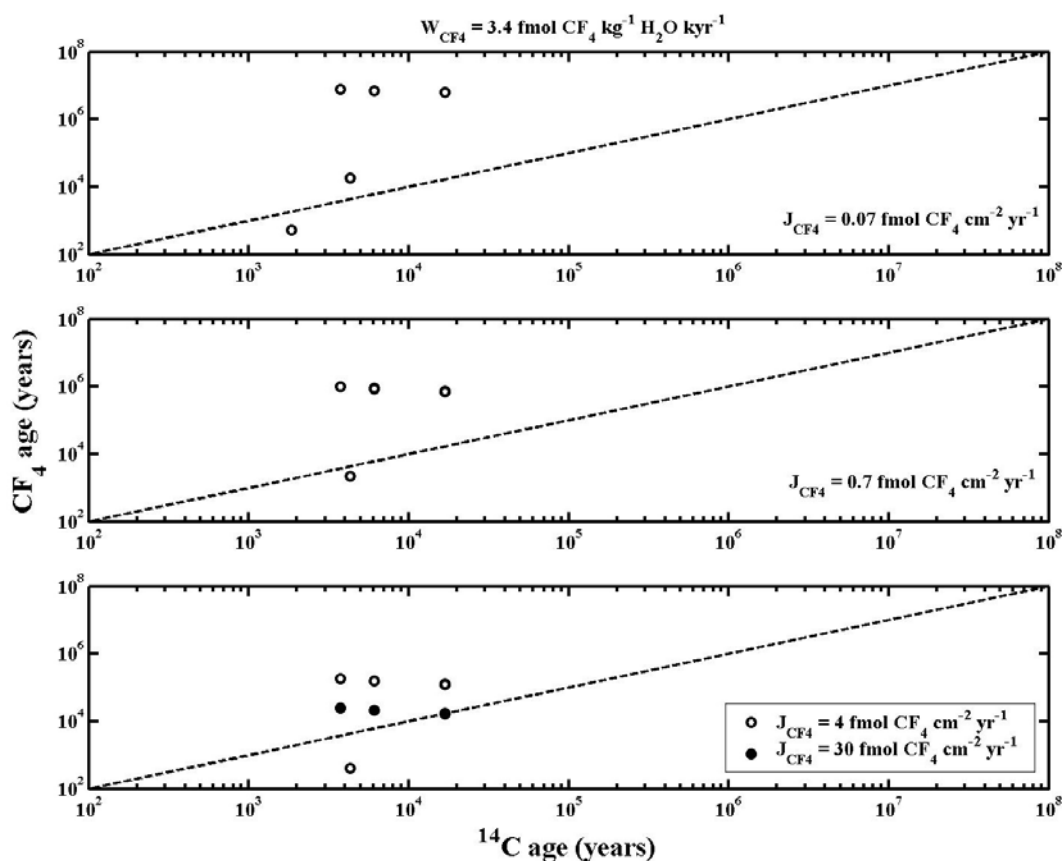
Figure 5.2 CF$_4$ water mass ages for Big Bear Lake Watershed groundwaters plotted against radiocarbon-based water mass ages. CF$_4$ ages are derived from excess CF$_4$ using a weathering release rate and a range of crustal fluxes representative of the geochemistry of CF$_4$ in Mojave Desert groundwaters. A large crustal flux (30 fmol CF$_4$ cm^{-2} yr^{-1}) is needed to account for the highly elevated CF$_4$ concentrations in groundwaters to the west of Baldwin Lake.

Although there is considerable scatter in Figure 5.3, the dissolved SF$_6$ concentrations in all cases can be explained using weathering and crustal SF$_6$ fluxes of similar magnitude to those observed in the neighboring Mojave Desert (Fig 5.3). Unlike CF$_4$, crustal SF$_6$ fluxes are not enhanced in wells tapping hydrothermal waters to the west of Baldwin Lake. The crustal flux of SF$_6$ estimated for well 2N/1E-12H1, 6×10^{-5} fmol SF$_6$ cm^{-2} yr^{-1} is almost identical to the depressed crustal SF$_6$ flux estimated for

well 5N/5W-4A1 (Table 4.1), 5×10^{-5} fmol SF_6 cm^{-2} yr^{-1}. Of the wells studied in the Mojave River Basin, 5N/5W-4A1 draws waters closest from the active Shadow Mountain fault. This supports the assertion that fluid flow in the Big Bear hydrothermal system is facilitated by the presence of a fault zone, and that fracturing of the granitic basement resulting from tectonic activity enhances the crustal flux of CF_4 to Big Bear groundwaters.
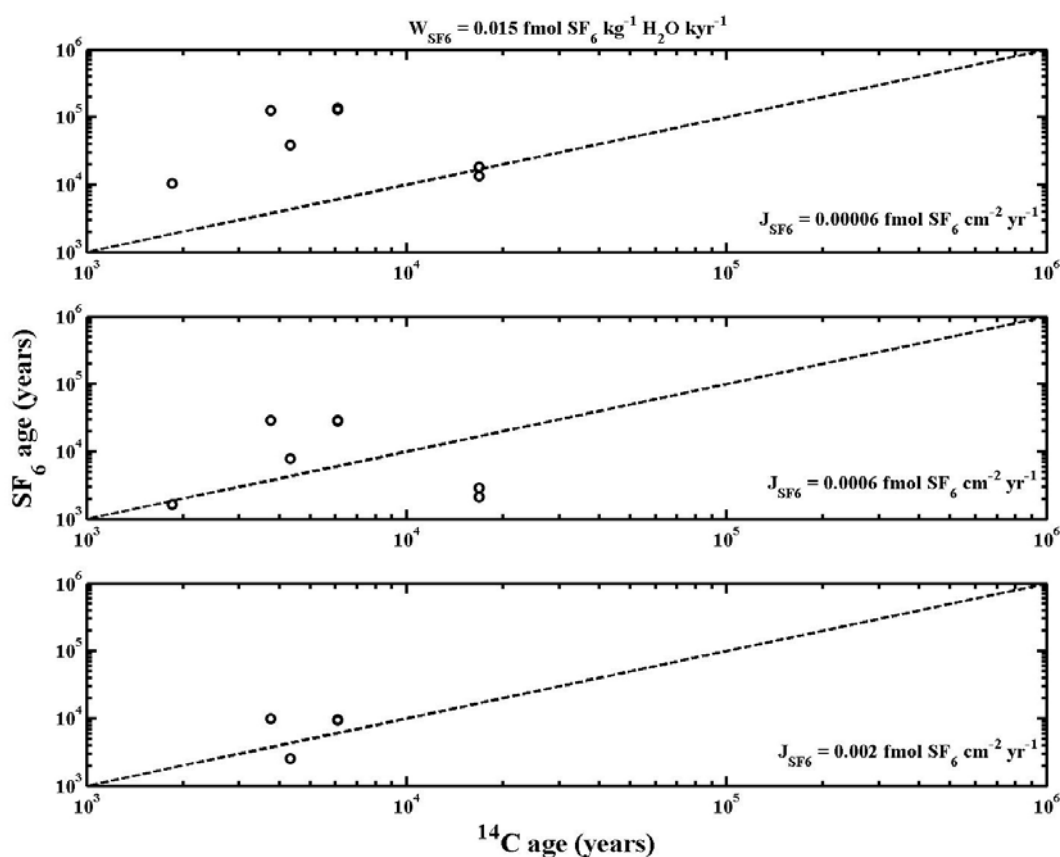
Figure 5.3 SF_6 water mass ages for Big Bear Lake Watershed (BBLW) groundwaters plotted against radiocarbon-based water mass ages. SF_6 ages are derived from excess SF_6 using a weathering release rate and a range of crustal fluxes representative of the geochemistry of SF_6 in Mojave Desert groundwaters. The range of crustal SF_6 fluxes observed in the Mojave Desert is sufficient to account for observed SF_6 concentrations in the BBLW.

5.4.2 Elevated crustal CF$_4$ fluxes in the BBLW: Implications for the global lithospheric CF$_4$ flux to the atmosphere

In Chapter 4, I used the relationship between crustal CF$_4$ and He fluxes in the Mojave Desert to estimate the global crustal degassing flux of CF$_4$ to the atmosphere. The upper limit to the crustal degassing CF$_4$ flux extrapolated from the Mojave Desert may be too low, since the crustal flux of CF$_4$ in thermal waters drawn from the BBLW is even higher than crustal CF$_4$ fluxes observed in the Mojave Desert.

Crustal helium fluxes for the BBLW can be estimated from Equation 5.1 using the excess ^{4}He concentrations and radiocarbon ages listed in Table 5.1 and replacing the weathering term in Equation 5.1 with an in-situ helium production rate of 4.4×10^{-12} cm^3 He @STP g^{-1} yr^{-1} for Big Bear aquifer material (J. Kulongoski, personal communication). The crustal ^{4}He flux for well 2N/1E-12H1 is 2.3×10^{-6} cm^3 He @ STP cm^{-2} yr$^{-1,}$ or 1.0×10^{-10} mol He cm^{-2} yr^{-1}, giving a CF$_4$/^{4}He molar crustal flux ratio of 3.0×10^{-4}. This is larger, but of similar magnitude to the range of CF$_4$/^{4}He molar crustal flux ratios observed in the Mojave Desert, 3×10^{-5} to 1.5×10^{-4}. If the BBLW crustal CF$_4$/^{4}He flux ratio is adopted as a new upper limit to the range of CF$_4$/^{4}He crustal flux ratios observed in the Mojave Desert, and the He flux from granitic rocks is estimated at 3×10^8 mol yr^{-1} (see Chapter 4 for derivation), then the global crustal degassing of CF$_4$ is estimated to be $800 - 8{,}000$ kg yr^{-1}. The total lithospheric flux of CF$_4$ to the atmosphere, including release by weathering, would then be $(0.9 - 9) \times 10^3$ kg CF$_4$ yr^{-1}.

For a lithospheric CF_4 source of $(0.9 - 9) \times 10^3$ kg CF_4 yr^{-1} to sustain a steady-state preindustrial atmospheric mixing ratio of 34.7 ppt CF_4, the preindustrial atmospheric lifetime would need to be between 62 and 620 kyr. The current estimate of the modern atmospheric CF_4 lifetime is 50 kyr, based on loss of CF_4 to high temperature combustors at the Earth's surface (Ravishankara et al., 1993). If the preindustrial atmospheric CF_4 lifetime were within the range presented here, 62 – 620 kyr, then the modern atmospheric lifetime of CF_4 would be between 28 – 46 kyr, raising the possibility that the modern atmospheric lifetime of CF_4 is significantly shorter than previously estimated.

5.5 Conclusion

Groundwaters collected from the Big Bear Lake Watershed contain concentrations of CF_4 and SF_6 that are well in excess of air-saturated water concentrations. This excess in CF_4 and SF_6 concentrations can be reasonably explained by a combination of release during weathering of the surrounding granitic rock and a crustal flux from depth. Concentrations of CF_4 are exceptionally high in hydrothermal waters drawn near Baldwin Lake. The crustal CF_4 and SF_6 fluxes estimated for Big Bear hydrothermal waters are similar to crustal fluxes observed down-flow of an active fault in the Mojave River Basin, suggesting that hydrothermal flow in the Big Bear Lake Watershed is facilitated by episodic crustal fracture events driven by local tectonics. If the ratio of the crustal CF_4 and He fluxes in thermal

BBLW waters are added to the Mojave Desert data set of CF_4/He flux ratios, the upper limit of the global crustal degassing CF_4 flux estimate is doubled. The corresponding lower limit to the preindustrial atmospheric lifetime of CF_4 decreases from 100 to 62 kyr, suggesting that CF_4 may be naturally removed from the atmosphere at a faster rate than previously estimated.

5.6 Acknowledgements

5.7 References

Aeschbach-Hertig W., Peeters F., Beyerle U. and Kipfer R. (2000) Palaeotemperature reconstruction from noble gases in ground water taking in to account equilibration with entrapped air, *Nature* **405**, 1040-1044.

Butler J. H., Battle M., Bender M., Montzka S. A., Clarke A. D., Saltzman E. S., Sucher C., Severinghaus J., and Elkins J. W. (1999), A twentieth century record of atmospheric halocarbons in polar firn air, *Nature* **399**, 749-765.

California Department of Water Resources, 2003, California's groundwater: Bulletin 118, update 2003: Sacramento, Calif., State of California, The Resources Agency,

Department of Water Resources, accessible at:
http://www.dpla2.water.ca.gov/publications/groundwater/bulletin118/basins/pdfs_desc/8-9.pdf

Flint L. E., Hevesi J. A., Flint A. L., Christensen A. H., Sneed M., Martin P., Jachens R. and Brandt J. (2008) Geohydrology of Big Bear Valley, California: Phase 1 – Geologic framework, recharge and geochemistry. USGS Scientific Investigations Report (in preparation).

GeoScience Support Services, Inc., 2003, Focused geohydrologic evaluation of the maximum perennial yield of the North Shore and Grout Creek hydrologic subunit tributary subareas: Report prepared for the City of Big Bear Lake Department of Water and Power, Dec. 2, 2003.

Höhener, P., Werner, D., Balsiger, C., Pasteris, G., 2003. Worldwide occurrence and fate of chlorofluorocarbons in groundwater. *Crit. Rev. Env. Sci. Tec.* **33**, 1-29.

Izbicki J. A. and Michel R. L. (2004) Movement and age of ground water in the western part of the Mojave Desert, southern California, USA. USGS Water-Resources Investigations Report 03-4314.

Kulongoski J. T., Hilton D. R. and Izbicki J.A. (2003) Helium isotope studies in the Mojave Desert, California: implications for groundwater chronology and regional seismicity. *Chem. Geol.* **202**, 95-113.

Kulongoski J. T., Hilton D. R. and Izbicki J. A. (2005) Source and movement of helium in the Morongo groundwater basin: the influence of regional tectonics on crustal and mantle helium fluxes. *Geochim. Cosmochim. Acta* **69**, 3857-3872.

Londquist C. J. and Martin P. (1991) Geohydrology and groundwater-flow simulation of the Surprise Spring Basin aquifer system, San Bernardino county, CA. USGS Water-Resources Investigations Report 89-4099.

Miller, F.K., 2004, Preliminary geologic map of the Big Bear City 7.5' quadrangle, San Bernardino County, California: U.S. Geological Survey Open-File Report 2004-1193, scale 1:24,000.

Morris R. A., Miller T. M., Viggiano A. A., Paulson J. F., Solomon S. and Reid G. (1995) Effects of electron and ion reactions on atmospheric lifetimes of fully fluorinated compounds. *J. Geophys. Res* **100 (D1)**, 1287-1294.

Ravishankara A. R., Solomon S., Turnipseed A. A. and Warren R. F. (1993) Atmospheric lifetimes of long-lived halogenated species. *Science* **259**, 194-199.

Reeves C. E., Sturges W. T., Sturrock G. A., Preston K., Oram D. E., Schwander J., Mulvaney R., Barnola J. M. and Chappellaz J. (2005) Trend of halon gases in firn air: Implications for their emissions distributions. *Atmos. Chem. Phys.* **5**, 2055-2064.

Stute M., Sonntag C., Deak J. and Schlosser P. (1992) Helium in deep circulating groundwater in the Great Hungarian Plain: Flow dynamics and crustal helium fluxes, *Geochim. Cosmochim. Acta* **56**, 2051-2067.

Chapter 6

Halogenated Gas Fluxes from Kilauea Volcano

Preface

The question of whether halogenated gases may be present in volcanic emissions has surfaced several times during my graduate studies at SIO. The first time I considered this question was during a collaborative study of volcanic gas seeping through soil in a tree-kill zone near Horseshoe Lake, Mammoth Lakes, California, with Tom Rahn and Martin Vollmer. We collected gas samples through several meters of snowpack near Horseshoe Lake in April of 2002. The snowpack effectively retained soil emissions of volcanic gas, allowing us to collect samples with CO_2 mole fractions of up to 70% CO_2. This considerable amount of carbon dioxide posed a serious analytical concern, as it could damage the cryofocusing traps used in the sampling module of the Medusa-GC/MS. Methods to reduce the CO_2 mole fractions to manageable abundances were only partly successful, and preliminary analyses of aliquots of collected gases for SF_6, CFC-12, CFC-11 and CFC-113 by GC/ECD (Vollmer and Weiss, 2000) indicated that these gases were atmospheric in origin. It no longer seemed reasonable to continue the project, and so

we put the project on hold in order to pursue other more promising research.

In the fall of 2005 I had the chance to measure halogenated gas abundances in aliquots of hydrothermal gases collected by Harmon Craig from hot springs and fumaroles in Yellowstone National Park (YNP) (Craig, 1953). The samples analyzed were a 10% split of the non-condensable fraction of 50 mL hydrothermal gas samples. I analyzed hydrothermal gases collected from two locations in YNP, Sizzling Basin and Black Dragon Cauldron, which have helium isotope ratios of $R/R_A \sim 16$, indicating the presence of a strong mantle component in hydrothermal gases at these locations.

CF_4 was undetectable in gas samples collected in YNP. The detection limit of CF_4 in YNP samples was high, ~100 ppt CF_4, mainly resulting from the small sample volumes involved in the analyses. This detection limit provides an upper limit to a hypothetical mantle CF_4 contribution to collected gases, and, when combined with the ^{3}He mole fraction of 1.3×10^{-7} for gases from Sizzling Basin (Welhan et al., 1988), and a mantle ^{3}He flux of <2300 mol yr^{-1} (Porcelli and Ballentine, 2002), constrains the mantle flux of CF_4 to the atmosphere to <2 moles CF_4 yr^{-1}.

This chapter focuses on my third and final visit to the question of a volcanic source of halogenated gases to the atmosphere. It details the collection and analysis of significantly larger volumes of volcanic gas from the summit fumaroles of Kilauea Volcano, Hawaii, and shows with greater confidence that a mantle flux of CF_4 must be a negligible player in the atmospheric geochemistry of CF_4.

6.1 Abstract

Volcanic gas samples were collected from fumarolic emissions at Kilauea summit for the analysis of a large group of halogenated gases by Medusa-GC/MS. Most of the analytes measured by Medusa-GC/MS that are present in collected gas samples can be attributed to the entrainment of ambient air through cracks and fissures and entrainment of gases exsolved from Kilauea's hydrothermal system. Elevated concentrations of CFC-11 (CCl_3F), which are normally attributed to a volcanic source, may instead indicate that the hydrothermal system of Kilauea contains dissolved gases that are fractionated by equilibration with a CFC-free vapor phase. No volcanic source of CF_4 or SF_6 is necessary to explain observed CF_4 and SF_6 concentrations in collected gases. A hypothetical undetected mantle source of CF_4 and SF_6 is at most 0.01% of the flux of CF_4 and SF_6 from the continents, indicating that the mantle is a negligible source of perfluorinated gases to the atmosphere.

6.2 Introduction

For the past several decades, there has been considerable debate surrounding the detection of chlorofluorocarbon gases (CFCs) in volcanic emissions (e.g., Gaffney, 1995; Gribble,1995; Isidorov, 1995). The most recent studies indicate that, with the possible exception of CFC-11 ($CFCl_3$), CFCs present in volcanic gases are a result of entrainment of modern air into fumarolic emissions (Jordan et al., 2000; Frische et al.,

2007). However, the discovery of elevated tetrafluoromethane (CF_4) concentrations in the presence of mantle volatiles migrating through the continental crust (see Chapter 4) suggests that perfluorinated gases, a group of long-lived, halogenated greenhouse gases, may be released to the atmosphere through volcanic degassing.

In this study, I analyzed enriched trace gas samples collected from three summit fumaroles on Kilauea volcano, Hawaii, for the two most abundant perfluorinated gases in the atmosphere, CF_4 and SF_6, as well as a broad suite of halogenated trace gases, including CFC-12 (CF_2Cl_2), CFC-11, and CFC-113 ($CFCl_2CF_2Cl$). Kilauea volcano is an ideal site to investigate a potential mantle source of CF_4 and SF_6 to the atmosphere, as it has a clear mantle component in summit fumaroles (Hilton et al., 1997) and is comprised of basaltic minerals that do not contain appreciable amounts of lithospheric CF_4 and SF_6 (Harnisch and Eisenhauer, 1998; Busenberg and Plummer, 2000). Two of the sampling sites are fumaroles in the vicinity of Halemaumau crater (fumaroles "B" and "C") while the other sampling site is a borehole previously drilled into the northeast region of the crater rim ("Sulphur Banks") (Fig. 6.1). Measured halogenated gas contents for emissions from Kilauea summit fumaroles are presented and the implications for the global geochemistry of CF_4 and SF_6 are discussed.
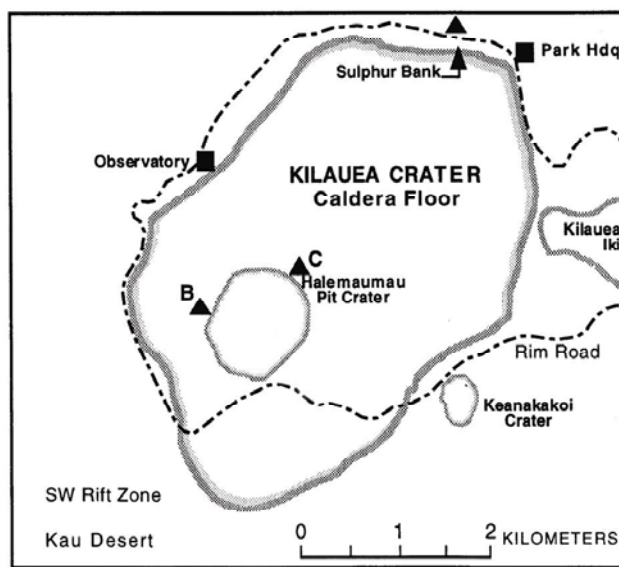
Figure 6.1 A map of Kilauea summit, indicating the location of fumaroles sampled in this study, Halemaumau crater, the USGS Hawaiian Volcano Observatory, and the Hawaii Volcano National Park Headquarters. Modified from Hilton et al. (1997).

6.3 Methods

Samples were collected into 250 mL Pyrex flasks, each containing 100 mL of 5N NaOH solution. During addition of NaOH solution to a flask, both the NaOH stock solution and flask headspace were purged with analyte-free N_2 gas. Each prepared flask was then vacuum-distilled twice at -78 °C, to remove the N_2 headspace as well as any residual modern contaminants. Vacuum distillation at -78 °C ensured minimal loss of water during headspace evacuation, keeping the normality of the NaOH solution effectively constant. One flask (the "preparation blank") was packaged and set aside in the laboratory to test for outgassing of halogenated gases from the Teflon stopcock of the flask or the surrounding shipping packaging. The remaining flasks

were shipped into the field, valve-side down, so that the NaOH solution provided a diffusion barrier to prevent incursion of modern air into the flask headspace.

At fumaroles B and C, a ~1 m titanium tube was inserted into the fumarole as far as possible (around 2/3 of a meter) to avoid collection of ambient air. A sampling flask was then connected to a rubber stopper/glass tube fitting on the exposed end of the Ti tube by a short (0.3 m) length of silicone tubing. On the down-flow side of the flask's valve a ~1 m length of rubber tubing was added. All tubing was purged using a hand pump, after which the tubing down-flow of the flask was clamped shut. The flask was then inverted and opened, allowing sample to bubble through the NaOH solution into the flask headspace, removing almost all of the gas (>99%) through condensation (for H_2O) or reaction with the NaOH solution (mainly CO_2 and SO_2). After roughly an hour of collection, the flask headspace contained a large enrichment of volcanic trace gases.

While volcanic emissions were steady and relatively rapid at fumaroles B and C, the borehole at Sulphur Banks often had no observable emissions of steam/volatiles. The titanium tube was inserted as far as possible into a rock pile covering the borehole in an attempt to avoid air contamination. However, collection of gas ceased after roughly five minutes of sampling at Sulphur Banks, indicating that the flask headspace had equilibrated mostly with ambient air rather than acidic volcanic gases.

Gravimetric measurements of a flask before and after sample collection provided an estimate of the total mass of gas collected in each sample. The four flasks

collected from fumaroles near Halemaumau crater collected sample masses of $22 - 28$ g, while there was no observable change in the mass of the flask used for sample collection at Sulphur Banks. This is consistent with collection of a significant amount of volcanic gas at all sites except Sulphur Banks. An average molecular weight for the collected gas of 21 ± 1 g mol^{-1} can be estimated from recent H_2O, CO_2 and SO_2 mole fraction measurements of fumarolic emissions near Halemaumau crater (Goff and McMurtry, 2000; Hurwitz et al., 2003). This molecular weight estimate can be used to calculate the total number of moles of gas collected in each sample.

In the laboratory, the headspace of a flask was extracted into a 40 mL stainless steel tube immersed in liquid helium, as described in Chapter 3. N_2 gas was then used to push the extracted gas into the Medusa cryotrapping gas chromatograph/mass spectrometer (Medusa-GC/MS) instrument system of Miller et al. (2008). Results were corrected for carrier gas blanks and calibrated with known volumes of a working standard of dry whole air with assigned dry-air mixing ratios based on the SIO-2005 gravimetric calibration scale (Prinn et al., 2000; C. Harth, personal communication).

6.4 Results and Discussion

6.4.1 Storage/Preparation Blanks

For the majority of halogenated gases measured by Medusa-GC/MS, the preparation blank was a relatively small proportion (<5%) of measured abundances in fumarolic gas samples. However, for CH_3I, CH_3Br, HFC-152a ($C_2H_4F_2$) and HFC-134a ($C_2H_2F_4$), the preparation was a large fraction of the measured values and the results for these compounds cannot be reliably interpreted. CF_4 and SF_6 were not detected in the preparation blank.

6.4.2 Sulphur Banks

The observed $CF_4/$ SF_6 mole ratio for gas collected from Sulphur Banks was 13.1 ± 0.6, close to the atmospheric mole ratio of 12.6 ± 0.1 observed in recent routine measurement of the remote troposphere (Miller et al., 2008). This indicates that the probable source of CF_4 and SF_6 to the Sulphur Banks sample was ambient air. The amount of modern air calculated from the molar amounts of CF_4 and SF_6 for this sample would be 4.4 ± 0.3 millimoles air, or 120 ± 9 mL of air at the ambient conditions of Kilauea summit. This is close to the expected headspace volume of 140 ± 4 mL for this flask, confirming the collection of predominately ambient air at Sulphur Banks. This quantity of air is sufficient to account for observed molar

amounts of Halon 1301 ($CBrF_3$), CFC-11, CFC-12, CFC-113, CFC-114 ($C_2F_4Cl_2$), CFC-115 (C_2F_5Cl) and HCFC-142b (CF_2ClCH_3) (Table 6.1).

Table 6.1 Measured halogenated gas content (X) for the gas sample collected at Sulphur Banks. X_C values are measured halogenated gas contents corrected for the addition of 120 mL of ambient air during sampling. Boldface values of X_C are within the uncertainty of measurement of zero and are thus negligible.

Compound	X (pmol)	X_C (pmol)	Compound	X (pmol)	X_C (pmol)
CF_4	0.332	**0.007**	$CBrF_3$	0.0151	**0.0014**
C_2F_6	0.048	0.033	$CBrClF_2$	0.0062	-0.01
C_3F_8	0.024	0.022	CH_3CCl_3	0.042	-0.026
SF_6	0.0253	**-0.0005**	C_2HCl_3	0.046	0.043
SO_2F_2	0	-0.008	C_2Cl_4	0.148	0.132
CCl_3F	1.196	0.136	$C_2H_3ClF_2$	0.083	**0.006**
CCl_2F_2	2.437	0.122	$C_2H_3Cl_2F$	0.113	0.030
$CClF_3$	0.0147	**0.0025**	C_2HClF_4	0.040	0.033
CH_3Cl	0.626	-1.73	C_2HF_5	0.315	0.29
CH_2Cl_2	1.301	1.15	$C_2Cl_3F_3$	0.327	**-0.006**
$CHCl_3$	0.002	**0.0022**	$C_2Cl_2F_4$	0.068	**-0.003**
$CHClF_2$	-0.12	-0.93	C_2ClF_5	0.039	**0.003**
$CHBr_3$	0.0005	-0.0041	$C_2Br_2F_4$	0.004	0.002

Methyl chloride (CH_3Cl), methyl chloroform (CH_3CCl_3), bromoform ($CHBr_3$), and HCFC-22 (CHF_2Cl) have molar amounts in the Sulphur Banks sample that are lower than expected based on the estimated modern air contribution, suggesting that they were destroyed during flask transit to the laboratory. The probable loss mechanism is dehydrohalogenation by the NaOH solution in the flask (e.g. CH_3CCl_3 +

NaOH => $CH_2=CCl_2$ + NaCl + H_2O). Other Cl- and Br- containing halohydrocarbons (e.g. dichloromethane, CH_2Cl_2) may also be lost to dehydrohalogenation but may have been significantly abundant to persist in collected samples until analysis. The C-F bond is very strong (O'Hagan, 2008) and so dehydrohalogenation of fluorinated halohydrocarbons (e.g. HFC-125, CF_3CHF_2) is probably insignificant. SO_2F_2 was not detected in the collected samples, which is consistent with its hydrolysis in basic solutions (Cady and Sudhindra, 1974)

All other analytes measured by Medusa-GC/MS were elevated above the molar amounts expected from the quantity of ambient air collected into the flask (Table 6.1). These gases may result from degassing of tubing plastics and polymers or hand-pump grease during sampling (Reynolds et al., 1990), or may be elevated in the ambient air at Kilauea summit due to volcanic emissions.

6.4.3 Halemaumau fumaroles

The halogenated gas composition of samples collected from fumaroles B and C are presented in Tables 6.2 and 6.3, respectively. Most compounds are present at molar amounts of less than 1 pmol, with the exception of several gases, including CFC-11, CFC-12, and CFC-113. Of these three CFCs, only CFC-11 is thought to have a volcanic source. Volcanic emissions from Kilauea contain up to 8 pmol CFC-11, or 7 ppt CFC-11 when sample masses are considered. This is somewhat smaller than the range of volcanic CFC-11 mole fractions of 30 − 980 ppt reported by Jordan et al.

(2000), supporting the assertion of Jordan et al. (2000) that volcanoes are an insignificant source of CFC-11 to the atmosphere.

Table 6.2 Halogenated gas content (X_i) for samples #1 and #2 (fumarole B)

Compound	X_1 (pmol)	X_2 (pmol)	Compound	X_1 (pmol)	X_2 (pmol)
CF_4	0.071	0.094	C_2HCl_3	0.12	0.35
C_2F_6	0.136	0.226	C_2Cl_4	0.75	3.87
C_3F_8	0.35	0.13	$C_2H_3ClF_2$	0.075	0.261
SF_6	0.0054	0.0099	$C_2H_3Cl_2F$	0.41	0.78
CCl_3F	2.963	8.110	C_2HClF_4	0.047	0.049
CCl_2F_2	1.593	3.353	C_2HF_5	2.82	0.72
$CClF_3$	0.006	0.010	$C_2Cl_3F_3$	1.16	2.50
CH_2Cl_2	2.02	3.94	$C_2Cl_2F_4$	0.052	0.082
$CBrF_3$	0.004	0.009	C_2ClF_5	0.014	0.022
$CBrClF_2$	0.015	0.023	$C_2Br_2F_4$	0.014	0.027

Table 6.3 Halogenated gas content (X_i) for samples #3 and #4 (fumarole C).

Compound	X_3 (pmol)	X_4 (pmol)	Compound	X_3 (pmol)	X_4 (pmol)
CF_4	0.217	0.130	C_2HCl_3	0.08	0.24
C_2F_6	0.100	0.127	C_2Cl_4	3.36	1.66
C_3F_8	0.81	1.07	$C_2H_3ClF_2$	0.235	0.080
SF_6	0.0169	0.0099	$C_2H_3Cl_2F$	0.74	0.29
CCl_3F	6.091	2.596	C_2HClF_4	0.115	0.105
CCl_2F_2	3.423	1.670	C_2HF_5	4.66	5.51
$CClF_3$	0.017	0.015	$C_2Cl_3F_3$	2.49	1.21
CH_2Cl_2	2.65	2.13	$C_2Cl_2F_4$	0.116	0.057
$CBrF_3$	0.012	0.008	C_2ClF_5	0.037	0.022
$CBrClF_2$	0.017	0.012	$C_2Br_2F_4$	0.025	0.013

6.4.3.1 Identifying non-volcanic contributions using halogenated gas mole ratios

The stable isotope and tritium concentrations of water in steam exiting summit fumaroles around Halemaumau crater are consistent with local meteoric water recharging Kilauea's hydrothermal system in the northeast region of Kilauea caldera (Hurwitz et al., 2003). Tritium concentrations in fumarolic steam from Kilauea suggest residence times of <1-5 years for hydrothermal waters (Goff and McMurtry, 2000). Some portion of CFCs detected in fumarole samples in this study should therefore be derived from air-saturated meteoric water recently recharging into Kilauea's hydrothermal system. Previous studies have also proposed that CFCs are introduced into volcanic emissions by entrainment of ambient air through cracks and fissures in the volcano (Jordan et al, 2000).

It is possible to distinguish and to constrain air and air-saturated water contributions using the suite of analytes measured by Medusa-GC/MS, since their differing solubilities and atmospheric mole fractions give distinct molar ratios for these two sources. For example, the ratios of the molar amounts of Medusa-GC/MS analytes in Tables 6.2 and 6.3 to CFC-12 are displayed in Table 6.4. Molar X_i/CFC-12 ratios in air-saturated water are based on compiled solubility data (see Appendix B). Some gases could not be incorporated into Table 6.4 because of the lack of sufficient solubility data in the literature.

Table 6.4 Mole ratios of Medusa-GC/MS analytes to CFC-12 ($R_i = X_i/X_{F12}$). R_A is the mole ratio of gas X to CFC-12 in ambient air. R_H is the mole ratio of gas X to CFC-12 in air-saturated water at the temperature of recharge (T~16 °C). Bold-face values with a gray background are within error of the range described by R_A and R_H and can thus be attributed to a combination of the two sources.

Compound	R_A	δR_A (%)	R_1	R_2	δR_i (%)	R_3	R_4	δR_H (%)	R_H
CF_4	$1.4 * 10^{-1}$	0.2	$\mathbf{4.4 * 10^{-2}}$	$\mathbf{2.8 * 10^{-2}}$	8	$\mathbf{6.4 * 10^{-2}}$	$\mathbf{7.8 * 10^{-2}}$	4	$9.0 * 10^{-3}$
C_2F_6	$6.6 * 10^{-3}$	0.3	$8.5 * 10^{-2}$	$6.7 * 10^{-2}$	0.5	$2.9 * 10^{-2}$	$7.6 * 10^{-2}$	6	$1.3 * 10^{-4}$
SF_6	$1.1 * 10^{-2}$	0.6	$\mathbf{3.4 * 10^{-3}}$	$\mathbf{3.0 * 10^{-3}}$	4	$\mathbf{4.9 * 10^{-3}}$	$\mathbf{5.9 * 10^{-3}}$	4	$8.5 * 10^{-4}$
CCl_3F	$4.6 * 10^{-1}$	0.3	$1.9 * 10^{0}$	$2.4 * 10^{0}$	0.1	$1.8 * 10^{0}$	$\mathbf{1.6 * 10^{0}}$	4	$1.7 * 10^{0}$
$CClF_3$	$5.3 * 10^{-3}$	3	$\mathbf{4.0 * 10^{-3}}$	$\mathbf{3.0 * 10^{-3}}$	15	$\mathbf{5.0 * 10^{-3}}$	$9 * 10^{-3}$	4	$1.4 * 10^{-3}$
$CBrF_3$	$5.9 * 10^{-3}$	2	$2 * 10^{-3}$	$\mathbf{3 * 10^{-3}}$	47	$\mathbf{3 * 10^{-3}}$	$\mathbf{5 * 10^{-3}}$	6	$4.1 * 10^{-3}$
$CBrClF_2$	$8.3 * 10^{-3}$	0.5	$\mathbf{9.6 * 10^{-3}}$	$6.8 * 10^{-3}$	5	$4.8 * 10^{-3}$	$7.4 * 10^{-3}$	6	$1.9 * 10^{-2}$
C_2HCl_3	$1.2 * 10^{-3}$	2	$7.7 * 10^{-2}$	$1.0 * 10^{-1}$	1	$2.5 * 10^{-2}$	$1.5 * 10^{-1}$	6	$3.0 * 10^{-3}$
C_2Cl_4	$7.2 * 10^{-3}$	0.7	$4.7 * 10^{-1}$	$1.2 * 10^{0}$	0.1	$9.8 * 10^{-1}$	$9.9 * 10^{-1}$	4	$2.3 * 10^{-3}$
C_2HF_5	$9.0 * 10^{-3}$	1	$1.8 * 10^{0}$	$2.2 * 10^{-1}$	0.3	$1.4 * 10^{0}$	$3.3 * 10^{0}$	6	$9.2 * 10^{-2}$
$C_2Cl_3F_3$	$1.4 * 10^{-1}$	0.4	$7.3 * 10^{-1}$	$7.4 * 10^{-1}$	0.1	$7.3 * 10^{-1}$	$7.2 * 10^{-1}$	4	$1.6 * 10^{-1}$
C_2ClF_5	$1.6 * 10^{-2}$	0.9	$\mathbf{8.6 * 10^{-3}}$	$\mathbf{6.7 * 10^{-3}}$	9	$\mathbf{1.1 * 10^{-2}}$	$\mathbf{1.3 * 10^{-2}}$	4	$1.6 * 10^{-3}$

Of the gases that can be displayed in Table 6.4, CF_4, SF_6 and CFC-115 are attributable to a mixture of air and hydrothermal contributions. This suggests that no volcanic source of CF_4 or SF_6 is necessary to explain their observed concentrations in collected samples. Molar CFC-11/CFC-12 ratios are almost always higher than can be explained by a mixture of air and water, which may support an additional source of CFC-11 to collected samples, although in all cases the molar CFC-11/CFC-12 ratio is close to that for air-saturated water.

Halon-1301 and Halon-1211 have molar X_i/CFC-12 ratios that are typically lower than, but of similar order of magnitude to, molar X_i/CFC-12 ratios for air and water contributions. This suggests that they may be reasonably attributed to air-water additions, and that there is no significant volcanic source of these gases.

In most cases CFC-113 and PCE have molar X_i/CFC-12 ratios that are higher than the range described by ambient air and water. Molar amounts of these gases vary in magnitude with order of sampling, with the first sample collected (#3) containing more CFC-113 and PCE than the following samples (#4, then #1). The final sample (#2) was collected a day after the other Halemaumau fumarole samples, and shows similar molar amounts of CFC-113 and PCE as the first sample collected on the previous day (#3). The probable source of these gases is degassing of polymers in the sampling line, with the source decreasing in significance as the line cleans with use.

6.4.3.2 Quantifying non-volcanic inputs using a two-member mixing model – Ambient

air + hydrothermal waters

If the quantity of a gas in volcanic emissions is entirely attributable to ambient air and hydrothermal water contributions, then the observed molar content of gas X in a collected sample (n_i) can be described by:

$$n_X = n_A \cdot Z_X + m_{H_2O} \cdot [X]$$

(6.1)

where n_A is the amount of air added (in moles), Z_X is the atmospheric mole fraction of gas *X*, m_{H_2O} is the hydrothermal water contribution (in kg water), and [*X*] is the air-saturated water concentration for gas X at the temperature and elevation of recharge (in molality units).

If two gases are derived from non-volcanic (i.e. air and water) sources, then the amount of non-volcanic contributions can be constrained using Equation 6.1. In terms of the CFC-12 content of collected gases, Equation 6.1 can be rearranged to solve for m_{H_2O}:

$$m_{H_2O} = \frac{\left(n_{CFC\text{-}12} - n_A \cdot Z_{CFC\text{-}12}\right)}{[CFC\text{-}12]}$$

(6.2)

Substituting Equation 6.2 into Equation 6.1 gives:

$$n_i = n_A \cdot Z_i + \frac{\left(n_{CFC\text{-}12} - n_A \cdot Z_{CFC\text{-}12}\right)}{[CFC\text{-}12]} \cdot [i] \qquad (6.3)$$

Equation 6.3 can be rearranged to solve for the number of moles air added to the sample:

$$n_A = \left(n_X - n_{CFC\text{-}12} \cdot \frac{[X]}{[CFC\text{-}12]}\right) \Big/ \left(Z_X - Z_{CFC\text{-}12} \cdot \frac{[X]}{[CFC\text{-}12]}\right) \quad (6.4)$$

To estimate the number of moles of air entrained into collected volcanic gases, Equation 6.4 was solved for each gas in Table 6.4 that can be attributed solely to hydrothermal and atmospheric sources. The error-weighted average of these n_A values, along with the estimated uncertainties in the average (δn_A) can be found in Table 6.5.

The air contents estimated by Equation 4 can be input into Equation 6.2 to solve for the hydrothermal content of collected fumarole gas samples. The resulting m_{H_2O} range from $0.5 - 1.4$ kg H_2O (Table 6.5). Runoff from precipitation the night before and the morning of the collection of sample #2 may have directly contaminated fumarole B and led to a more significant air-saturated water contribution than for other samples.

Table 6.5 The estimated air content ($n_A \pm \delta n_A$, in moles) and estimated air-saturated water content ($m_{H_2O} \pm \delta m_{H_2O}$, in kilograms) of gas samples collected from fumaroles around Halemaumau crater.

Sample	#1	#2	#3	#4
n_A	$8.8 * 10^{-4}$	$1.19 * 10^{-3}$	$2.6 * 10^{-3}$	$1.42 * 10^{-3}$
δn_A	$3 * 10^{-5}$	$6 * 10^{-5}$	$1 * 10^{-4}$	$6 * 10^{-5}$
m_{H_2O}	0.57	1.39	1.02	0.46
δm_{H_2O}	0.02	0.04	0.04	0.02

Using the air and hydrothermal water contents listed in Table 6.5, the non-volcanic contributions to measured halogenated gas abundances are removed to assess whether a residual, possibly volcanic, component is present. Residual halogenated gas contents for samples #1 – 4 (X_C, where in this case $X_C = X_i - n_A \cdot Z_X - m_H \cdot [X]$) are presented in Table 6.6.

A mixture of ambient air and gas exsolved from Kilauea's hydrothermal system can explain the observed abundances of CF_4, SF_6, CFC-12, Halon-1301, and Halon-1211 in all samples. CFC-13 and CFC-115 residuals are of similar magnitude to their respective errors and may not be significant. CFC-11 residuals are positive, requiring an additional, possibly volcanic, source of CFC-11 to emissions from Kilauea summit fumaroles.

Table 6.6 Residual halogenated gas abundances for fumaroles B (#1-2) and C (#3-4), after accounting for addition of ambient air and hydrothermal gases to collected gases. Boldface values of X_C are within δX_C of zero and are thus negligible

Compound	X_{C1} (pmol)	X_{C2} (pmol)	X_{C3} (pmol)	X_{C4} (pmol)	δX_C (pmol)
CF_4	**-0.006**	**-0.02**	**-0.002**	**0.014**	0.03
C_2F_6	0.133	0.221	0.091	0.122	0.001
SF_6	**-0.001**	**0.0004**	**-0.0008**	**0.0005**	0.001
CCl_3F	0.8	3.1	2.0	0.7	0.1
CCl_2F_2	**0**	**0**	**0**	**0**	–
$CClF_3$	**0.002**	**0.003**	0.007	0.010	0.003
$CBrF_3$	**-0.004**	**-0.006**	**-0.005**	**-0.001**	0.006
$CBrClF_2$	**-0.01**	**-0.03**	**-0.03**	**-0.01**	0.03
C_2HCl_3	0.119	0.340	0.077	0.241	0.001
C_2Cl_4	0.743	3.863	3.343	1.648	0.003
C_2HF_5	2.71	0.47	4.47	5.42	0.02
$C_2Cl_3F_3$	0.91	1.97	1.96	0.95	0.02
C_2ClF_5	0.004	0.008	0.012	0.009	0.003

6.4.3.3 Quantifying non-volcanic inputs using a two-member mixing model – Ambient air + fractionated hydrothermal waters

One possible explanation for excess CFC-11 in collected fumarolic gases is that the hydrothermal system is partially stripped of gases during its transit from the recharge site to Halemaumau crater. If an analyte-free vapor phase were introduced into the system, the CFCs present in the hydrothermal system would repartition into the vapor phase and liquid phase based on their solubilities. CFCs that are retained in

the aqueous phase would then be fractionated with respect to their air-saturated water values, with more soluble gases (e.g. CFC-11) being retained more significantly than the less soluble gases (e.g. CFC-12, CF_4 and SF_6) (Ballentine et al., 2002). Long-period seismic events suggest that volcanic gases condense at 200 – 400 m depths below the northeastern and central parts of Halemaumau crater (Almendros et al., 2001). If partial condensation of volcanic gas occurrs to the northeast of Halemaumau crater, or if gases exsolved from the groundwater by heating during transit remain in contact with the liquid phase, then hydrothermal waters could equilibrate with an initially analyte-free vapor phase, resulting in loss of the sparingly-soluble chlorofluorocarbon gases from the aqueous phase. The steam exiting fumaroles in the vicinity of Halemaumau crater would then have an apparent excess of CFC-11 with respect to CFC-12 and other low solubility halocarbons.

Ballentine et al. (2002) considered the phase partitioning of noble gases when gas bubbles with no noble gas content pass through a water column containing air-saturated noble gas concentrations. The water column in their model is split into cells, with no exchange of fluids or dissolved gases between cells. A bubble is added to the first cell, where it is assumed to equilibrate completely with the dissolved gases present. The partitioning of the dissolved gases is described by:

$$\frac{[X]_G}{[X]_L + [X]_G} = \left(\frac{V_L}{V_G} \cdot K_X + 1 \right)^{-1}$$

(6.5)

where $[X]_i$ is the number of moles of gas X in the liquid (L) and gas (G) phases, V_i is the volume of liquid or vapor phase, and K_X is the Henry's coefficient for the gas. After equilibration, the bubble is placed in the next cell, where it establishes a new equilibrium with the dissolved gas. Once the bubble has been in contact with all cells in the column, the next bubble (with no noble gas content) is added to the first cell and the process is repeated.

As gas is lost to equilibration with bubbles passing through the column, the molar ratio of two dissolved gases (X and Y) in the aqueous phase diverges from their molar ratio in air-saturated water. Their molar ratio can be related to the fraction of gas remaining and the original air-saturated water mole ratio by the Rayleigh fractionation law:

$$\left(\frac{[X]}{[Y]}\right)_L = \left(\frac{[X]}{[Y]}\right)_0 P^{(\alpha-1)} \qquad (6.6)$$

where [i] are molar amounts of gas i in the fractionated liquid phase (L) and original air-saturated water, P is the fraction of gas Y remaining in the liquid phase, and α is the fractionation coefficient, equal to K_X/K_Y, where K_i is the Henry's coefficient for the gas.

For this study, the extent of fractionation of the hydrothermal system and the contribution of ambient air to sample gases can be solved iteratively using a trio of halogenated gases for which reliable solubility data are available. The three gases I

selected for this process is CFC-12, CFC-11 and SF_6, because of their distinct solubilities, atmospheric mole fractions and lack of apparent contamination.

For the initial iteration, I assumed that CFC-12 and CFC-11 originate solely from a hydrothermal contribution to the fumarolic gases. The extent of fractionation could then be solved from Equation 6.6, using a CFC-12/CFC-11 mole ratio for air-saturated water at 16°C as the initial condition (Nullet and Sanderson, 1993). The value of α was estimated using solubilities at a temperature of 16°C. Initial P values calculated in this manner range from 0.88 to 0.99 for three of the samples, indicating that only a small amount of fractionation is necessary to explain observed CFC-12/CFC-11 mole ratios. The final sample (#4) had an initial P value of 1.04, which is unrealistic, and so P was set to 1 (i.e. no fractionation) for this sample. Equation 6.6 was then used to estimate the fractionated hydrothermal SF_6/CFC-11 mole ratio, which, when multiplied by the observed molar amounts of CFC-11, gave an initial estimate of the hydrothermal contribution of SF_6 to collected gas samples.

The SF_6 content of gas samples, once corrected for addition of hydrothermal SF_6, was then used to estimate the air content of collected gases. This in turn was used to calculate CFC-12 and CFC-11 air contributions, which were subtracted from observed CFC-12 and CFC-11 contents to obtain new estimates of the hydrothermal component for these gases. These new hydrothermal values were input into Equation 6.6, P values were re-estimated, and the process was repeated until fractionation factors and air contents converged. Results from the final iteration are presented in Table 6.7.

Table 6.7 Air content (n_A, in moles) and hydrothermal fractionation factors (P) for fumarolic gas collected near Halemaumau crater.

Sample	#1	#2	#3	#4
n_A	$8.9 * 10^{-4}$	$1.63 * 10^{-3}$	$2.79 * 10^{-3}$	$1.63 * 10^{-3}$
P	0.87	0.80	0.83	0.84

Since Kilauea's hydrothermal system is heated during the transit between the site of recharge and its discharge as steam at Halemaumau, it was also necessary to check whether changes in solubility ratios with temperature would have an influence on air content and fractionation factor estimates. For this test the iteration was performed again at the temperature of steam leaving the fumaroles (T~98°C). High-temperature solubilities for halogenated gases were extrapolated from low-temperature solubilities using the technique of Trew et al. (2001). The air contents of collected gases are not significantly different at T = 98 °C from the T = 16 °C case, while the fractionation factor estimates are roughly 5% lower. Regardless, residual halogenated gas contents for the 16 °C and 98 °C cases agree to within the uncertainty of measurement, indicating that the fractionation model is relatively insensitive to the changes in temperature observed in Kilauea's hydrothermal system, at least for the low-solubility halogenated gases studied here. The residual gas contents for Halemaumau fumarole samples using a fractionated hydrothermal component (T = 16 °C) are presented in Table 6.8.

Table 6.8 Residual halogenated gas content for fumaroles B (#1-2) and C (#3-4), after accounting for addition of ambient air and fractionated hydrothermal gases to sample gas. Boldface values of X_C are within δX_C of zero and are thus negligible. Since SF_6, CFC-11 and CFC-12 were used as constraint, they have zero residual content.

Compound	X_{C1} (pmol)	X_{C2} (pmol)	X_{C3} (pmol)	X_{C4} (pmol)	δX_C (pmol)
CF_4	**0.003**	**-0.03**	**0.005**	**0.006**	0.03
C_2F_6	0.133	0.220	0.090	0.122	0.001
SF_6	**0**	**0**	**0**	**0**	0.001
CCl_3F	**0**	**0**	**0**	**0**	0.1
CCl_2F_2	**0**	**0**	**0**	**0**	–
$CClF_3$	**0.003**	0.005	0.009	0.011	0.003
$CBrF_3$	**-0.002**	**-0.004**	**-0.003**	**0.0001**	0.006
$CBrClF_2$	**-0.01**	-0.07	-0.05	**-0.01**	0.03
C_2HCl_3	0.118	0.336	0.075	0.240	0.001
C_2Cl_4	0.744	3.866	3.346	1.649	0.003
C_2HF_5	2.65	0.24	4.32	5.37	0.02
$C_2Cl_3F_3$	0.90	1.94	1.94	0.94	0.02
C_2ClF_5	0.006	0.009	0.014	0.008	0.003

CF_4, SF_6, CFC-11, CFC-12 and Halon-1301 contents in Halemaumau crater fumarolic emissions can be attributed to air entrainment and to gases exsolved from a fractionated hydrothermal system. CFC-13, Halon-1211 and CFC-115 residuals in the fractionated hydrothermal case are mostly non-zero, but of very similar magnitude to their respective errors, and therefore are probably insignificant. Regardless, a model including a hydrothermal source of halogenated gas that is fractionated according to gas solubility reproduces the observed data well, and explains the elevated CFC-11

content of volcanic gas that has been previously attributed in other locales to a volcanic source.

6.4.4 Constraining volcanic fluxes of CF_4 and SF_6 to the atmosphere

No volcanic source of CF_4 and SF_6 is necessary to explain their observed abundances in fumarolic gas samples collected near Halemaumau crater. Given the strong presence of mantle gas in fumarolic emissions from Kilauea (Hilton et al., 1997), this evidence suggests that there is no significant flux of CF_4 or SF_6 from the mantle to the atmosphere through volcanic emissions.

If an undetected source of volcanic CF_4 and SF_6 exists, its magnitude may be constrained by considering the upper limit to the detectable amount of volcanic CF_4 or SF_6, given as $X_C + \delta X_C$ (Table 6.8). Adding δX_C values for CF_4 and SF_6 to the average of their respective X_C values gives upper limits of 0.02 pmol CF_4 and 0.001 pmol SF_6. The quantity of gas collected from fumaroles near Halemaumau crater ranges from 1.00 to 1.36 moles, based on the mass of gas collected, 22.3 to 27.8 g, and an estimated molecular weight of 21 ± 1 g mol^{-1} for the fumarolic gas. The upper limit to a hypothetical mole fraction of CF_4 and SF_6 in the fumarolic gas is then <0.02 ppt CF_4 and <0.001 ppt SF_6.

The upper limit to a possible volcanic flux of CF_4 and SF_6 from Kilauea, and the upper limit to a possible global volcanic source to the atmosphere can then be estimated, albeit with considerable uncertainty, by analogy to well-constrained gas

fluxes, such as the SO_2 or ^{3}He fluxes from Kilauea (Hilton et al., 1997; Sutton et al., 2001). The SO_2 molar content of fumarolic gases near Halemaumau crater typically ranges from 1.8 – 2.0 % (Goff and McMurtry, 2000; Hurwitz et al., 2003). The maximum hypothetical CF_4/SO_2 and SF_6/SO_2 mole ratios would then be <1.1 and <0.06 pmol/mol, respectively. Sutton et al. (2001) estimate the total SO_2 degassing from Kilauea at 7.2 x 10^9 moles SO_2 yr^{-1}, and thus the flux of CF_4 and SF_6 from Kilauea to the atmosphere is at most <0.008 mole CF_4 yr^{-1} and <0.0004 mole SF_6 yr^{-1}. While Kilauea may be representative of the mantle flux of CF_4 and SF_6 to the atmosphere, it may not represent the total global flux of CF_4 and SF_6 from volcanoes, since it is possible that volcanoes overlying thick sections of the continental crust emit gases that contain continental lithospheric CF_4 and SF_6.

The global mantle flux of CF_4 and SF_6 could be constrained using a more easily identified mantle gas, such as ^{3}He (Porcelli and Ballentine, 2002). The ^{3}He flux from Kilauea has been estimated at 4.2 – 5.9 moles ^{3}He yr^{-1} (Hilton et al., 1997). Assuming that the maximum $CF_4/^3$He and $SF_6/^3$He molar ratios for a hypothetical volcanic flux from Kilauea are representative of their ratios in mantle volatiles, and using a total ^{3}He flux of <2300 mol ^{3}He yr^{-1} (Porcelli and Ballentine, 2002) to the atmosphere, then the global mantle flux of CF_4 and SF_6 would be <3 mol CF_4 yr^{-1} and <0.2 mol SF_6 yr^{-1}. The upper limits to mantle CF_4 and SF_6 fluxes presented here are negligible when compared to the estimated fluxes of (1 – 5) x 10^5 moles CF_4 and (0.9 – 5) x 10^2 moles SF_6 from the continental crust (Deeds et al., 2008).

6.5 Conclusions

A considerable number of halogenated gases, including CF_4 and SF_6, are present in fumarolic gases discharged near Halemaumau crater on Kilauea summit. Most of these gases can be attributed to entrainment of air and addition of gas exsolved from Kilauea's hydrothermal system. Residual CFC-11 that is typically attributed to a volcanic source (Jordan et al., 2000) may be explained by a fractionation of dissolved hydrothermal gases due to prior equilibrium with a vapor phase containing no halogenated gas content. No volcanic source is necessary to explain the observed CF_4 and SF_6 content of fumarolic emissions at Kilauea. The uncertainty in CF_4 and SF_6 analyses constrains the upper limit of a hypothetical mantle flux of these gases to less than 0.01% of the lithospheric flux of CF_4 and SF_6 from the continental crust to the atmosphere, reinforcing the assertion that mantle emissions of CF_4 and SF_6, if present, are an insignificant factor in the global geochemistry of these gases.

6.6 Acknowledgements

I thank K. Phillips for the opportunity to join her student-run field trip to Hawaii to pursue this research. I thank D. Hilton for providing me with a huge amount of excellent advice regarding volcanic gas sampling. I am also grateful to J. Sutton and

6.7 References

Almendros J., Chouet B., and Dawson P. (2001) Spatial extent of a hydrothermal system at Kilauea Volcano, Hawaii, determined from array analyses of shallow long-period seismicity,2, Results. *J. Geophys. Res.* **106,** 13581-13598.

Ballentine C.J., Burgess R. and Marty B. (2002) Tracing fluid origin, transport and interaction in the crust. In *Noble gases in geochemistry and cosmochemistry*, vol. 47 (eds. D. Porcelli, C. J. Ballentine and R. Wieler), Mineral. Soc. Am., Washington D. C. pp. 539-614.

Busenberg E. and Plummer L. N. (2000) Dating young groundwater with sulfur hexafluoride: natural and anthropogenic sources of sulfur hexafluoride. *Water Resour. Res.* **36**, 3011-3030.

Cady, G. H., and Sudhindra M. (1974) Hydrolysis of sulfuryl fluoride. *Inorg. Chem.* **13,** 837-41.

Craig H. (1953) The geochemistry of the stable carbon isotopes. *Geochim. Cosmochim.Acta,* **3** 53-92.

Deeds D. A., Vollmer M. K., Kulongoski J. T., Miller B. R., Mühle J., Harth C. M., Izbicki J. A., Hilton D. R. and Weiss R. F. (2008) Evidence for crustal degassing of CF_4 in Mojave Desert groundwaters. *Geochim. Cosmochim. Acta* **72,** 999-1013.

Frische M., Garofalo K., Hansteen T. H., Borchers R. And Harnisch J. (2006) The origin of stable halogenated compounds in volcanic gases, *Environ. Sci. Pollution Res.* **13**, 406-413.

Gaffney J. S. (1995) Volcanic CFCs. *Environ. Sci. Tech.* **29**, 8A.

Goff F. and McMurtry G. M. (2000) Tritium and stable isotopes of magmatic waters. *J. Volcanol. Geotherm. Res.* **97**, 347-396.

Gribble G. (1995) Author's response. *Environ. Sci. Tech.* **29**, 8A.

Harnisch J. and Eisenhauer A. (1998) Natural CF_4 and SF_6 on Earth. *Geophys. Res. Lett.* **25**, 2401-2404.

Hilton D. R., McMurtry G. M. and Kreulen R. (1997) Evidence for extensive degassing of the Hawaiian mantle plume from helium-carbon relationships at Kilauea volcano. *Geophys. Res. Lett.* **24**, 3065-3068.

Hurwitz S., Goff F., Janik C. J., Evans W. C., Counce D. A., Sorey M. L. and Ingebritsen S. E. Mixing of magmatic volatiles with groundwater and interaction with basalt on the summit of Kilauea Volcano, Hawaii. *J. Geophys. Res.* 108(B1), 2028, doi:10.129/2001JB001594, 2003.

Isidorov V. A. (1995) Isidorov's response. *Environ. Sci. Tech.* **29**, 8A.

Jordan A., Harnisch J., Borchers R., Le Guern F. and Shinohara H. (2000) Volcanogenic halocarbons, *Environ. Sci. Technol.* **34**, 1122-1124.

Miller B. R., Weiss R. F., Salameh P. K., Tanhua T., Greally B. R., Mühle J. and Simmonds P. G. (2008) Medusa: a sample preconcentration and GC/MS detector system for in situ measurements of atmospheric trace halocarbons, hydrocarbons and sulfur compounds, *Anal. Chem.* **80**, 1536 – 1545.

Nullet D. and Sanderson M. (1993) Radiation and energy balances and air temperature. In: *Prevailing Trade Winds, Weather and Climate in Hawaii*, University of Hawaii Press, Honolulu, Hawaii, pp. 37 – 56.

O'Hagan D. (2008) Understanding organofluorine chemistry. An introduction to the C-F bond. *Chem. Soc. Rev.* **37**, 308-319.

Porcelli D. and Ballentine C. J. (2002) Models for the distribution of terrestrial noble gases and the evolution of the atmosphere, In *Noble gases in geochemistry and cosmochemistry*, vol. 47 (eds. D. Porcelli, C. J. Ballentine and R. Wieler), Mineral. Soc. Am., Washington D. C. pp. 411-480.

Prinn R.G., Weiss R. F., Fraser P. J., Simmonds P. G., Cunnold D. M., Alyea F. N., O'Doherty S., Salameh P., Miller B. R., Huang J., Wang R. H. J., Hartley D. E., Harth C., Steele L. P., Sturrock G., Midgley P. M. and McCulloch A. (2000) A history of chemically and radiatively important gases in air deduced from ALE/GAGE/AGAGE. *J. Geophys. Res.* **105 (D14)**, 17751-17792.

Reynolds G. W., Hoff J. T. and Gillham R. W. (1990) Sampling Bias Caused by Materials Used to Monitor Halocarbons in Groundwater. *Environ. Sci. Technol.* **24**, 135-142.

Sutton A. J., Elias T., Gerlach T. M. and Stokes J. B. (2001) Implications for eruptive processes as indicated by sulfur dioxide emissions from Kilauea Volcano, Hawaii, 1979 – 1997. *J. Volcanol. Geotherm. Res.*, **108**, 283-302.

Trew M., O'Sullivan M. J. and Yasuda Y. (2001) Modeling the phase partitioning behavior of gas tracers under geothermal reservoir conditions. *Geothermics* **30**, 655-695.

Vollmer M. K. and Weiss R. F. (2002) Simultaneous determination of sulfur hexafluoride and three chlorofluorocarbons in water and air. *Mar. Chem.* **78**, 137-148.

Welhan J. A., Poreda R. J., Rison W. and Craig H. (1988) Helium isotopes in geothermal and volcanic gases of the western United States, I. Regional Variability and magmatic origin. *J. Volcanol. Geotherm. Res.* **34**, 185-199.

Chapter 7

Tetrafluoromethane in the deep North Pacific Ocean

7.1 Abstract

Dissolved tetrafluoromethane (CF_4) has been measured for the first time in the North Pacific Ocean. Surface water collected during calm weather is near equilibrium with the modern atmosphere. Deep water, isolated from atmospheric exchange for centuries, is near equilibrium with the preindustrial atmosphere, after accounting for an expected 5% addition of this low-solubility gas due to air injection during high-latitude deep-water formation. These results strongly suggest that dissolved CF_4 is conservative in seawater and that the oceanic imprint of anthropogenic increases in atmospheric CF_4 can be used as a time-dependent tracer of ocean ventilation and subsurface circulation processes. Although the continental lithosphere is a source of natural atmospheric CF_4, we find no evidence of an oceanic lithospheric CF_4 input into deep Pacific waters. The estimated upper limit of a potential oceanic lithospheric CF_4

flux to the global atmosphere is on the order of 2.5% of that from the continental lithosphere.

7.2 Introduction

Dissolved chlorofluorocarbons (CFCs) such as CFC-12 (CCl_2F_2) and CFC-11 (CCl_3F) are used widely as time-dependent tracers of oceanic ventilation, mixing and circulation processes (e.g., Weiss et al., 1985; Warner et al., 1996), since they are relatively inert in seawater, their seawater solubilities are known, and their atmospheric histories are well-documented (Walker et al., 2000). However, international regulations imposed by the Montreal Protocol on Substances that Deplete the Ozone Layer and its subsequent amendments (UNEP, 2006) have severely curtailed emissions of these compounds to the atmosphere. As a result, atmospheric abundances of CFCs are no longer rising as they did before regulation and are now beginning to decline according to the balance between their atmospheric lifetimes and greatly reduced remnant emissions (Prinn et al., 2000). These changes have reduced the usefulness and complicated the interpretation of dissolved atmospheric CFC-12 or CFC-11 as time-dependent ocean tracers, especially for waters that have acquired their CFC signatures since the Montreal protocol came into force in the late 1980s.

A potential alternative tracer is dissolved atmospheric tetrafluoromethane (CF_4), an effectively inert trace gas with an estimated atmospheric lifetime of >50,000

years (Ravishankara et al., 1993). The atmospheric abundance of CF_4 has roughly doubled over the past three-quarters of a century due to aluminum production and other industrial activity, as is documented by our laboratory and by others (Harnisch et al., 1996; Worton et al., 2007) based on measurements of air trapped in polar firn layers and recent atmospheric measurements. As is done with CFC tracers (Doney and Bullister, 1992), apparent water mass ages could be estimated by comparing the partial pressure of CF_4 in equilibrium with a water parcel (pCF_4) with the atmospheric history of CF_4.

Since the atmospheric lifetime of CF_4 is very long, the preindustrial natural atmospheric abundance of CF_4 may be explained by relatively minor natural emissions from the solid Earth. CF_4 is naturally present in granites and fluorites in the continental crust (Harnisch and Eisenhauer, 1998; Harnisch et al., 2000), and Deeds et al. (2008) have shown that CF_4 liberated by weathering and alteration is transported out of the continental lithosphere to the atmosphere by groundwater fluid flow. If similar CF_4 emissions occur from the oceanic mantle, crust, or overlying sediments, then CF_4 would be expected to accumulate in the deep ocean, especially in the deep Pacific where water residence times are long, in a manner analogous to the accumulation of dissolved crustal and mantle helium in the deep Pacific (e.g., Lupton, 1998). By comparing the deep Pacific CF_4 concentration with the concentration expected in these waters as a result of their exposure to the preindustrial atmosphere it should be possible to assess the role of the oceanic lithosphere as a potential source of atmospheric CF_4, as well as assessing the extent to which lithospheric sources may

complicate the use of the anthropogenic increase in atmospheric CF_4 as a time-dependent tracer of oceanic ventilation processes.

Although present methods for measuring dissolved CF_4 with the required sub-femtomolar precision are time-consuming and require large water samples, and are not yet suitable for high spatial resolution oceanic tracer studies, they are quite suitable for evaluating the potential of further work in this area and for assessing the existence of a potential CF_4 source from the oceanic lithosphere.

7.3 Methods

North Pacific Deep Water (NPDW) samples were collected in 10 liter Niskin PVC bottles from ~2000 m depth near the Hawaii Ocean Time-series (HOT) ALOHA station (~23°N, ~158°W), in the North Pacific subtropical Gyre, as part of a HOT-affiliated cruise in early December of 2006. NPDW samples were immediately sub-sampled in 2 L aliquots into evacuated 2.5 L glass flasks. Only 4 – 5 L of seawater were drawn from each bottle (i.e. two 2 L samples plus flushing) in order to avoid collection of seawater contaminated with modern air in the upper portion of the Niskin bottle. Seawater samples were extracted and measured in our laboratory at the Scripps Institution of Oceanography (SIO) in the subsequent weeks. The loss of several flasks to breakage during transport left only sufficient flasks for two NPDW CF_4 analyses. Surface seawater samples collected in a 10 liter Niskin bottle at roughly 5 m depth off the SIO pier (~32°N, ~117°W) were extracted using similar methods.

In the laboratory, the headspaces of three flasks were extracted and combined into an evacuated cold finger immersed in liquid helium, so that each measurement is based on ~6 L of seawater. Due to its low solubility (Scharlin and Battino, 1995), almost all the CF_4 in each seawater sample (>99%) was present in the headspace of its flask, so only a small correction was necessary to account for residual dissolved CF_4 left in each sample after extraction. The cold finger was removed from the liquid helium, warmed to the touch and the collected gases were transferred to the "Medusa" cryotrapping quadrupole gas chromatograph/mass spectrometer (GC/MS) system (Miller et al., 2008) for CF_4 analysis. Results are blank-corrected, and are calibrated using a known 1 L volume of whole air standard with an assigned CF_4 dry-air mixing ratio of 75.0 ± 0.4 ppt (parts per trillion), based on the SIO-2005 gravimetric calibration scale (Prinn et al., 2000; C. Harth, personal communication). The analytical precision of our dissolved CF_4 measurements in seawater is estimated at ±3%, based on a propagation of errors, and is of similar magnitude to the reproducibility of duplicate groundwater samples containing similar molar quantities of CF_4 to seawater samples in this study (Deeds et al., 2008).

In addition to CF_4, the Medusa-GC/MS simultaneously measures a broad suite of halogenated gases, including SF_6, CFC-12 and CFC-11. Since there are no known natural sources of CFC-12 and CFC-11 (Butler et al., 1999), and since SF_6 is undetectable at ALOHA station below 1000 m depth (Bullister et al., 2006), measured SF_6 and CFC concentrations can be used to constrain modern contributions to seawaters that last equilibrated with the preindustrial atmosphere. SF_6 is not released

from degassing of polymers (Busenberg and Plummer, 2000), and so it provides a check against sampling artifacts that might prevent reliable interpretation of the CFC data. Measured SF_6, CFC-12 and CFC-11 concentrations for NPDW samples in this study are 0.27 – 0.29 fmol SF_6 kg^{-1} H_2O and 0.02 - 0.04 pmol CFC kg^{-1} H_2O for both CFCs. Molar ratios of these gases lie between the molar ratios for modern air and modern seawater (e.g. molar CFC-12/CFC-11 ratios are ~0.9, lying between the molar ratios of ~2 for modern air and ~0.5 for modern seawater). A two end-member mixing model between modern air and modern water contaminants can therefore be used to describe the observed SF_6 and CFC concentrations.

Accordingly, the amount of modern air and water present in our NPDW samples are 0.6 – 0.9 cm^3 air STP kg^{-1} H_2O and 4 – 5 g H_2O kg^{-1} sample, corresponding to a contaminant contribution to measured CF_4 concentrations of roughly 2 – 3 fmol CF_4 kg^{-1} H_2O. Modern air contaminant concentrations are of similar magnitude to modern air contamination observed previously for this analytical technique (Deeds et al., 2008) and probably result from entrainment of small quantities of lab air during dissolved gas extraction and analysis. Modern water contamination concentrations reflect the mixing of small amounts of water in contact with the modern atmosphere from the upper portion of Niskin bottles into samples collected from the lower reaches of the bottle. We estimate the error in the CF_4 contamination corrections at ±0.2 fmol CF_4 kg^{-1} H_2O (i.e. roughly ±10% of the estimated corrections), which increases the total error of reported contaminant-corrected CF_4 concentrations for NPDW to ±4%.

7.4 Results

Measured CF$_4$ concentrations, [CF$_4$], and expected equilibrium CF$_4$ concentrations, [CF$_4$]*, for surface and deep Pacific seawater are listed in Table 1, together with the percentage supersaturation of CF$_4$ in collected samples (ΔCF$_4$), defined as:

$$\Delta CF_4 = \left(\frac{[CF_4]}{[CF_4]^*} - 1 \right) \cdot 100 \qquad (1)$$

Equilibrium CF$_4$ concentrations are calculated from measured salinities (S) and potential temperatures (θ) assuming a sea surface pressure of 1 atmosphere. Deep Pacific seawater samples were assumed to be in equilibrium with a mean preindustrial atmospheric CF$_4$ dry air mole fraction of 34.8 $\pm$ 0.2 ppt based on analyses in our laboratory (J. Mühle, personal communication) of ancient air in Greenland ice and Antarctic firn. This preindustrial atmospheric CF$_4$ background agrees well with published literature values (Harnisch et al., 1996; Worton et al., 2007). Surface seawater samples were assumed to be in equilibrium with the mean atmospheric CF$_4$ mole fractions for the month prior to sampling, as calculated from routine air CF$_4$ analyses by Medusa-GC/MS at SIO.

The solubility of CF$_4$ in seawater has received little attention, with only four measurements available in the literature, covering a range of 15 – 30°C and a salinity of 35.086 psu (Scharlin and Battino, 1995). For this study, we derived Ostwald

solubility coefficients for CF_4 in seawater as a function of both salinity and temperature by modifying fitted freshwater solubility data (Clever et al., 2005) with the Setschenow equation:

$$\ln\left(\frac{L}{L_0}\right) = k_s \cdot S \qquad\qquad (7.2)$$

where L and L_o are the seawater and freshwater solubilities, k_s is the salting-out coefficient and S is the salinity. Salting-out coefficients for CF_4 as a function of temperature were also obtained from the Setschenow equation using the seawater and freshwater data of Scharlin and Battino (1995). The standard error of seawater CF_4 solubility estimates for this method, in Ostwald solubility units, is ±0.0001, or roughly ±2% on average. This is the major source of error in calculated CF_4 solubilities, and results mainly from the considerable disagreement (up to 5%) between compiled freshwater CF_4 solubilities at low temperatures (<20°C).

There is good agreement between measured and equilibrium CF_4 concentrations in surface seawater samples. Measured CF_4 concentrations are on average (0.8 ± 2) % undersaturated with respect to atmospheric equilibrium (Table 1). Sparingly soluble gases tend to be supersaturated in seawater due to the dissolution of air bubbles submerged by wave action, or "air injection" (Craig and Weiss, 1971; Hamme and Emerson, 2002), but calm weather during sampling (average wind speeds of about 2 m s^{-1}) may explain a relatively small air injection contribution to our surface water samples. Our surface seawater results therefore suggest that the

analytical method used here measures CF_4 seawater concentrations with a systematic uncertainty on the order of 2%. Although our deep Pacific seawater CF_4 measurements are limited in number, they represent mean CF_4 concentrations in these deep Pacific seawaters with a similar systematic uncertainty.

7.5 Discussion

Measured dissolved CF_4 concentrations in deep Pacific seawater are oversaturated with respect to seawater in equilibrium with the preindustrial atmospheric CF_4 background (Table 1). To estimate the supersaturation of CF_4 during deep water formation, we use the quasi-steady-state mixed-layer model of Schudlich and Emerson (1996). The model includes diffusive gas exchange with the atmosphere, seawater temperature changes, and air-injection. Air injection is modeled as a combination of completely collapsing small bubbles, and large bubbles that only partially dissolve before returning to the atmosphere. When the mixed-layer model of Schudlich and Emerson (1996) is constrained using measured neon and argon saturations at 2000 m depth at ALOHA station (Hamme and Emerson, 2002; Hamme and Severinghaus, 2007), the CF_4 supersaturation during deep water formation is $(5 \pm 1)\%$, which is consistent with the observed CF_4 supersaturation of $(4 \pm 3)\%$.

CF_4 is thought to be inert in the oceans on timescales of thousands of years (Cicerone, 1979; Ravishankara et al., 1993). However, we cannot completely discount the possibility that an oceanic sink of CF_4 exists which coincidentally balances an

Table 7.1 North Pacific deep (ALOHA) and surface (SIO) North Pacific seawater CF_4 results. ΔCF_4 is the percentage supersaturation of the measured CF_4 concentration $[CF_4]$ relative to the saturation value, $[CF_4]^*$, expected in equilibrium with the listed preindustrial and modern atmospheric CF_4 dry air mole fractions $x(CF_4)$ for deep and surface waters, respectively (see text). θ is the potential temperature, S is the salinity, and z is the depth. Errors for mean values are the root-mean-squares of the individual errors.

Location	Sample Date	θ (°C)	S (psu)	$x(CF_4)$ (ppt)	$[CF_4]^*$ (fmol CF_4 kg^{-1})	$[CF_4]$ (fmol CF_4 kg^{-1})	ΔCF_4 (%)
ALOHA 23°N 158°W z ≈ 2000 m	14 Dec. 2006	1.91 ± 0.01	34.61 ± 0.01	34.8 ± 0.2	11.1 ± 0.3	12.0 ± 0.5	8.1 ± 5
						11.1 ± 0.5	0 ± 5
						Mean	4.0 ± 3
	8 Dec. 2006	16.48 ± 0.05	33.44 ± 0.02	76.6 ± 0.2	15.4 ± 0.3	15.4 ± 0.6	0 ± 4
SIO 32°N 117°W z ≈ 5 m						16.0 ± 0.6	−1.2 ± 4
	28 Feb. 2007	14.7 ± 0.2	33.34 ± 0.02	76.7 ± 0.1	16.2 ± 0.3	16.3 ± 0.6	0.6 ± 4
							−2.5 ± 4
						Mean	−0.8 ± 2

oceanic source of CF_4 at 2000 m depth at ALOHA station, thus producing an artificial agreement between the observed and estimated supersaturation of CF_4 in deep Pacific seawaters. Regardless, the most straightforward and most likely explanation remains that CF_4 is conservative in seawater, and that the agreement between measured and expected deep Pacific CF_4 seawater concentrations therefore shows no evidence of a significant oceanic lithospheric source of CF_4.

To consider whether a significant oceanic source may be hidden solely by analytical limitations, we constrain the upper limit to a hypothetical oceanic CF_4 source by comparing the measured and predicted CF_4 supersaturations at the extreme range of their positive and negative uncertainties, respectively. This comparison yields a maximum of 3% of the measured $[CF_4]$ value, or 0.35 fmol CF_4 kg^{-1} H_2O. If this CF_4 excess is assumed to originate from an ubiquitous lithospheric source emanating from the oceanic crust, and if the excess accumulates over a time period on the order of 1400 years, as estimated from radiocarbon measurements (Key et al., 2004), then the oceanic CF_4 source must contribute less than $\sim 2.5 \times 10^{-4}$ fmol CF_4 kg^{-1} H_2O per year.

If one assumes that this flux is characteristic of the roughly 1.0×10^{21} kg of seawater that lie below the ~1 km depth of surface and intermediate waters in the deep basins of the world ocean, then the hypothetical global flux of CF_4 into the deep ocean from the oceanic lithosphere is constrained to an upper limit on the order of 250 mol CF_4 per year. The continental lithospheric flux of CF_4 to the atmosphere is estimated at $(1 - 5) \times 10^4$ moles CF_4 per year (Deeds et al., 2008). If an oceanic source of CF_4

exists it is therefore at most only about 2.5% of the continental flux, indicating that weathering and alteration of the continental crust are the dominant sources of natural CF_4 to the atmosphere (Harnisch and Eisenhauer, 1998). This is consistent with the lack of detectable amounts of CF_4 in mafic rocks (Harnisch and Eisenhauer, 1998; Harnisch et al., 2000) and volcanic gases (Jordan et al., 2000; Frische et al., 2007), which suggest that neither the oceanic crust nor the mantle are significant sources of CF_4. It may still be possible that in coastal oceans dissolved CF_4 seawater concentrations are elevated due to release from underlying continental crust or from mixing with groundwaters discharging from the continents, but more research is necessary to show if this is the case.

The long exchange time of radiocarbon in the surface ocean with the atmosphere, and the introduction of radiocarbon with remineralization of sinking organic material at depth may bias the radiocarbon-based estimate of the length of time over which lithospheric gases may accumulate in deep seawaters. A better age tracer for deep seawaters for the purposes of this discussion may be ^{39}Ar, since it is entirely gas-based and enters the oceans solely from exchange with the atmosphere (Loosli, 1983). The argon-39 age of deep Pacific seawater at ALOHA station at 2.2 km depth is 790 years (Loosli, 1989), which is significantly younger than the radiocarbon age (~1400 years) for NPDW at this location. The upper limit to a hypothetical ocean lithospheric flux of CF_4 into the oceans, constrained with the ^{39}Ar age, would be 440 mol yr^{-1}, or ~4% of the lithospheric CF_4 flux from the continents. Although this is somewhat larger than the upper limit to the oceanic CF_4 flux

estimated using the ^{14}C age of NPDW at ALOHA station, the main conclusion that there is no evidence for an oceanic source of CF_4 is unchanged.

According to Worton et al. (2007) the atmospheric mole fraction of CF_4 increased from 40 ppt to 78 ppt between 1955 and 2003. This change would increase surface seawater CF_4 concentrations by about 7.7 fmol CF_4 kg^{-1} H_2O, based on our analysis of CF_4 solubility and assuming a mean global sea surface temperature of 16°C and salinity of 35 psu, with a mean growth rate of about 0.16 fmol CF_4 kg^{-1} H_2O per year. For the duplicate measurement technique used here this corresponds to a precision of ~3 years in apparent pCF_4 age over this period. Improvements in measurement technique would reduce this uncertainty proportionally.

7.4 Conclusion

Measured concentrations of CF_4 in surface seawaters during calm weather are in equilibrium with modern atmospheric CF_4 mole fractions. Deep Pacific seawaters contain CF_4 concentrations slightly in excess of those expected for equilibrium with the preindustrial atmospheric CF_4 mole fraction, due mainly to injection of air bubbles into surface seawaters during deep water formation. No oceanic lithospheric source is required to explain our measurements of dissolved CF_4 in the deep Pacific Ocean. We estimate from these first results that the upper limit of a potential oceanic lithospheric CF_4 flux to the atmosphere is on the order of 4% of that from the continental lithosphere. Within the limits of our analytical methods, dissolved atmospheric CF_4 is

conservative in the oceans over time scales of 10^3 years, and is therefore a suitable anthropogenic time-dependent tracer of ocean ventilation and subsurface circulation processes that involve waters that have been exposed to the atmosphere since the onset of anthropogenic CF_4 emissions. Unlike the case for the use of anthropogenic CFCs as ocean tracers, the existence of a natural atmospheric CF_4 background makes it possible to verify the conservativeness of this tracer directly from ocean measurements. Measurements of dissolved CF_4 at other locations and depths will be useful in further testing the conclusions we have drawn from these first observations of dissolved oceanic CF_4 distributions.

7.5 Acknowledgements

Chapter 7 is submitted for publication as Deeds D. A., J. Mühle and R. F. Weiss (2008) Tetrafluoromethane in the deep North Pacific Ocean, *Geophys. Res. Lett.*, in review. I collected the deep and surface seawater samples presented in the manuscript,

measured their dissolved CF_4 concentrations by GC/MS, interpreted the results and prepared this manuscript.

7.6 References

Bullister, J.L., D.P. Wisegarver and R.E. Sonnerup, (2006), Sulfur Hexafluoride as a Transient Tracer in the North Pacific Ocean. Geophys. Res. Lett., vol 33, doi: 10.1029/2006GL026514, 2006

Busenberg, E. and L. N. Plummer (2000) Dating young groundwater with sulfur hexafluoride: Natural and anthropogenic sources of sulfur hexafluoride, *Water Resources Research* **36**, 3011 – 3030.

Butler, J. H., M. Battle, M. L. Bender, S. A. Montzka, A. D. Clarke, E. S. Saltzman, C. M. Sucher, J. P. Severinghaus and J. W. Elkins (1999), A record of atmospheric halocarbons during the twentieth century from polar firn air, *Nature* **399**, 749–755.

Cicerone R. J. (1979) Atmospheric carbon tetrafluoride: a nearly inert gas, *Science* **206**, 59–61.

Clever, H. L., R. Battino, B. Jaselskis, Y. P. Yampolskii, P. Scharlin and C. L. Young (2005), IUPAC-NIST solubility data series 80. Gaseous fluorides of boron, nitrogen, sulfur, carbon and silicon and solid xenon fluorides in all solvents, *J. Phys. Chem. Ref. Data* **34**, 201–435.

Craig, H. and R. F. Weiss (1971), Dissolved gas saturation anomalies and excess helium in the ocean, *Earth Planet. Sci. Lett.* **10**, 289–296.

Deeds D. A., Vollmer M. K., Kulongoski J. T., Miller B. R., Mühle J., Harth C. M., Izbicki J. A., Hilton D. R. and Weiss R. F. (2008) Evidence for crustal degassing of CF_4 in Mojave Desert groundwaters. *Geochim. Cosmochim. Acta* **72,** 999-1013.

Doney, S. C., and J. L. Bullister (1992), A chlorofluorocarbon section in the eastern north-Atlantic, *Deep-Sea Res. I* **39**, 1857–1883.

Frische, M., K. Garofalo, T. H. Hansteen, R. Borchers and J. Harnisch (2006), The origin of stable halogenated compounds in volcanic gases, *Environ. Sci. Poll. Res.* **13**, 406–413.

Hamme, R. C., and S. R. Emerson (2002), Mechanisms controlling the global oceanic distribution of the inert gases argon, nitrogen and neon, *Geophys. Res. Lett.* **29**, 2120, doi: 10.1029/2002GL015273.

Hamme, R. C., and J. P. Severinghaus (2007), Trace gas disequilibria during deep-water formation, *Deep-Sea Res., A* **54**, 939–950.

Harnisch, J., and A. Eisenhauer (1998), Natural CF_4 and SF_6 on Earth, *Geophys. Res. Lett.* **25**, 2401–2404.

Harnisch, J., R. Borchers, P. Fabian and M. Maiss (1996), Tropospheric trends for CF_4 and C_2F_6 since 1982 derived from SF_6 dated stratospheric air, *Geophys. Res. Lett.* **23**, 1099–1102.

Harnisch, J., M., Frische, R. Borchers, A. Eisenhauer and A. Jordan (2000), Natural fluorinated organics in fluorite and rocks, *Geophys. Res. Lett.* **27**, 1883–1886.

Jordan, A., J., Harnisch, R. Borchers, F. Le Guern and H. Shinohara (2000), volcanogenic halocarbons, *Environ. Sci. Technol.* **34**, 1122–1124.

Key, R. M., A. Kozyr, C. L. Sabine, K. Lee, R. Wanninkhof, J. L. Bullister, R. A. Feely, F. J. Millero, C. Mordy, and T. H. Peng (2004), A global ocean carbon climatology: results from Global Data Analysis Project (GLODAP), *Global Biogeochem. Cycles* **18**, GB4031, doi: 10.1029/2004GB002247.

Loosli H. H. (1983) A dating method with ^{39}Ar, *Earth and Planet. Sci. Lett.* **63**, 51 – 62.

Loosli H. H. (1989) Ar: A tool to investigate ocean water circulation and mixing, in *Handbook of Environmental Isotope Chemistry*, vol. 3, *The Marine Environment* (Eds: P. Fritz and J. C. Fontes), Elsevier Sci., New York, pp. 385 – 392.

Lupton, J. (1998), Hydrothermal helium plumes in the Pacific Ocean, *J. Geophys. Res.* **103**, 15,853–15,868.

Miller B. R., Weiss R. F., Salameh P. K., Tanhua T., Greally B. R., Mühle J. and Simmonds P. G. (2008) Medusa: a sample preconcentration and GC/MS detector system for in situ measurements of atmospheric trace halocarbons, hydrocarbons and sulfur compounds, *Anal. Chem.* **80**, 1536 – 1545.

Prinn, R.G., R. F. Weiss, P. J. Fraser, P. G. Simmonds, D. M. Cunnold, F. N. Alyea, S. O'Doherty, P. Salameh, B. R. Miller, J. Huang, R. H. J. Wang, D. E. Hartley, C. Harth, P. L. Steele, G. Sturrock, P. M. Midgley and A. McCulloch (2000), A

history of chemically and radiatively important gases in air deduced from ALE/GAGE/AGAGE, *J. Geophys. Res.* **105**, 17,751–17,792.

Ravishankara, A. R., S. Solomon, A. A. Turnipseed and R. F. Warren (1993), Atmospheric lifetimes of long-lived halogenated species, *Science* **259**, 194–199.

Scharlin, P., and R. Battino (1995), Solubility of CCl_2F_2, $CClF_3$, CF_4 and CH_4 in water and seawater at 288.15 – 303.15K and 101.325 kPa, *J. Chem. Eng. Data* **40**, 167–169.

Schudlich, R., and S. Emerson (1996), Gas supersaturation in the surface ocean: the roles of heat flux, gas exchange and bubbles, *Deep-Sea Res., II* **43**, 569–589.

UNEP (United Nations Environment Programme) (2006), *Handbook for the Montreal Protocol on Substances that Deplete the Ozone Layer*, 7th Edition, Ozone Secretariat, UNEP, Nairobi.

Walker, S. J., R. F. Weiss and P. K. Salameh (2000), Reconstructed histories of the annual mean atmospheric mole fractions for the halocarbons CFC-11, CFC-12, CFC-113, and carbon tetrachloride, *J. Geophys. Res.* **105**, 14,285–14296.

Warner, M. J., J. L. Bullister, D. P. Wisegarver, R. H. Gammon and R. F. Weiss (1996), Basin-wide distributions of chlorofluorocarbons CFC-11 and CFC-12 in the north Pacific: 1985-1989, *J. Geophys. Res.* **101**, 20,525–20,542.

Weiss, R. F., J. L. Bullister, R. H. Gammon and M. J. Warner (1985), Atmospheric chlorofluoromethanes in the deep equatorial Atlantic, *Nature* **314,** 608–610.

Worton, D. R., W. T. Sturges, L. K. Gohar, K. P. Shine, P. Martinerie, D. E. Oram, S. P. Humphrey, P. Begley, L. Gunn, J.-M. Barnola, J. Schwander and R. Mulvaney (2007), Atmospheric trends and radiative forcings of CF_4 and C_2F_6 inferred from firn air, *Environ. Sci. Technol.* **41**, 2,184–2,189.

Chapter 8

Concluding Remarks

In this thesis, I present the first measurements of tetrafluoromethane in waters drawn from the ocean and continents, and add to the limited number of sulfur hexafluoride measurements previously available for continental groundwaters (Busenberg and Plummer, 2000). Dissolved tetrafluoromethane and sulfur hexafluoride concentrations in Mojave Desert groundwaters provide in-situ evidence for a lithospheric source of these gases to the atmosphere. I also present measurements of CF_4 and SF_6, as well as a broad suite of halogenated gases in fumarolic emissions from Kilauea volcano, and attribute their presence to air and hydrothermal sources, adding to the body of evidence that volcanoes are not a significant source of halogenated gases to the atmosphere (Jordan et al., 2000; Frische et al., 2008). My measurements of dissolved CF_4 concentrations in deep seawaters demonstrate the conservative nature of CF_4 in seawater, showing the potential of CF_4 as a time-dependent tracer of ocean circulation and mixing processes and indicating that the oceanic crust is not a significant source of atmospheric CF_4.

As discussed in Chapters 4 and 5, almost all groundwaters studied contain concentrations of tetrafluoromethane and sulfur hexafluoride in excess of equilibrium

133

concentrations at the conditions of recharge, indicating subsurface sources of these gases. The spatial variability in excess CF_4 and SF_6 in groundwaters can be explained by a combination of two subsurface processes: i) release during the weathering of granitic aquifer material and ii) advection into the aquifer through the underlying basement (a "crustal flux" of CF_4 and SF_6). The crustal flux of CF_4, but not SF_6, is elevated in groundwaters drawn from the vicinity of active faults in the Mojave Desert, suggesting that CF_4 is released from the deep crust during tectonically-driven fracture events, similar to the release of deep crustal ^{4}He (Kulongoski et al., 2003; 2005). When these groundwater measurements are extrapolated to the global scale and combined with the estimated global weathering flux of these gases (Harnisch and Eisenhauer, 1998), the resulting lithospheric fluxes to the atmosphere can explain the measured preindustrial atmospheric abundances of CF_4 and SF_6.

In Chapter 6, I show that the tetrafluoromethane and sulfur hexafluoride content of fumarolic emissions from Kilauea volcano can be attributed to entrainment of air into rising magmatic volatiles, arguing against the presence of a volcanic flux of these gases from the mantle to the atmosphere. Halogenated gases present in collected volcanic gases are derived not only from entrained air but also from the hydrothermal system of Kilauea summit. The mole ratios of halogenated gases in fumarolic emissions from Kilauea summit indicate that Kilauea's hydrothermal system has been fractionated due to equilibrium with a vapor phase free of these halogenated gases. An excess of trichlorofluoromethane (CFC-11) in volcanic emissions, which has been

previously attributed to a volcanic source (Jordan et al., 2000), can instead be explained by a fractionated hydrothermal source.

Dissolved CF_4 concentrations in deep North Pacific seawaters presented in Chapter 7 are supersaturated with respect to equilibrium with the preindustrial atmosphere. The degree of CF_4 supersaturation in deep seawater, ~4%, can be attributed to the entrainment and partial dissolution of air bubbles into surface waters prior to deep-water formation. There is no evidence for an oceanic lithospheric source of CF_4 to the atmosphere, CF_4 is conservative in seawater, and therefore dissolved anthropogenic CF_4 concentrations may be used as a time-dependent tracer of ocean circulation processes. This finding is especially valuable to the oceanographic community, as recent emissions regulations have reduced the usefulness of dissolved CFC-12 and CFC-11 as ocean tracers. If an oceanic source of CF_4 exists, it is less than ~4% of the continental lithospheric flux to the atmosphere.

The global picture that emerges from the work presented in this thesis is that, of all the regions of the lithosphere, only the continental crust is a significant natural source of CF_4 (and SF_6) to the atmosphere (Figure 8.1). Based on the lithospheric flux of CF_4 estimated in Chapter 4, $(1 - 5) \times 10^4$ mol CF_4 yr^{-1}, the lifetime of CF_4 in the preindustrial atmosphere is $100 - 620$ kyr. The previous range of preindustrial atmospheric lifetimes for CF_4, estimated from a lithospheric flux estimate of $0.1 - 1$ t CF_4 yr^{-1} (Harnisch and Eisenhauer, 1998), is $550 - 5,500$ kyr, which is inconsistent with the best estimate preindustrial CF_4 lifetime of 110 kyr (Ravishankara et al., 1993; Morris et al., 1995). However, the range of preindustrial atmospheric lifetimes

estimated from the work presented in this thesis encompasses this best estimate atmospheric lifetime, and thus represents a significant step toward understanding the natural geochemistry of CF_4.
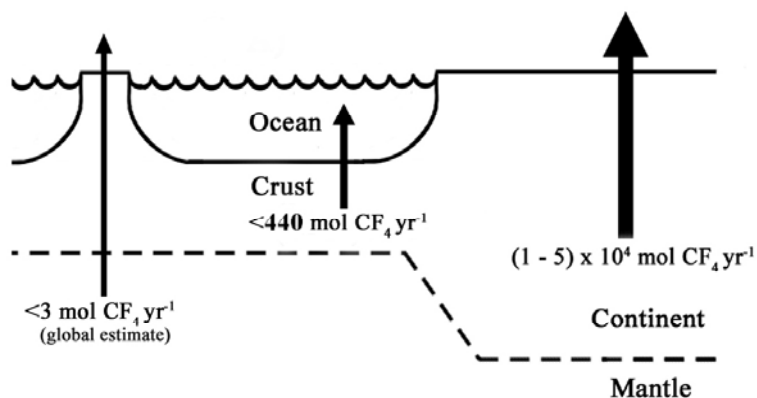
Figure 8.1 A cartoon of the lithospheric CF_4 flux to the atmosphere, including upper constraints to the flux of CF_4 from the mantle and the oceanic crust. The continental crust flux estimate is extrapolated from crustal CF_4 fluxes into Mojave Desert groundwaters (Chapter 4).

The atmospheric lifetime of CF_4 in the modern atmosphere has been estimated to be 50 kyr, based solely on loss of CF_4 to high temperature combustors at the Earth's surface (Ravishankara et al., 1993). If the natural sinks of CF_4 are considered in parallel to its loss to high temperature combustion, then the range of probable modern atmospheric lifetimes is 28 – 46 kyr. Atmospheric CF_4 lifetimes in this range have the same effect on the 100-year timescale used by policymakers for comparative studies of greenhouse gas Global Warming Potentials (Forster et al., 2007). However, these results indicate that the lasting climate forcing associated with CF_4 emissions may persist for only about half as long as previously anticipated.

There is a significant amount of research yet to be done to build upon the results presented in this thesis. A more sensitive study of the CF_4 and SF_6 content of granitic rocks is clearly necessary given the frequency with which SF_6 has remained undetected in granites. The discussion of Chapter 4 and Chapter 5 depends heavily on the assumed constancy of $CF_4/^4He$ and $SF_6/^4He$ molar ratios in granites in the crust, and so concurrent measurement of He and other noble gases in granites from locations outside the Mojave Desert are needed to verify the global lithospheric CF_4 and SF_6 degassing estimates presented herein. Harnisch et al. (2000) propose the presence of small quantities of CFC-11 and CFC-12 in granites. If this were verified by further measurements it could reveal the chemical mechanisms responsible for the formation of CF_4 in the fluid inclusions of granites.

Further measurements of CF_4 and SF_6 in groundwaters should help constrain global weathering fluxes of these gases. Measurement of CF_4 and SF_6 concentrations in a non-granitic aquifer could provide support evidence for the crustal degassing mechanism proposed in Chapter 4. SF_6 concentrations have been shown to be elevated in carbonate aquifers (Busenberg and Plummer, 2000), so it would be interesting to measure CF_4 concentrations in these groundwaters as well.

Evidence against a volcanic source of CF_4 and SF_6 could be strengthened by the measurement of the CF_4 and SF_6 content of emissions from a volcano overlying a thick section of continental crust. Further CFC measurements at other locations besides Kilauea may confirm that CFC-11 excesses commonly observed in volcanic emissions are a result of the exsolving of gases from a hydrothermal source whose

dissolved gases have been fractionated as a result of previous equilibrium with a CFC-free vapor phase.

Although CF_4 has been shown to be conservative in seawater, the analytical technique presented in this thesis must be improved before anthropogenic CF_4 concentrations in seawater can be used effectively as a time-dependent ocean tracer with high spatial and temporal resolution. The 3 year temporal resolution and the small sample number afforded by the current analytical technique could nevertheless illustrate the effective use of CF_4 as a time-dependent tracer.

8.1 References

Busenberg, E. and L. N. Plummer (2000) Dating young groundwater with sulfur hexafluoride: Natural and anthropogenic sources of sulfur hexafluoride, *Water Resources Research* **36**, 3011 – 3030.

Forster, P., Ramaswamy V., Artaxo P., Berntsen T., Betts R., Fahey D.W., Haywood J., Lean J., Lowe D.C., Myhre G., Nganga J., Prinn R., Raga G., Schulz M. and Van Dorland R. (2007) Changes in Atmospheric Constituents and in Radiative Forcing. *In: Climate Change 2007: The Physical Science Basis. Contribution of Working Group I to the Fourth Assessment Report of the Intergovernmental Panel on Climate Change* [Solomon, S., D. Qin, M. Manning, Z. Chen, M. Marquis, K.B. Averyt, M.Tignor and H.L. Miller (eds.)] Cambridge University Press, Cambridge, United Kingdom and New York, NY, USA.

Frische, M., K. Garofalo, T. H. Hansteen, R. Borchers and J. Harnisch (2006), The origin of stable halogenated compounds in volcanic gases, *Environ. Sci. Poll. Res.* **13**, 406–413.

Harnisch J. and Eisenhauer A. (1998) Natural CF_4 and SF_6 on Earth. *Geophys. Res. Lett.* **25**, 2401-2404.

Harnisch, J., M., Frische, R. Borchers, A. Eisenhauer and A. Jordan (2000), Natural fluorinated organics in fluorite and rocks, *Geophys. Res. Lett.* **27**, 1883–1886.

Jordan, A., J., Harnisch, R. Borchers, F. Le Guern and H. Shinohara (2000), volcanogenic halocarbons, *Environ. Sci. Technol.* **34**, 1122–1124.

Kulongoski J. T., Hilton D. R. and Izbicki J.A. (2003) Helium isotope studies in the Mojave Desert, California: implications for groundwater chronology and regional seismicity. *Chem. Geol.* **202**, 95-113.

Kulongoski J. T., Hilton D. R. and Izbicki J. A. (2005) Source and movement of helium in the Morongo groundwater basin: the influence of regional tectonics on crustal and mantle helium fluxes. *Geochim. Cosmochim. Acta* **69**, 3857-3872.

Morris R. A., Miller T. M., Viggiano A. A., Paulson J. F., Solomon S. and Reid G. (1995) Effects of electron and ion reactions on atmospheric lifetimes of fully fluorinated compounds. *J. Geophys. Res* **100 (D1)**, 1287-1294.

Ravishankara A. R., Solomon S., Turnipseed A. A. and Warren R. F. (1993) Atmospheric lifetimes of long-lived halogenated species. *Science* **259**, 194-199.

Thesis Appendix A

Absolute Molar Calibration of CF$_4$

A.I Calibration technique

Routine air measurements by Medusa-GC/MS are reported in relative molar quantities (i.e. mole fractions), since relative molar quantities are less sensitive to systematic biases present in an analytical routine than measurements based on an absolute molar calibration. As an example, the MEMS integrating digital mass-flow controller used to quantifiably sample a specified volume of gas for analysis by GC/MS contains a non-zero reference vacuum that results in an underestimation of the total integrated sample volume introduced into the instrument. Since the mole fraction of a gas in an analyzed sample is calibrated relative to the mole fraction of the gas in the standard, which is not dependent on the amount of standard introduced into the instrument, the systematic bias in the volume of gas analyzed will not be an analytical concern, so long as the standard and sample are treated in an identical manner.

For the gas analyses presented in my thesis, it is the absolute number of moles collected that are required for dissolved CF$_4$ and SF$_6$ concentration calculations (see Chapter 3). In this case, an underestimation of the standard volume introduced into the Medusa-GC/MS will result in a significant overestimation of the number of moles

analyte in an extracted gas sample. It was therefore necessary to develop a method to reliably calibrate the Medusa-GC/MS's mass-flow controller for a series of groundwater CF_4 analyses.

The apparatus used to calibrate the MEMS flow controller is a volume-calibrated 6-liter flask immersed in a water bath. The volume of the 6-liter flask is calibrated to within 10 mL by repeat equilibration with nitrogen gas stored in a 35-liter flask whose internal volume has been accurately determined as a function of room temperature and pressure (Bullister, 1984). The water bath surrounding the 6-liter flask has sufficient thermal mass that the relatively small temperature fluctuations associated with the thermostatted lab air are not transmitted to the flask. The temperature of the water bath is measured with a mercury thermometer to within 0.1 °C prior to each standard calibration. The internal pressure of the flask is measured to within 0.1 mTorr by a Paroscientific piezoelectric pressure sensor. The computer controlling the Medusa-GC/MS communicates directly with the pressure sensor, automatically and consistently logging the measured internal pressure of the flask prior to and after each standard calibration.

For most analyses the flask was filled with roughly 40 psia of the working standard used to calibrate accompanying analyses. This standard was then drawn directly from the 6-liter flask, with the volume of standard withdrawn determined by the measured decrease in the internal pressure of the flask. In this case the standard volume reported by the MEMS flow controller was unnecessary, and the number of moles standard withdrawn could be calculated to within $\pm\, 0.2 - 0.4\%$.
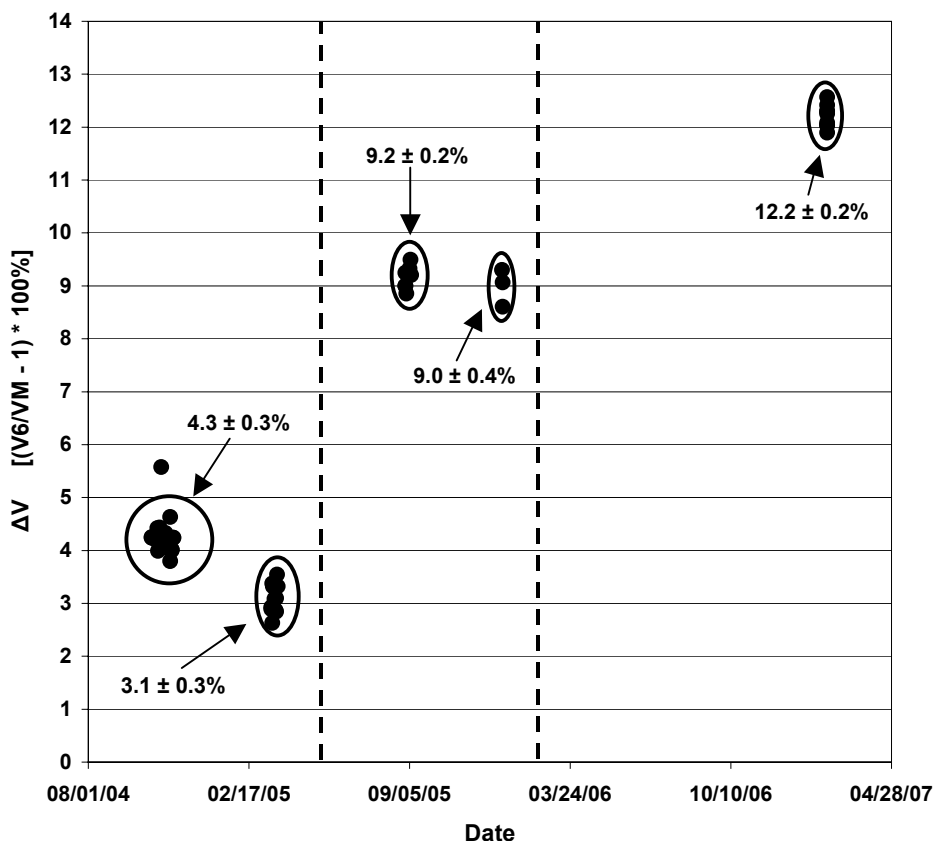
Figure A.1 The percent offset (ΔV) between the volume of sample removed from the volume-calibrated 6 liter flask (V6), as determined from its internal pressure change, and the sample volume reported by the MEMS flow controller (VM). The MEMS flow controller consistently underestimates sample volume by as much as 120 milliliters due to a non-zero reference vacuum. Mean offsets for a series of comparisons (circled) are also shown. Dashed vertical lines indicate where the MEMS flow controller on the instrument was replaced by an identical unit. Although the accuracy of an individual MEMS flow controller does not vary considerably over the timespan of a month, there is significant variability in the accuracy between MEMS flow controllers.

After several sets of analyses had been completed it became clear that the MEMS flow controller is relatively stable within a time period of about a month (Figure A.1). Thus the standard volumes reported by the MEMS could be used, assuming that either before or after a series of analyses the 6-liter flask was used to calibrate the volume bias in the flow controller. The working standard could then be

drawn directly from its original tank, reducing the likelihood of contamination, and the 6-liter flask could be filled to 40 psia with a more easily replaceable gas, such as nitrogen gas, for the calibration of the MEMS flow controller. Standard volumes reported by the MEMS were underestimated by 30 – 120 mL (3 – 12 %).

A.II The virial expansion

Although it is convenient to assume ideality for a real gas, attractive and repulsive interactions between gas molecules can significantly influence the physical response of a real gas to compression or expansion, resulting in deviations from the ideal gas law. It is only at low densities (or high temperatures) that molecules in a real gas are sufficiently separated on average that they can be considered non-interacting (i.e. ideal). As the gas is compressed and the average distance between molecules decreases, attractive forces between molecules act to facilitate compression of the real gas. At even higher pressures, the average distance between molecules shrinks to the point where repulsive forces begin to dominate, hindering further compression of the gas. When considering compressed air in the 6-liter flask used to calibrate the MEMS flow controller, deviations from ideality may significantly influence the number of moles introduced into the GC/MS and result in a miscalibration of the MEMS and a bias in CF_4 measurements.

An alternative to the ideal gas law is the virial equation of state for gases, which is a power-series expansion of the ideal gas law whose additional terms account for intermolecular interactions. One version of the virial equation is:

$$pV_m = RT\left(1 + B'(T)p + C'(T)p^2 + ...\right)$$

(A.1)

where p is the pressure, V_m is the molar volume, R is the universal gas constant and T is the temperature, and B'(T) and C'(T) are temperature-dependent coefficients that are gas-specific. The "second virial coefficient", B'(T), accounts for interactions between pairs of molecules, while the "third virial coefficient", C'(T), includes 3-body interactions. Although the virial equation of state can be expanded to additional terms for greater accuracy, in general additional terms are unnecessary, as $C'(T)p^2 \ll B(T)p$. The compressibility of a gas $(Z = pV_m/RT)$ provides an indication of the deviation of a real gas from ideality, since an ideal gas always has a compressibility of 1. Figure A.2 is a plot of the compressibility of air as a function of its pressure, as described by the virial equation. The 6 liter flask used to calibrate the MEMS is never filled to pressures higher than 3 atmospheres due to the fragility of the digital pressure sensor. At pressures of <3 atmospheres, the deviation from ideality is small (Fig. A.2), less than 0.2%, which is an order of magnitude less than the typical correction to sample volumes reported by the MEMS.
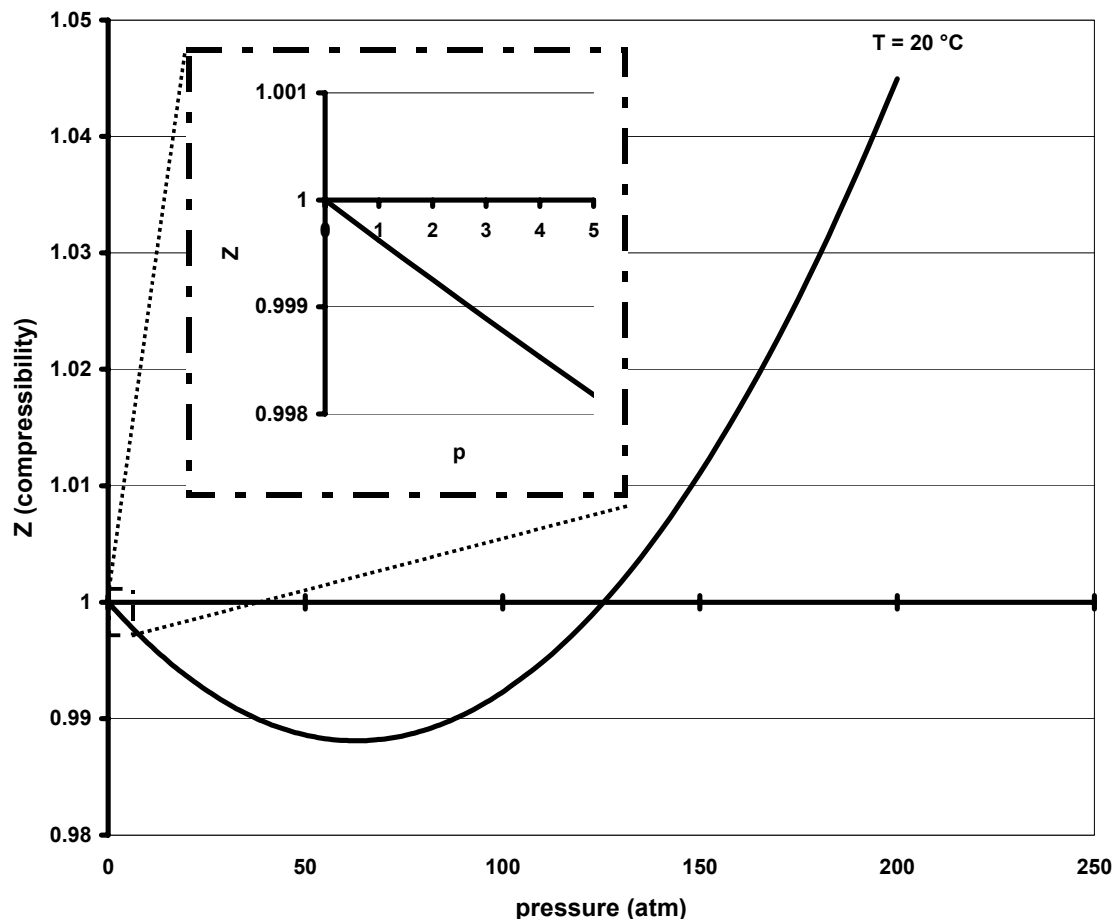
Figure A.2 The compressibility (Z) of air as a function of pressure (p) and at a temperature of 20 °C, as described by the virial equation (i.e. $Z = pV_m/RT = 1 + B'p + C'p^2$). At low pressures the compressibility of air is close to Z = 1, which is the compressibility of an ideal gas. As the pressure increases, air becomes slightly more compressible than an ideal gas (Z<1) due to attraction between air molecules. As the pressure continues to increase, repulsive forces between air molecules begin to dominate, and air becomes significantly less compressible than an ideal gas (Z>1). The internal pressure of the calibration apparatus is always at most roughly 3 atmospheres, and so the deviation from ideality is small, on the order of 0.1 – 0.2% (see insert).

A.III References

Bullister J. (1984) Atmospheric Chlorofluorocarbons as Tracers of Ocean Circulation and Mixing: Measurement and Calibration Techniques and Studies in the Greenland and Norwegian Seas, PhD Thesis, University of California, San Diego, pp. 61-64.

Thesis Appendix B

Halogenated Gas Solubilities

My doctoral studies required a reliable method for estimating dissolved CF_4 concentrations in water over a wide range of temperatures, from cold seawater in the depths of the Pacific, to cool meteoric water recharging the Mojave from nearby mountainsides, to the relatively warm conditions of the laboratory. Unfortunately, for most of my studies no one source existed that collected and compiled all available CF_4 solubility data from the literature to best describe the dependence of CF_4 solubility on temperature. I therefore compiled CF_4 solubility data from available literature and fit it as a function of temperature, as described in the following section. Many of the publications containing CF_4 solubility data also reported solubilities for other halogenated trace gases measured by the Medusa-GC/MS. In anticipation that they may be studied in natural waters in the future by members of the Weiss lab, I also compiled all available solubility data for other halogenated gases measured by Medusa-GC/MS, with the exception of the well-studied chlorofluorocarbons (CFC-12, CFC-11, and CFC-113) and SF_6.

B.I Freshwater CF$_4$ Solubilities

Freshwater CF$_4$ solubility data were collected from Ashton et al. (1968), Wen and Muccitelli (1979), Smith et al. (1981), Cosgrove and Walkley (1981), Park et al. (1982), Scharlin and Battino (1992) and Mainer (2000). The solubility data were converted to a common solubility unit (Ostwald solubilities) and fitted with a Clark-Glew-Weiss (CGW) function of temperature:

$$L = -146.348 + \frac{208.0542}{T/100K} + 65.2749 \times \ln\left(T/100K\right) \qquad \textbf{(B.1)}$$

where L is the Ostwald solubility and T is the temperature in Kelvin. The resulting fit is valid over a temperature range of 273 – 323 K and agrees with the compiled data to within 2% in most cases. Figure B.1 displays the compiled solubility data, the CGW function presented above, as well as a CGW function of an almost identical data set compiled by Clever et al. (2005).

The Ostwald solubility can be defined as the ratio of the concentration of gas dissolved in the liquid phase (C_g^L) to the concentration of gas in the vapor phase (C_g^V), in units of moles gas per liter solution:

$$L = \left(\frac{C_g^L}{C_g^V}\right)_{equil} \qquad \textbf{(B.2)}$$
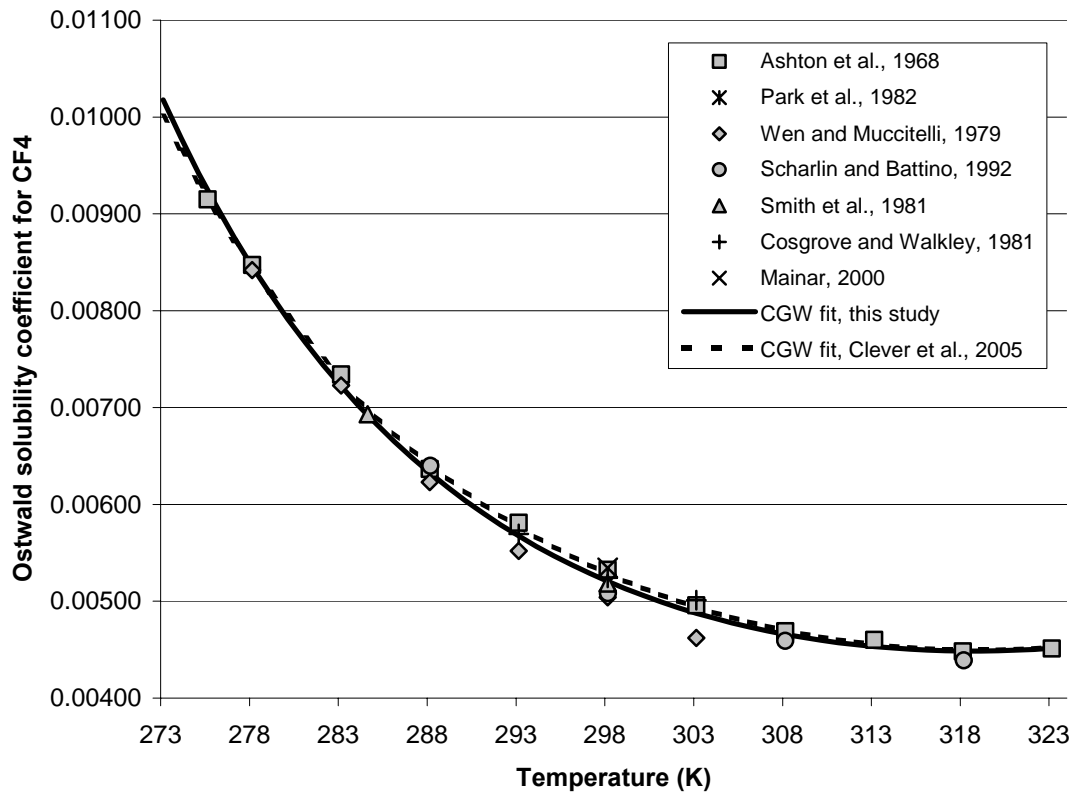
Figure B.1 Ostwald solubility coefficients for CF_4 as a function of temperature. Clarke-Glew-Weiss (CGW) fits to the data from this study and from Clever et al. (2005) are also shown. The CGW fit used in this study agrees to within 2% with the majority of the data.

For air-saturated water, and assuming that the ideal gas law holds, C_g^V can be estimated from:

$$C_g^V = \frac{(p - p_{sat}(T))}{R \cdot T} \cdot x_g \tag{B.3}$$

where p is atmospheric pressure, $p_{sat}(T)$ is the saturation vapor pressure of water, a function of the ambient temperature, T, R is the universal gas constant and x_g is the

atmospheric mole fraction of the gas. Substituting Equation B3 into Equation B2, the concentration of a dissolved gas in an air-saturated water sample, in moles per liter water, can then be estimated from:

$$C_g^L = \frac{\left(p - p_{sat}(T)\right)}{R \cdot T} \cdot x_g \cdot L$$ (B.4)

B.II Seawater CF$_4$ solubilities

The solubility of CF$_4$ in seawater is relatively unstudied, with only 4 data points available in the literature (Scharlin and Battino, 1995), covering a relatively short range of temperatures (15°C – 30°C) and disregarding the dependence of seawater solubility on salinity. Given that the freshwater solubility for CF$_4$ has been more thoroughly studied, it would be advantageous to define the solubility of CF$_4$ in seawater based on its freshwater solubilities.

The solubility of a gas in a mixed-electrolyte solution, such as seawater, can be determined from the fresh water solubility using a modified version of the Setschenow equation (Masterton, 1975):

$$\ln\left(L/L_0\right) = -k_s \cdot I_v$$ (B.5)

where L is the solubility of the gas in the electrolyte solution, L_0 is the freshwater solubility, I_v is the ionic strength of solution, and k_s is an empirically-derived, temperature-dependent constant called the "salting coefficient". Using the freshwater and seawater solubilities for CF_4 (Scharlin and Battino, 1995), salting coefficients for CF_4 as a function of temperature can be estimated. The dependence of the resulting salting coefficients on temperature can be fit very well with a second-order polynomial (Masterton, 1975):

$$k_s = 0.00029863 \times T^2 \ 0.17074 \times T + 24.707 \qquad \textbf{(B.6)}$$

The seawater solubility of CF_4 can then be estimated by combining Equations B.1, B.5 and B.6:

$$L(T, I_V) = \left[A + \frac{100 \cdot B}{T} + C \cdot \ln\left(\frac{T}{100}\right) \right] \times \exp\left(-\left[aT^2 + bT + c\right] \cdot I_V\right) \qquad \textbf{(B.7)}$$

The values for capitalized constants are given in Equation B.1, while those for lowercase constants are given in Equation B.6. One simple method for estimating the ionic strength of seawater from its salinity is:

$$I_V = \frac{0.03600}{1.80655} \times S \times \rho_{H_2O}(T, S) \qquad \textbf{(B.8)}$$

where S is the salinity (in g kg^{-1}) and $\rho_{H_2O}(T,S)$ is the density of seawater (in kg L$^{-1)}$, estimated using an equation of state for seawater (Millero and Poisson, 1981). Once the Ostwald solubility for CF$_4$ in seawater is estimated using Equations B.7 and B.8, the concentration of the gas in seawater can be estimated with Equation B.4, keeping in mind that the saturation vapor pressure of water in this case is also a function of salinity.

B.III Freshwater solubilities for other "Medusa" analytes

Many of the manuscripts containing CF$_4$ solubilities also contained solubilities for other halogenated trace gases analyzed by the Medusa-GC/MS. I compiled this data with supplementary data from the literature (Wilhelm et al., 1977; Horvath and Getzen, 1995; Meylan et al., 1996; Hovorka and Dohnal, 1997; Horvath et al., 1999; Alexander et al., 2001; Abraham et al., 2001; Bonifacio et al., 2001), and obtained sufficient data to fit freshwater solubility curves for 18 additional Medusa analytes (Table B.1). Data were converted to a common solubility unit, in this case Bunsen solubilities (α, $\alpha = L \times T / 273.15$ K), and fit with CGW curves similar to CF$_4$.

Table B.1 CGW coefficients for Bunsen solubilities of halogenated trace gases

Compound	A	B	C	T_{min} (K)	T_{max} (K)
CFC-13	-34.7447	53.1175	11.9348	288	343
CFC-115	7.7555	-4.6742	-10.1559	298	348
CH_3Cl	-55.7000	95.2618	22.5156	278	353
CH_2Cl_2	-109.9320	159.1689	53.1494	273	308
$CHCl_3$	-45.5056	67.9165	21.1735	273	333
CCl_4	-150.2787	209.3940	71.3191	273	308
CH_2F_2	382.5767	-524.8648	-189.4262	289	302
CHF_3	27.4570	-26.6468	-18.0919	278	348
CH_3Br	-53.5628	94.3649	21.2424	278	353
$CHBr_3$	-21.8293	27.5201	10.3813	283	303
CH_3I	-42.8008	62.4380	20.7563	273	313
Halon 1301	-89.8586	140.1702	36.3776	273	323
Halon 1211	-163.085	248.8417	71.0524	273	323
HCFC-22	-101.7181	162.6169	42.9495	298	348
HFC-125	649.6003	-906.4999	-316.6113	298	303
HFC-134a	-15.3731	36.9605	1.8164	278	338
HFC-152a	-14.5973	33.1985	3.1389	273	338
PFC-116	-114.0755	166.7571	47.1396	278	328
TCE	-36.4882	51.0431	16.3367	273	333
PCE	-45.6286	61.7913	19.5115	273	343
CGW curve: $\ln(\alpha) = A + B \times \dfrac{100}{T} + C \times \ln\left(\dfrac{T}{100}\right)$					
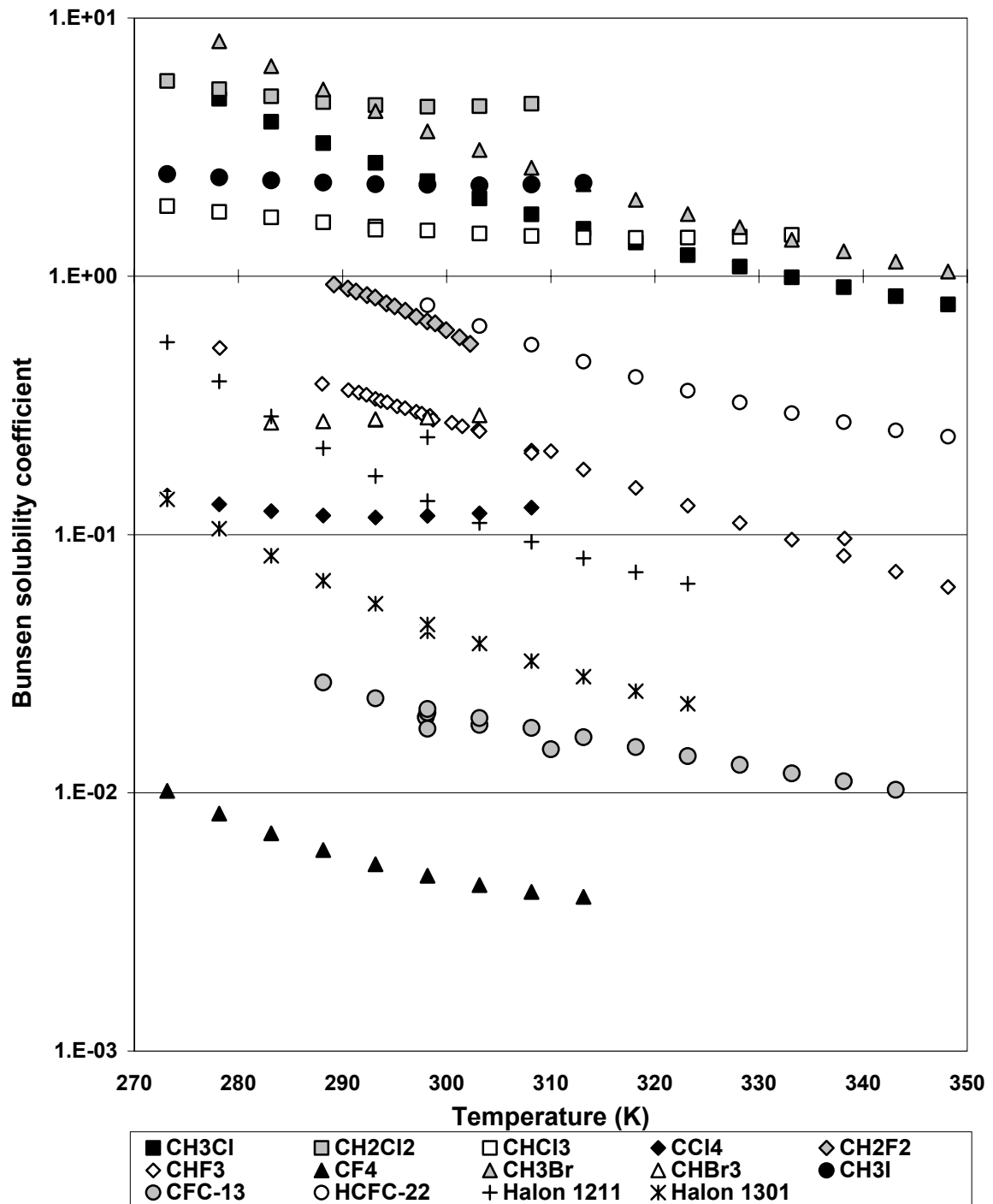
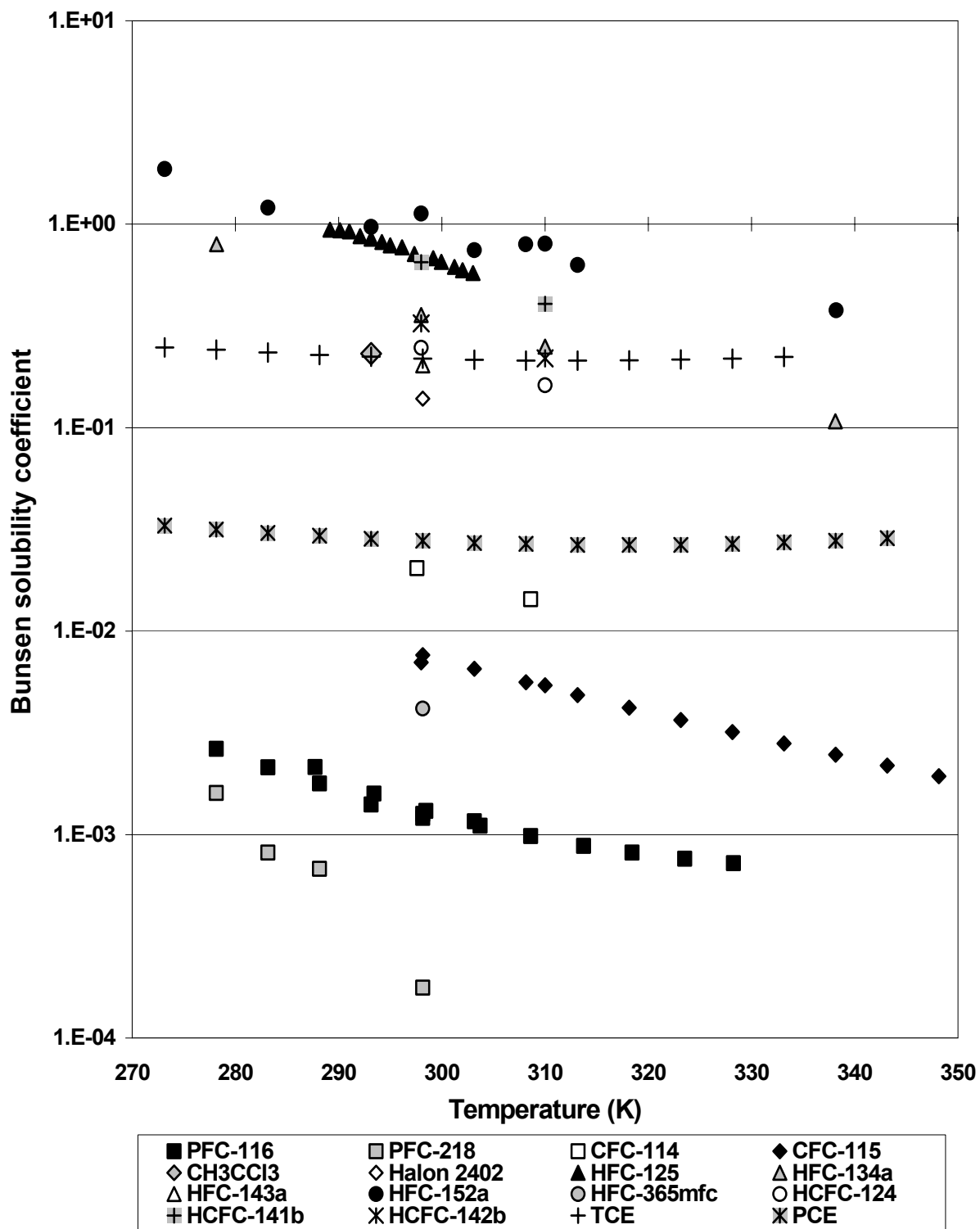**Figure B.2** Bunsen solubilities for halogenated methanes in freshwater.

Figure B.3 Bunsen solubilities for C2–C3 halocarbons in freshwater.

For the remaining trace gases there was not a sufficiently large enough data set to reliably fit the solubility data as a function of temperature. These compounds are displayed in Figure B.2 and B.3, along with the 18 compounds for which CGW fits were possible. For Halon-2402 and HFC-365mfc, no solubility data were available, and so solubility estimates at 298 K were made using the bond contribution model of Meylan and Howard (1991). Trifluoromethane solubilities from Alexander et al. (2000) are a factor of 1.63 times higher than other solubilities drawn from the literature. I scaled their data set by a factor of 1/1.63 to bring it into better agreement with other studies, but the reader should keep in mind that their unaltered solubilities may be correct.

B.IV References

Abraham M. H., Gola J. M. R., Cometto-Muñiz J. E. and Cain W. S. (2001) Solvation properties of refrigerants, and the estimation of their water-solvent and gas-solvent partitions. *Fluid Phase Equil.* **180**, 41-58.

Alexander A. F. M., Abel A. G. M. and Fonseca I. M. A. (2000) Solubility of some new refrigerants in water. *Fluid Phase Equil.* **173**, 97-107

Ashton J. T., Dawe R. A., Miller K. W., Smith E. B. and Sticking B. J. (1968) Solubility of certain gaseous fluorine compounds in water. *J. Chem. Soc. A* **8**, 1793-1796.

Bonifácio R. P., Pádua A. A. H. and Costa Gomes M. F. (2001) Perfluoroalkanes in water: Experimental Henry's Law coefficients for hexafluoroethane and computer simulations for tetrafluoromethane and hexafluoroethane. *J. Phys. Chem. B* **105**, 8403-8409.

Clever H. L., Battino R., Jaselskis B., Yampolskii Y. P., Scharlin P. and Young C. L. (2005) IUPAC-NIST solubility data series 80. Gaseous fluorides of boron, nitrogen, sulfur, carbon and silicon and solid xenon fluorides in all solvents, *J. Phys. Chem. Ref. Data* **34**, 201-435.

Cosgrove B. A. and Walkley J. (1981) Solubilities of gases in H_2O and ^2H_2O. *J. Chrom.* **216**, 161-167.

Horvath A. L. and Getzen F. W. (1995) IUPAC-solubility data series 60. Halogenated methanes with water. Oxford University Press, Oxford, UK.

Horvath A. L., Getzen F. W. and Maczynska Z. (1999) IUPAC-solubility data series 67. Halogenated Ethanes and Ethenes with Water. *J. Phys. Chem. Ref. Data* **28**, 395-627.

Hovorka S. and Dohnal V. (1997) Determination of air-water partitioning of volatile halogenated hydrocarbons by the inert gas stripping method. *J. Chem. Eng. Data* **42**, 924-933.

Mainer A. M., Dissertation, University of Zaragoza, Spain, 2000.

Masterton W. L. (1975) Salting coefficients for gases in seawater from scaled-particle theory. *J. Sol.Chem.* **4**, 523-534.

Meylan W. M., Howard P. H. and Boethling R. S. (1996) Improved method for estimating water solubility from octanol water partition coefficient. *Environ. Toxicol. Chem.* **15**, 100-106.

Millero F. J. and Poisson A. (1981) International one-atmosphere equation of state of seawater. *Deep Sea Res. A* **28**, 625-629.

Park T., Rettich T. R., Battino R., Peterson D. and Wilhelm E. (1982) Solubility of gases in liquids – 14. Bunsen coefficients for fluorine-containing gases (freons) dissolved in water at 298.15 K, *J. Chem. Eng. Data* **27**, 324-326.

Scharlin P. and Battino R. (1992) Solubility of 13 nonpolar gases in deuterium-oxide at 15-degrees-C-45-degrees-C and 101.325-KPa – thermodynamics of transfer of nonpolar gases from H_2O to D_2O. *J. Sol. Chem.* **21**, 67-91.

Scharlin P and Battino R (1995) Solubility of CCl_2F_2, $CClF_3$, CF_4 and CH_4 in water and seawater at 288.15 – 303.15K and 101.325 kPa. *J. Chem. Eng. Data* **40**, 167-169.

Smith R. A., Porter E. G. and Miller K. W. (1981) The solubility of anesthetic-gases in lipid bilayers. *Biochim. Biophys.* Acta **645**, 327-338.

Wen W. Y. and Muccitelli J. A. (1979) Thermodynamics of some perfluorocarbon gases in water. *J. Sol. Chem.* **8**, 225-246.

Wilhelm E., Battino R. and Wilcock R. J. (1977) Low-pressure solubility of gases in liquid water. *Chem. Rev.* **77**, 219-262.